

EXPERIMENTAL RESIN TESTING: MASS TRANSFER  
CHARACTERISTICS AND SPECTROSCOPIC  
ANALYSIS OF NEW AND USED RESINS

By

ALAGAPPAN ARUNACHALAM

Bachelor of Engineering (Honors)

Birla Institute of Technology and Science

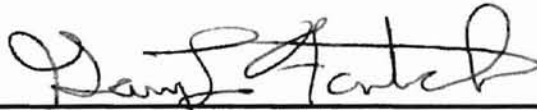
Rajasthan, India

1994

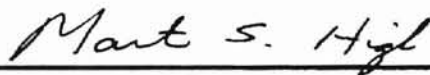
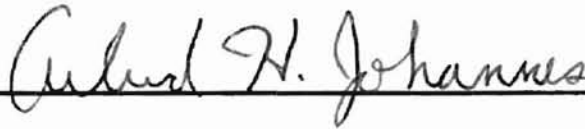
Submitted to the Faculty of the  
Graduate College of the  
Oklahoma State University  
in partial fulfillment of  
the requirements for  
the Degree of  
MASTER OF SCIENCE  
July, 1996

EXPERIMENTAL RESIN TESTING: MASS TRANSFER  
CHARACTERISTICS AND SPECTROSCOPIC  
ANALYSIS OF NEW AND USED RESINS

Thesis Approved:



Thesis Adviser



Dean of the Graduate College

## ACKNOWLEDGEMENTS

I wish to express my sincere appreciation to my major advisor, Dr. Gary L. Foutch for his irreplaceable assistance, constructive guidance, inspiration and total candor throughout the course of this study. My sincere appreciation extends to my other committee members Dr. Arland H. Johannes and Dr. Martin High, for their guidance and encouragement without which this work would never have been accomplished. I would like to thank Dr. Vikram N. Chowdiah for his frank and sincere advice, guidance, and suggestions which were invaluable to me during the course of my graduate studies.

I would like to thank the other members of my research group, Jidong Lou, Yunquan Liu, Sunkavalli Vinay, Dennis Hussey, Kalyan Wunnava, Ashwin Gramopadhye, Brian Gill, and John Carmett for their patience and support while performing my experiments.

Special thanks must be given to my parents whose emotional and financial support, encouragement, and inspiration was unfailing throughout my stay at Oklahoma State University.

## TABLE OF CONTENTS

Chapter	Page
I. INTRODUCTION.....	1
II. LITERATURE REVIEW.....	5
Ion Exchange Equilibria.....	5
Ion Exchange Kinetics.....	9
Ionic Mass Transfer Coefficient.....	11
III. MASS TRANSFER PROPERTIES OF MONOVALENT AND DIVALENT IONS IN NEW AND USED RESINS.....	16
Introduction.....	16
Mass Transfer Equation.....	17
Experimental Procedure.....	20
Experimental Results and Discussion.....	23
Extraction of Particle Mass Transfer Properties.....	42
Results and Discussion.....	46
Conclusions and Recommendations.....	49
IV. SPECTROSCOPIC ANALYSIS OF USED RESINS.....	52
Introduction.....	52
Theory.....	54
Results and Discussion.....	55
Conclusions.....	62
BIBLIOGRAPHY.....	63
APPENDIXES.....	67
APPENDIX A — EXPERIMENTAL SYSTEM.....	68



---

Chapter	Page
APPENDIX B — EXPERIMENTAL PROCEDURE.....	74
APPENDIX C — ION CHROMATOGRAPHIC APPARATUS .....	80
APPENDIX D — ERROR ANALYSIS .....	94
APPENDIX E — EXPERIMENTAL DATA.....	99

## LIST OF TABLES

Table	Page
I Experimental Influent Concentrations and Flow Rates .....	21
II Source of Used Ion Exchange Resins Tested .....	21
III Physical Properties of DOWEX Monosphere Resin .....	22
IV Operating Conditions of Condensate Polishers at Riverside CPs 1 and 2 and Northeast CPs 3 and 4.....	34
V MTCs of New Monosphere Resin (Film MTC), Riverside station CPs 1 and 2, Northeast station CPs 3 and 4 .....	47
VI Mass Transfer Coefficients Based on Overall Mass Transfer Coefficients estimated by Harries and Ray's Equation (Table V) .....	48
VII Effective Particle Diffusivity Based on Linear Driving Force Equation (Film MTCs based on Harries and Ray's equation .....	49
VIII List of Equipment .....	72
IX Characteristics of Chemicals for Regenerant and Eluant .....	83
X Mass Transfer Coefficient Data of Monosphere Resin estimated by Harries and Ray's Equation.....	99
XI Maximum and Minimum Relative Errors of Mass Transfer Coefficients Due to Experimental Uncertainties.....	106

## LIST OF FIGURES

Figure	Page
1 Mass transfer coefficients of sodium for new monosphere resin in a mono bed at different flow rates .....	24
2 Mass transfer coefficients of chloride for new monosphere resin in a mono bed at different flow rates .....	25
3 Mass transfer coefficients of sodium for new monosphere resin in a mixed bed at different flow rates .....	27
4 Mass transfer coefficients of chloride for new monosphere resin in a mixed bed at different flow rates4 .....	28
5 Comparison of mass transfer coefficients of sodium and chloride for new monosphere resin in a mixed bed and a mono bed at 500 ml/min flow rate ....	30
6 Comparison of mass transfer coefficients of sodium in a mixed bed for new monosphere resin and used resin (RS CP1) at different flow rates .....	31
7 Comparison of mass transfer coefficients of sodium in a mixed bed for new monosphere resin and used resin (RS CP2) at different flow rates .....	32
8 Comparison of mass transfer coefficients of chloride in a mixed bed for new monosphere resin and used resin (RS CP 1) at different flow rates.....	33
9 Mass transfer coefficients of magnesium for new monosphere resin in a mono bed at different flow rates .....	35
10 Mass transfer coefficients of magnesium for new monosphere resin in a mixed bed at different flow rates .....	36
11 Comparison of mass transfer coefficients of magnesium for new monosphere resin and used resin (RS CP 1) in a mixed bed at different flow rates .....	38

Figure	Page
12 Mass transfer coefficients of calcium for new monosphere resin in a mono bed at different flow rates .....	39
13 Mass transfer coefficients of calcium for new monosphere resin in a mixed bed at different flow rates .....	40
14 Mass transfer coefficients of calcium for used monosphere resin (RS CP 1) in a mixed bed at different flow rates .....	41
15 Comparison of mass transfer coefficients of calcium, magnesium, and sodium for new monosphere resin in a mixed bed at 750 ml/min.....	43
16 Raman Spectroscopic analysis of new anion monosphere resin bead (surface scan at 400 mW intensity laser beam) .....	56
17 Raman Spectroscopic Analysis of used anion resin from Riverside Station CP 2 (surface scan at 400 mW intensity laser beam) .....	57
18 Raman Spectroscopic Analysis of a second bead of new anion monosphere resin (surface scan at 200 mW intensity laser beam) .....	58
19 Raman Spectroscopic Analysis of used anion monosphere resin from Northeast station CP2 (surface scan at 400 mW intensity laser beam) .....	59
20 Flow Diagram of Experimental System .....	73
21 Calibration Curve for sodium as obtained from Dionex Software .....	89
22 Calibration Curve for magnesium as obtained from Dionex Software .....	90
23 Calibration Curve for calcium as obtained from Dionex Software .....	91
24 Calibration Curve for chloride as obtained from Dionex Software.....	92
25 Calibration Curve for sulfate as obtained from Dionex Software .....	93

## NOMENCLATURE

A	cross sectional area of a column, $m^2$
$a_s$	specific surface area of cation or anion resin, $m^2/m^3$ resin
ACI	advanced computer interface
B	temperature factor
C	constant depending on instrument response, slidewidth, collection angle
$C_i$	concentration of species i, ppb or $meq/m^3$
$d_p$	particle diameter of cation or anion resin, cm
$D_c$	intracrystalline selectivity, $m^2/s$
$D_p$	effective particle diffusivity, $m^2/s$
DAP	2,3-diaminopropionic acid monohydrochloride
$E_a$	absolute error of any measurement
$E_r$	relative error of any measurement
$H_2SO_4$	sulfuric acid
I	raman intensity of radiation
IC	ion chromatographic system
K	distribution coefficient in liquid phase $\cong 1$ /selectivity coefficient
$K_{o,i}$	overall MTC of ion i, m/s
$K_{f,i}$	film MTC of ion i, m/s

$K_{\max}$	maximum bound on mass transfer coefficient
$K_{\min}$	minimum bound on mass transfer coefficient
$k_H$	MTC estimated by Eq (10), m/s
$k$	overall mass transfer coefficient, $s^{-1} = a_s k_o$
MTC	mass transfer coefficient, m/s
ppm	parts per million
$q_i$	mean resin phase concentration of species i, meq/cm <sup>3</sup>
$Q_i$	total resin exchange capacity of resin i, meq/ml
R	universal gas constant
$R_i$	volume fraction of cation or anion resin in mixed bed
$R_p$	particle resin radius, m
r	coefficient of fit
RS1	resistivity meter 1
RS2	resistivity meter 2
$r_c$	microparticle radius, m
S	specific surface area, $S=a_s(1-\epsilon)$ , m <sup>2</sup> /m <sup>3</sup> resin
$S_i$	intrinsic molar scattering coefficient
T	temperature in degrees Kelvin
TBAOH	tetrabutylammonium hydroxide
$u_r$	superficial linear velocity, m/s
V	volumetric flow rate, m <sup>3</sup> /min
$X_m$	measured value

$X_i$	true value
$x_i$	equivalent fraction of species i in solution
$y_i$	equivalent fraction of species i in resin phase
$z$	distance from column inlet, m
$Z$	bed depth, m
$Z_i$	charge on ion i

#### Greek Letters

$\varepsilon$	bed void fraction
$\lambda_i$	equivalent conductance
$\nu$	frequency of vibration

#### Superscripts

*	interfacial equilibrium condition
eff	column effluent condition
f	feed condition
o	bulk solution condition

#### Subscripts

f	film
o	overall
p	particle
max	maximum
min	minimum

## CHAPTER I

### INTRODUCTION

Ion exchange is one of the major processes used on an industrial scale in the continuous production of ultrapure water. As requirements for high purity water have developed, systems consisting of single- and mixed-bed ion exchange resins along with a number of other pre- and post-treatment processes have evolved. For many industries, any deterioration in water quality obtained from ion-exchange mixed-beds has serious consequences on production processes and other items of the plant. Hence, the development of a tool that can predict the performance of an ion-exchange resin column as the resin in the beds gradually ages becomes essential.

Ion exchange resins are insoluble solid polymers, normally consisting of polystyrene beads with divinyl benzene cross-linking, which carry exchangeable cations or anions. When the resins are in contact with a solution, the exchangeable ions in the resin can be exchanged for a stoichiometrically equivalent amount of ions of the same sign (counter ions) from the solution. Since ion exchange is a reversible process, the resins can be regenerated so that they are converted to their original forms and are capable of carrying out further ion-exchange. Ion exchange is essentially a diffusion



process and has little relation to chemical reaction kinetics in the usual sense. The ion exchange resins are selective and take up certain counter ions in preference to others.

Ultrapure water is required in large volumes by power plants that use mixed-bed ion-exchange for condensate polishing and makeup water purification. Most condensate polishers utilize regenerable bead form resin in packed beds, though some use throw-away powdered ion exchange resins. To produce ultrapure water, the cation and anion exchange resins are regenerated to the hydrogen and hydroxide forms, respectively. This is normally referred to as the hydrogen/hydroxide cycle. This mode of operation continually removes amines that are added to boiler feed water to raise the pH and minimize corrosion of the steel components. Hence, normally an excess of cation exchange resin is provided in the mixed beds of most condensate purification plants. Some plants use cation resins in the ammonium form, referred to as amine cycle. This eliminates the removal of ammonium ions from the water and hence, reduces the sizes of the plants. Though this cycle eliminates the problem of continuous removal of ammonia, it suffers from the disadvantage of unfavorable equilibrium for the removal of sodium on ammonium form of cation exchange resin.

Another major problem with ion-exchange resins is their deterioration with continuous use. This problem is especially associated with anionic resin (Harries and Ray, 1984; Harries, 1986, 1987). The first observation with anion resin degradation is an increase in chloride and sulfate leakage from the condensate purification plants. There are a number of factors attributed to anion resin degradation. Organic molecules present in feedwater (humic and fulvic acids), cross contamination of anion resin during cation resin regeneration, degradation products of cation resins such as short chain aromatic

sulfonates, and manufacturing residues of cation resin are some of the causes of degradation of anion resin (Harries, 1984). McNulty et al. (1986) discussed thermal degradation of strong base capacity and coating of the resin surface by dense iron-oxide films as reasons for normal anion resin deterioration.

Kinetic problems with cation exchange resins are often attributed to poor regeneration or poor flow characteristics. Cation resin degradation is observed by increased sodium or ammonium leakage which has been ascribed to residual polymeric material, like oligomeric species, eluted from the anion resin (Harries, 1991). In both anion and cation resin degradation the foulants are unlikely to diffuse into the beads but instead form a physical layer at the surface that inhibits ion exchange by blocking the exchange sites. In addition, the foulants may set up their own potential barrier at the bead surface (Harries, 1984), spare anionic groups on the foulant repelling the anions approaching in the liquid phase.

Frisch and Kunin (1960) examined the kinetics of mixed bed ion-exchange and concluded that boundary-layer diffusion was the rate controlling step at low influent concentrations. When the overall reaction begins to slow due to resin fouling, the process can no longer be explained by film diffusion alone, but must take into account reaction and/or particle diffusion. The effects of resin degradation on mixed-bed ion exchange unit performance have been discussed by Foutch and Chowdiah (1992).

Normally, experimentally measured mass transfer coefficients (MTCs) are used to indicate the extent of deterioration in new and used ion exchange resins. Harries and Ray (1984) adapted the mass transfer equation of Frisch and Kunin (1960) for application to mixed beds. The same model is used in this study to evaluate MTCs of new resins and to

estimate resin degradation. This procedure uses a single-parameter experiment to obtain a single-parameter property, the overall MTC. This overall MTC is a lumped parameter that includes film, interfacial, and particle effects. The simplicity of this procedure makes it more attractive to use rather than the diffusion models used for particle mass transfer kinetics (Gopala Rao and Gupta, 1982). Lee (1994) used a similar methodology to study used resin kinetics. The flow rates used in his study were in the lower range of flow rates normally used in industry. He used a simple series resistance model to explain used resin kinetics.

The objectives of this study are:

1. To evaluate mass transfer coefficients of new and used resins (from Public Service of Oklahoma) for sodium, chloride, magnesium and calcium at higher flow rates than that used by Lee (1994) and at a wider influent concentration range than that used by Harries and Ray (1984). This range of flow rates and influent concentrations was chosen so that it covers the entire operating conditions spectrum in industry.
2. To study used resin kinetics using a combination of Harries and Ray's (1984) mass transfer equation and a modified form of the series resistance model.
3. To evaluate effective particle diffusivity in used resins to elucidate the role particle diffusion rate plays in fouled resins.
4. To analyze the surface of used resins using Laser Raman Spectroscopy.

## CHAPTER II

### LITERATURE REVIEW

Ion-exchange is the reversible stoichiometric exchange of ions between a solid and a liquid in which there is no substantial change in the structure of the solid. Basic definitions, equilibria, kinetics, and industrial applications of ion-exchange have been discussed in detail by Kunin (1960), Helfferich (1962, 1966), Grimshaw and Harland (1975), and Naden and Streat (1984). Mixed-bed ion-exchange is defined as the simultaneous exchange of cations and anions by an intimate mixture of cation and anion exchangers. Haub (1984), Yoon (1990), Zecchini (1990), and Noh (1992) have done extensive work in modeling the mixed-bed ion-exchange process. Harries (1978, 1986, 1987, 1988, 1991), Harries and Ray (1984), and Lee (1994) have documented, in detail, the kinetics of mixed-bed ion-exchange processes for new and used resins. Literature related to the present study is reviewed in this chapter.

#### Ion-Exchange Equilibria

Ion-exchange equilibrium is attained when an ion exchanger is placed in an electrolyte solution containing a counter ion which is different from that in the ion-

exchange resin. If the resin is initially in A form and the counter ion in the solution is B, the ion-exchange reaction is given by



The counter-ion ratio of the two competing counter ion species in the resin is usually different from that in the solution because the ion-exchange prefers one species with respect to the other. This is called selectivity.

Equilibrium between the resin and the solution can be described by means of rigorous thermodynamics with no model and no assumptions about the mechanisms of the phenomena. Different solutions can be obtained depending on the forms of equations selected based on components in the system and of the standard and reference state (Helfferich, 1962). Most theories in this approach consider the components of the resin to be "resinates," the dissolved ions, and the solvent along with the standard and reference states of the resinates are taken to be mono-ionic forms of the ion exchanger. Kielland (1935) was among the first researchers to take this approach. He outlined a thermodynamic method of treating base-exchange equilibria using activity coefficients. The practical value of the rigorous thermodynamic approach is limited because the quantities involved cannot be determined by measurements or predictions without assumptions. Hence, various models with properties similar to those of an ion-exchange resin have been developed. Such models are useful only for select systems where the actual properties are adequately represented by the model.

Gregor's (1948, 1951) "network of elastic springs" representation of ion-exchange resins was the first model introduced that reflected particular properties of ion-

exchangers. This model is purely mechanical and does not include electrostatic interactions. The model also does not involve the single ion as a discrete particle and hence, the model is termed “macroscopic.” Models on a “molecular scale” were proposed by Katchalsky (1953) and by Nagasawa and Rice (1961). Both models are similar in many respects and represent the matrix with fixed ionic groups as cross linked chains with rigid segments, carrying one electric charge each, that are interconnected by universal joints. Increase in entropy and the subsequent coiling of the chains is used to explain elasticity. A variety of other diverse approaches and models have been developed, with varying degrees of similarity with other theories and with varying degrees of usefulness (Helfferich, 1962). The most important rules from these models are deduced by simple qualitative reasoning.

In general, ion-exchange resins prefer counter ions of higher valences with the preference increasing with dilution of the solution (Helfferich, 1962). This effect is explained in terms of the Donnan Potential. The Donnan Potential attracts counter ions into the exchanger and thus balances their tendency to diffuse out into the solution. The force with which the Donnan potential acts on an ion is proportional to the ionic charge. Ion-exchange equilibria is also affected by swelling pressure of the resin and the sizes of the solvated counter ions. Ion exchangers prefer counter ions with smaller solvated equivalent volumes because of the tendency of their matrices to relax (Gregor, 1951). Hence, selectivity increases with dilution of the solution, with decreasing equivalent fractions of the smaller ion, and with increasing degrees of cross linking of the resin. Though in general, larger counter ions can displace smaller ones, very large organic ions and inorganic complexes may be mechanically excluded by sieve action (Helfferich,

1962). Sieve action occurs if the meshes of the matrix are too narrow for accommodating the ion, and is more strongly observed in highly cross-linked resins.

Deviations from ideality occur usually because of interactions of various components of the system. The most important interactions are those between counter ions and fixed ionic groups in which ion pairs or covalent bonds are formed. The ion-exchanger prefers the counter ion that forms the stronger ion pairs or bonds with the fixed ionic groups. Such interactions could occur if the fixed ionic groups are similar in structure to precipitating or complexing agents that react with the counter ion (Helfferich, 1962). Counter ions could also be held by fixed ionic groups by the electrostatic attraction between charges of opposite sign. This effect favors preference for the counter ion of higher valence and, in many cases, preference for the smaller counter ion (Boyd et al. 1947). In some cases, interactions of the solvent molecules with one another and London forces between the counter ion and the matrix may affect selectivity. Kressman (1949) found that styrene-type resins usually prefer counter ions with aromatic groups to those with aliphatic groups. Hence, when counter ions with organic groups that resemble the components of the matrix are present, the ion exchanger selectivity for these ions increases.

The temperature dependence of equilibria is related to the standard enthalpy change that accompanies the reaction (Helfferich, 1962). High temperature discourages the reaction that occurs with evolution of heat. Ion exchange is not a chemical reaction and, as a rule, occurs with little evolution/uptake of heat. Hence, temperature dependence of ion exchange equilibria is only minor. Similarly, pressure dependence that is related to



standard volume change accompanying a reaction, of ion-exchange equilibria is negligible.

### Ion-Exchange Kinetics

The theory of ion-exchange kinetics is not nearly as advanced as that of ion-exchange equilibria. The main difficulties with time-dependent phenomena are mostly mathematical (Helfferich, 1962). Experimental and theoretical work has led to a much better understanding of the mechanism and the rate-determining step of the ion-exchange process, but a lot of work is still to be done.

Ion exchange, as a rule, is a diffusion process with the rate-determining step established to be diffusion of the counter ions between the ion-exchanger and the solution it is in contact with (Helfferich, 1962). Any counterions leaving the exchanger are replaced by an equivalent amount of other counterions except in cases where electrolyte sorption and desorption accompanies ion-exchange, thus changing the ion-exchanger co-ion content. Under normal circumstances, Donnan exclusion keeps the co-ion content low so that deviations from stoichiometric exchange remain small.

The ion-exchange process can be controlled by one of three rate controlling mechanisms: interdiffusion of counterions within the ion exchanger itself (particle diffusion), interdiffusion of counterions in the adherent films (film diffusion), and the “chemical” exchange reaction at the fixed ionic groups (Boyd et al., 1947). Spalding (1961) has shown that the counterion exchange across the interface between ion exchanger and solution is highly unlikely to be the rate-determining step if transition



across the interface is purely a physical process such as diffusion. Rate control by the exchange reaction has been ruled out for ordinary ion-exchange processes (Boyd, 1947) but can occur in chelating group resins that form reacting complexes (Turse and Rieman, 1961). Hence, as a rule, either film diffusion control or particle diffusion control or a combination of the two is the rate controlling mechanism.

The rate of ion exchange is determined by the slower of the two processes. Film diffusion control prevails in systems with ion exchangers of high concentration of fixed ionic groups, low degree of crosslinking, and small particle size, with dilute solution, and with inefficient agitation (Gopala Rao, 1964). All factors with opposite tendencies support particle diffusion control using quantitative expressions for the effects of the various factors. Boyd et al. (1947) concluded that particle diffusion was the controlling mechanism for solution concentration of 0.1 M or greater, and film diffusion was the rate controlling mechanism for concentrations of 0.003 M or less with a combination of the two in the intermediate concentration range. Petruzzelli et al (1988) studied the particle diffusion mechanism using autoradiography and light microscopic observation inside a resin bead. Tittle (1981) verified experimentally the poor kinetics on used anion exchange resin.

An important feature of ion-exchange is the conservation of electroneutrality. This requires stoichiometric exchange of counter ions, otherwise a net electric charge would result. This equality of fluxes is enforced by an electric field set up by the diffusion process. In a solution with concentration gradients, the net flux is given by the Nernst-Planck equation

$$\begin{aligned}
 J_i &= (J_i)_{\text{diffusion}} + (J_i)_{\text{electrical}} \\
 &= -D_i \left( \nabla C_i + z_i C_i \frac{F}{RT} \nabla \phi \right)
 \end{aligned}
 \tag{II-2}$$

applies whenever an electric field exists. It does not matter whether the electric field is generated by an external source or by diffusion within the system. The effects of convection, gradients of pressure and activity coefficients are not used in the derivation of this equation. This equation applied to counterions in binary exchange is used to obtain the effective liquid phase or solid phase diffusivity. The mass-transfer coefficient in rate expressions can be calculated using this effective diffusivity (Kataoka et al., 1973).

Graham and Dranoff (1972) analyzed film-diffusion control at low concentration and low stirring rates, and intraparticle diffusion control at high concentrations and high stirring rates using anion exchange experiments in a well stirred batch reactor. They concluded that film diffusion control was the rate mechanism in the initial stages of ion-exchange until the outer layers of the exchanger are exhausted after which particle diffusion control becomes a major factor. Goto et al. (1981 a, b) carried out experiments using a batchwise stirred tank reactor and proposed a method of simultaneous evaluation of the interphase mass-transfer coefficient and intraparticle diffusivity using linear and nonlinear isotherms.

### Ionic Mass-Transfer Coefficient

Frisch and Kunin (1960) first derived a mass transfer equation for ionic leakage from an ion-exchange resin mixed bed at extremely low solute concentrations ( $< 10^{-5}$  N).

Their relation did not account for cation to anion resin ratio or their diameters because they assumed identical cation and anion exchange rates. Harries and Ray (1984) adapted this ionic leakage equation for application to either anion or cation exchangers in a mixed bed.

The ionic leakage is the effluent from the bed that originates from the feed solution, and is related to the physical characteristics of the resin and the hydraulics of the system. The leakage is characterized by the inability of the polisher to sufficiently reduce the influent ionic concentration to the target level (McNulty, 1984). Elution leakage is caused by the equilibrium exchange of impurity ions left on the resins after regeneration by the ions present in the water at the bottom of the bed. Displacement leakage occurs when impurity ions loaded onto the top of a bed during a condenser leak are displaced down the bed by the ammonium ions (Ammonium cycle) present in the condensate after the original leak is sealed (Bates and Johnson, 1984).

Van Brocklin and David (1972, 1975) investigated the effects of ionic migration for the case of film diffusion rate control. They accounted for ionic migration effects by considering a ratio of ionic to non-ionic mass-transfer coefficients. Harries and Ray's modification (1984) incorporated the cation to anion exchange volume ratio in a mixed bed and the volumetric flow rate. Using the modified Frisch and Kunin equation, they concluded that boundary layer diffusion was the rate controlling step at low influent concentration. They also found that

$$k_r = \frac{D}{\delta} \quad (\text{II-3})$$

holds for boundary layer diffusion. In this relation,  $D$  is the aqueous diffusion coefficient for the exchanging species and  $\delta$  is the fixed thickness of the boundary layer.  $\delta$  is a hydrodynamic function of the resins and so the mass transfer coefficient varies with flow rate. They studied mass transfer coefficient variations with bead size and concluded that the bead size affects the overall rate of exchange, but polymer/matrix types do not affect both chloride and sulfate exchange. The foulants likely to affect anion exchange resins were identified to be natural vegetation decay products, cation resin degradation products, and metallic oxides and oils from boilers, turbines and pumps.

Harries and Ray (1978) studied acid leakage from mixed beds and kinetic deterioration in used resins. They found that improper rinse after regeneration coupled with improper mixing of resin in a mixed bed contribute to acid leakage and anion-resin contamination. Anderson et al. (1955) showed the kinetics of sulfuric acid release during water rinse from strongly basic anion resin to be fairly rapid. Hence, slow acid release that leads to prolonged acid bleeding can be attributed to the weakly basic groups on the anion resin. Harries and Ray (1978) found that strongly basic anion exchange resin lose both total and strongly basic capacity and increase in weakly basic capacity as they age. Thus, aging and fouling of resins worsen the problem of acid contamination and subsequent acid release.

Harries (1987) studied variations of mass transfer coefficients of chloride and sulfate for new and used resins in mixed resins at a superficial velocity of 100 m/hr. He concluded that increasing the anion resin ratio in a mixed bed does not have any added advantage in removing chloride or sulfate ions. Experimental results showed that the

mass transfer coefficients of sulfate were smaller than those of chloride. McNulty (1984) made the same observation. The cations from the injected salt are removed less rapidly as the cation-to-anion exchange resin ratio decreases and the solution becomes more alkaline. Huang and Li (1973) used the film mass-transfer coefficient to obtain interphase-mass transfer coefficients which involved both film and particle resistances.

Emmett and Hebbs (1983) found that the mass transfer rate was proportional to the square root of the influent superficial velocity for both anion and cation exchange resins in mono beds. Tittle (1986) proposed the kinetic deterioration in anion exchangers comes from the preferential chemical degradation of exchange groups, particularly the strongly basic groups, at the bead surface.

Harries (1985) also proposed that variations in bead surface chemistry could be responsible for observed kinetics differences in new resins. Sulfate kinetics on used resins was more strongly affected than chloride kinetics. A study of the mass transfer coefficient with influent pH revealed a sharp drop in both chloride and sulfate exchange kinetics as the influent pH moved from acidic to neutral or alkaline in a mixed bed. From measurements of the resin bead size and their effects on mass transfer coefficients for chloride and sulfate Harries (1988) concluded that increased size caused a reduction of mass transfer coefficients for both ions, and the mass transfer coefficients of sulfate were more strongly influenced.

Harries (1991) studied the rates of anion exchange for chloride and sulfate when ammonia and morpholine were dosed into a mixed bed as corrosion controlling agents. He found the rate of exchange was faster when the corrosion controlling agents were dosed and attributed this to the pH of the aqueous phase.

Van Deemter et al. (1956) developed a relation approximating the overall mass transfer coefficients to be equal to the sum of the resistances in the mobile and immobile phase of a chromatographic column. The immobile phase (particle) mass transfer resistance was defined to be the Distribution Factor divided by the particle mass transfer coefficient. Glueckauf and Coates (1947) developed a simple linear driving force model with an estimated effective rate constant to avoid the complexity of the solution of a mathematical model with two mass transfer resistances. Ruthven (1984) found that the breakthrough curves calculated from the linear rate model for plug flow and from Rosen's solution for intraparticle diffusion control show good agreement when the equivalent rate constant is defined as  $15D/R_p^2$ . Using Moments analysis, he derived the following relation for a simple linear rate model for dispersed plug flow and macropore-micropore diffusion with external film resistance:

$$\frac{1}{kK} = \frac{R_p}{3k_f} + \frac{R_p^2}{15\epsilon_p D_p} + \frac{r_c^2}{15KD_c} \quad (\text{II-4})$$

In Equation II-4, the first term on the RHS accounts for film diffusion resistance, the second term on the RHS accounts for particle diffusion resistance, and the third term accounts for intraparticle micropore diffusion resistance.

## CHAPTER III

### MASS TRANSFER PROPERTIES OF MONOVALENT AND DIVALENT IONS IN NEW AND USED RESINS

#### Introduction

Ion exchange technology is capable of treating large volumes of water economically, and is widely used for ultrapure water processes such as steam-cycle condensate polishing. Mixed-bed ion-exchange is used to remove ionic impurities to sub-parts-per-billion concentrations. A major problem for these processes is deterioration of both, cationic and anionic resin. Degradation of anionic resin has been of particular concern in the power industry (Harries and Ray, 1984; Harries, 1986, 1987).

Anion resin degradation is usually identified by an increased ionic leakage from the column during a step-change increase in feedwater concentration. This ionic leakage (chloride or sulfate) occurs during repeated use of anion resins and is due to several effects such as organic foulants in feedwater and deactivation of resin exchange sites (Griffin, 1991). Poor cation-exchange kinetics is observed as sodium or ammonium leakage, and is caused by residual polymeric material, like oligomeric species, eluted from the anion resin (Harries, 1991). These foulants form a physical barrier on the resin

surface, inhibit the penetration of counter ions into the resin, and interrupt the exchange sites (Tittle, 1981; Harries and Ray, 1984). When the overall reaction begins to slow due to resin fouling, the process has to be modeled by taking reaction and/or particle diffusion rate into consideration along with film diffusion mechanism. The effects of resin degradation on the performance of mixed-bed ion-exchange have been discussed by Foutch and Chowdiah (1992).

In this study, an experiment that measures overall MTC is used to evaluate resin degradation. This method was used by Harries and Ray (1984), Harries (1986), and by McNulty et al. (1986). This procedure is commonly used in industry with various modifications. The extent of deterioration of resin can be identified by evaluating the difference in MTC of new and used resins, but the reasons for degradation cannot be identified. In order to quantify the effects of particle diffusion control in used ion-exchange resins, the data obtained from the kinetics testing of resins are analyzed using a relation developed by Van Deemter et al. (1956) approximating the overall MTC to be equal to the sum of resistances in the mobile and immobile phase of a chromatographic column. Effective particle diffusivities have been estimated using an extension of the linear driving force model developed by Ruthven (1984) for dispersed plug flow and macropore-micropore diffusion with external film resistance.

#### Mass Transfer Equation

The assumptions made in the development of the model to predict mass transfer coefficients are given below:



- Film diffusion is assumed to be the rate determining step because of the ultra low concentration of influent feed impurity
- Pseudo steady state exchange (variations of concentration with space are much more important than with time)
- No coion flux across the particle surface
- Ionic fluxes are equal because of electroneutrality constraint
- Uniform bulk and resin compositions
- Activity coefficients are unity
- Plug flow
- Isothermal and isobaric operation
- Negligible axial dispersion
- Interfacial concentration is negligible assuming low resin loadings

In a fixed bed ion-exchange column, the solute continuity equation ignoring axial dispersion for a certain ion 'i' is

$$\frac{u}{\varepsilon} \frac{\partial C_i}{\partial z} + \frac{\partial C_i}{\partial t} + R \left( \frac{1-\varepsilon}{\varepsilon} \right) \frac{\partial q_i}{\partial t} = 0 \quad (\text{III-1})$$

The first term of Equation III-1 represents the convective transport of ions axially, the second term accounts for accumulation in the fluid phase, and the third term accounts for accumulation in the solid phase. R is the volumetric fraction of cation or anion resin in the bed. For a shallow bed column, accumulation in the fluid phase can be neglected because of the short residence time and high flow rates through the column. Hence, the material balance (Equation III-1) for a shallow bed column is

$$\frac{u}{\varepsilon} \frac{\partial C_i}{\partial z} + R \left( \frac{1 - \varepsilon}{\varepsilon} \right) \frac{\partial q_i}{\partial t} = 0 \quad (\text{III-2})$$

The rate law (assuming initial breakthrough controlled by external film resistance), using a Nernst-film model is

$$\frac{\partial q_i}{\partial t} = K_{f,i} a_s (C_i - C_i^*) \quad (\text{III-3})$$

The interfacial concentration,  $C_i^*$  is assumed zero in all calculations (Frisch and Kunin, 1960; Koloini et al., 1977; Rahman and Streat, 1981). This assumption is appropriate for low levels of resin loading observed in kinetic leakage analysis. Using Equation III-3 and the following boundary conditions

$$C_i = C_i^f \text{ at } z=0 \quad (\text{III-4})$$

$$C_i = C_i^{\text{eff}} \text{ at } z=Z$$

Equation III-2 can be integrated to give the following expression for the mass transfer equation for a certain ion 'i'.

$$\ln \left( \frac{C_i^{\text{eff}}}{C_i^f} \right) = - \left( \frac{K_{f,i} Z R a_s (1 - \varepsilon)}{u} \right) \quad (\text{III-5})$$

The specific surface area ( $a_s$ ) for a spherical resin particle is given by  $a_s d_p = 6$ . Writing  $S = a_s (1 - \varepsilon)$  and volumetric flow rate,  $V = Au$  where  $A$  is the area of the bed, the final mass transfer equation for a certain ion, 'i' is (Harries and Ray, 1984)

$$\ln \left( \frac{C_i^{\text{eff}}}{C_i^f} \right) = - \left( \frac{K_{f,i} S Z A R}{V} \right) \quad (\text{III-6})$$

The ionic MTC,  $K_{f,i}$  is calculated using equation III-6 from the outlet concentration ( $C_i^{\text{eff}}$ ) for a given influent concentration ( $C_i^f$ ) with predetermined values of  $V$ ,  $Z$ ,  $A$ ,  $R$  and  $S$ .

## Experimental Procedure

Experiments were performed to study flow and concentration effects on MTC. The procedure is as described by Harries (1986). Table I lists the eight influent concentrations and three flow rates used. The flow rates were chosen to cover the entire spectrum of superficial velocities used in industry. The resins used in this study were the Dowex Monosphere resins 650C-H (cationic) and 550A-OH (anionic). Used monosphere resins were obtained from the Public Service of Oklahoma (PSO) site at Riverside (Tulsa). The used resins in this study for experiments were from the Riverside facility and were sampled from two condensate polishers (CP) in March, 1993.

Data obtained from resins used in Lee's (1994) study from four different sites are used to study particle mass transfer properties. The resin sampling sites and dates of installation and sampling are presented in Table II. Table III shows the physical characteristics of the resins as reported by the manufacturer. The effluent samples were analyzed by a Dionex Series 4500i Ion Chromatographic system. All resins were obtained in the hydrogen or hydroxide form, but were regenerated and rinsed in the laboratory to ensure identical treatment and to maximize their capacities before testing. Regeneration procedures for both, anion and cation exchange resin, are described in Appendix B. All containers were rinsed with deionized water. The effluent samples were analyzed within 2 days by ion chromatography.

All experiments were carried out at room temperature. The test column was one inch in diameter. The mixed bed in the column was made up consisting of a 2:1 cation:

anion resin by volume ratio (40 ml: 20 ml). The mono bed depth was made up with 40 ml by volume of cation or anion resin. The bed depths were measured each run. The 2:1 resin ratio is commonly used in industry, and hence selected for the experiment. The detailed experimental procedure is given in Appendix B.

**TABLE I**

**Experimental Influent Concentrations and Flow Rates**

Influent Concentrations (ppb)	
Cation	Anion
30	46
98	150
200	308
400	616
700	1078
980	1509
2000	3080
3000	4620
Superficial Velocities	
volumetric (ml/min)	linear x 10 <sup>-2</sup> (m/s)
500	1.65
750	2.47
1000	3.29

**TABLE II**

**Source of Used Ion Exchange Resins Tested**

Resin Type		Plant Sampling Information		
Cation	Anion	Name of Plant	Installed	Sampled
650C-H	550A-OH	Riverside No.1	Oct., 1990	Mar., 1993
		Riverside No.2	Mar., 1992	Mar., 1993
		Northeast Station No. 3	Dec., 1991	Apr., 1993
		Northeast Station No. 4	Feb., 1992	Apr., 1993

TABLE III

## Physical Properties of DOWEX Monosphere™ Resin

Parameter	Cation	Anion
Name	Monosphere™ 650C-H	Monosphere™ 550A-OH
Capacity (meq/ml)	1.90 (Na <sup>+</sup> form)	1.1 (Cl <sup>-</sup> form)
Selectivity	1.13 for Na-H	22.0 for Cl-OH
Void fraction	0.33-0.35	0.33-0.35
Diameter (cm)	0.065	0.059
Density (lb/ft <sup>3</sup> )	50.0	40.0
Water retention (%)	46-51	44-50
Diameter (cm)	0.065	0.059
Cross linkage (%)	8	6
Appearance	hard, black, spheres	hard, white, spheres
Particle within ±0.01 cm range of diameter (%)	95 minimum	95 minimum

## Accuracy and Reproducibility

Errors in this experimental study arose from a number of sources, such as the preparation of concentrated salt solutions, the measurement of cation and anion resins, the determination of the bed depth, measurement of volumetric flow rates and in the analysis of effluent concentrations using ion chromatography. The sources of these errors were identified and care was taken to minimize them. The overall error in the data was calculated to be bound between  $\pm 12\%$ . The degree of reproducibility of experimental data was determined by repeating an experimental run and comparing the results. The error analysis on experimental data is described in Appendix D.

## Experimental Results and Discussion

The effluent concentrations obtained using the ion chromatographic equipment are substituted into the mass transfer equation (equation III-6) and the mass transfer coefficients (MTCs) are determined for various influent concentrations and flow rates.

The results of the mass transfer experiments done on monobeds to evaluate the MTCs of sodium and chloride are shown in Figures 1 and 2. The mass transfer coefficients of both ions increase as the flow rate increases, indicating that kinetics are controlled by film diffusion. Film diffusion is inferred to be the rate controlling mechanism because the film thickness decreases as flow rate increases leading to improved kinetics. For film diffusion,  $K_f = \frac{D}{\delta}$  holds where  $D$  is the aqueous diffusion coefficient of the exchanging species. The film thickness boundary layer ( $\delta$ ) is a mathematical concept to provide a simplified method of describing diffusion processes involving liquid flow rate variation on a solid.

The mass transfer coefficient is independent of influent concentrations throughout most of the concentration range studied. At influent concentrations below 200 ppb sodium and 300 ppb chloride, however, the MTCs are affected by influent

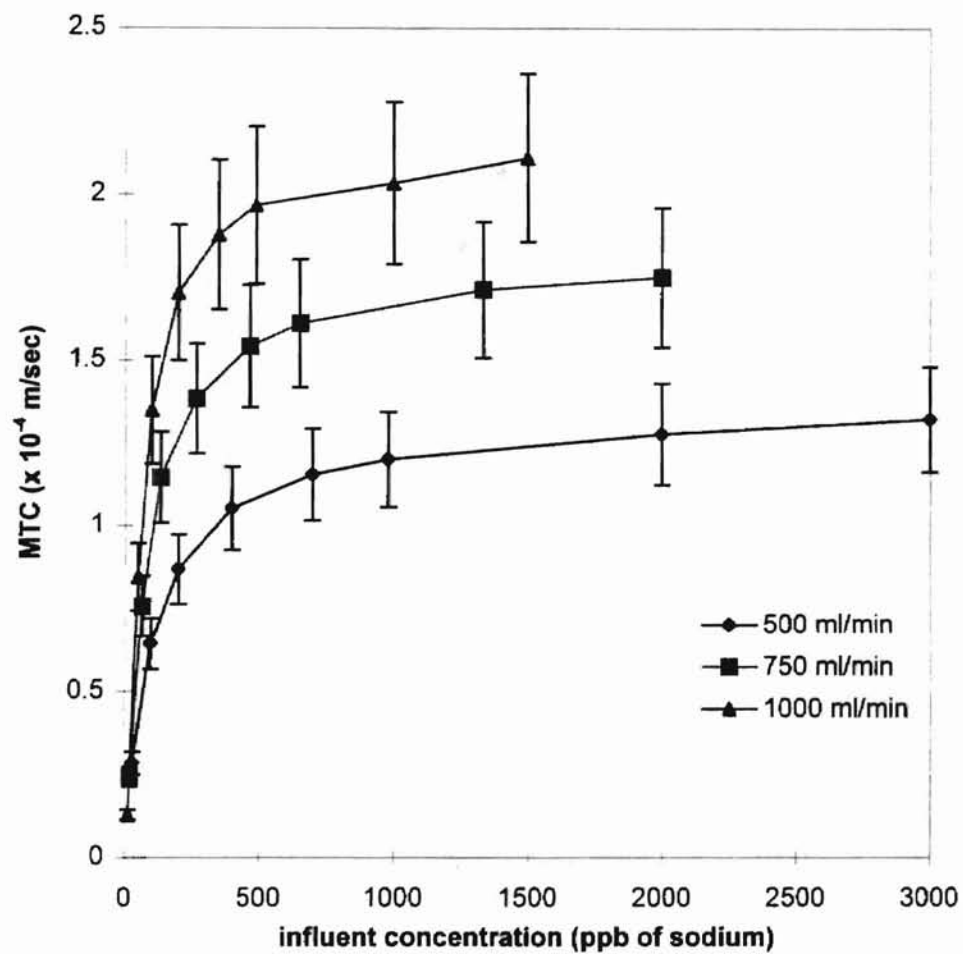


Figure 1. Mass transfer coefficients of sodium for new monosphere resin in a mono bed at different flow rates

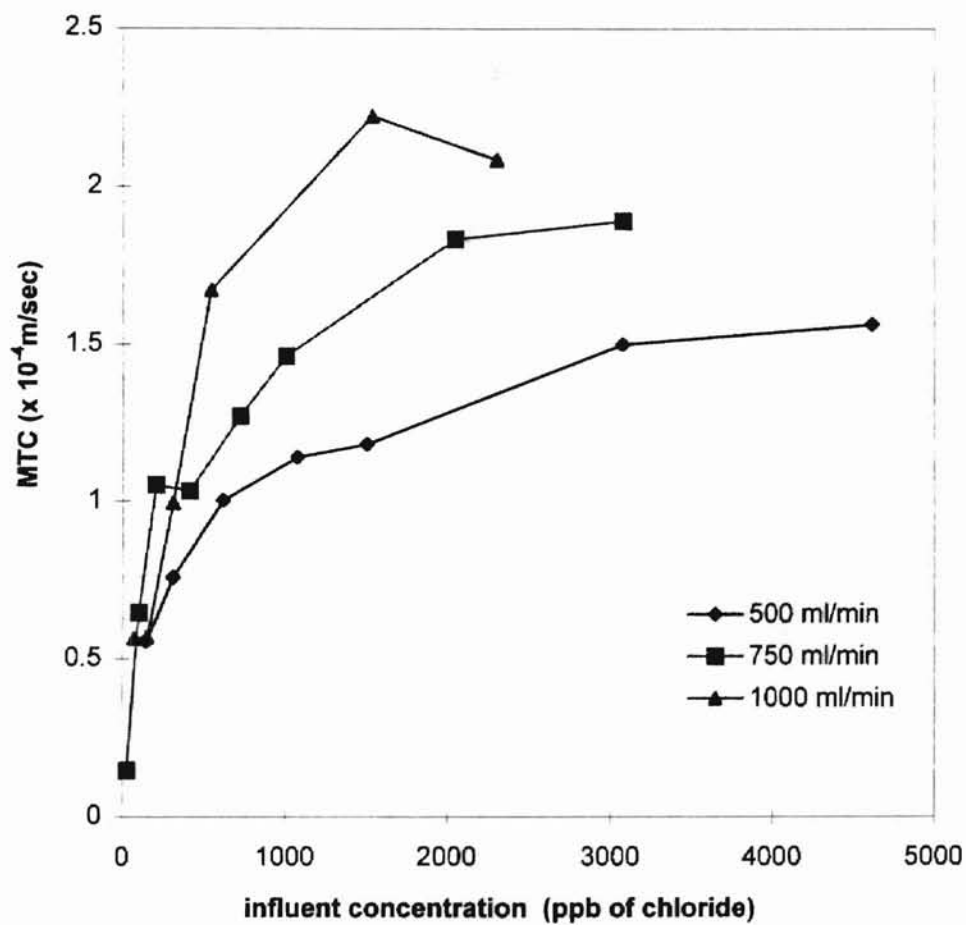


Figure 2. Mass transfer coefficients of chloride for new monosphere resin in a mono bed at different flow rates



concentration. This trend coincides with data from Harries and Ray (1984) that showed chloride and sulfate MTC decreasing as the influent concentration was lowered below 500 and 676 ppb respectively. One possible cause for this apparent dependence on influent concentration at low levels is most probably related to the concentration detection limit. The ion chromatographic system used to evaluate concentrations has a detection level of 0.2 ppb sodium and 0.3 ppb chloride. It is also likely that the MTC is, indeed, a function of influent concentration at the lower concentration range.

Modification of the current equipment along with greater control of the human error involved while carrying out the experiment would result in a better understanding of MTCs in this influent concentration region. A higher MTC does not indicate a smaller ionic leakage. The MTC is used to indicate the rate at which the influent ion reaches the resin surface for mass transfer. At low flow rates, the residence time through the bed is greater than at higher flow rates resulting in lower ionic leakage.

The MTCs for both cationic and anionic resins in monobed experiments were lower than those obtained from mixed-bed experiments (Figures 3 and 4). For an anionic monobed, the  $\text{OH}^-$  concentration increases during exchange, and reaction continues in a more basic solution. In contrast, cationic monobed exchange occurs in a more acidic solution than a mixed bed due to the same phenomenon. The MTCs of anionic exchange are higher in acidic solution, while those for cationic exchange are higher in basic solution. Harries (1991) attributed the lower MTC of a monobed to solution pH. The higher MTCs in mixed beds were explained by Haub and Foutch (1986) by considering neutralization in the bulk phase and liquid film. Since MTC is an overall system parameter, the ionic flux through the film is a complex function of all species present. As

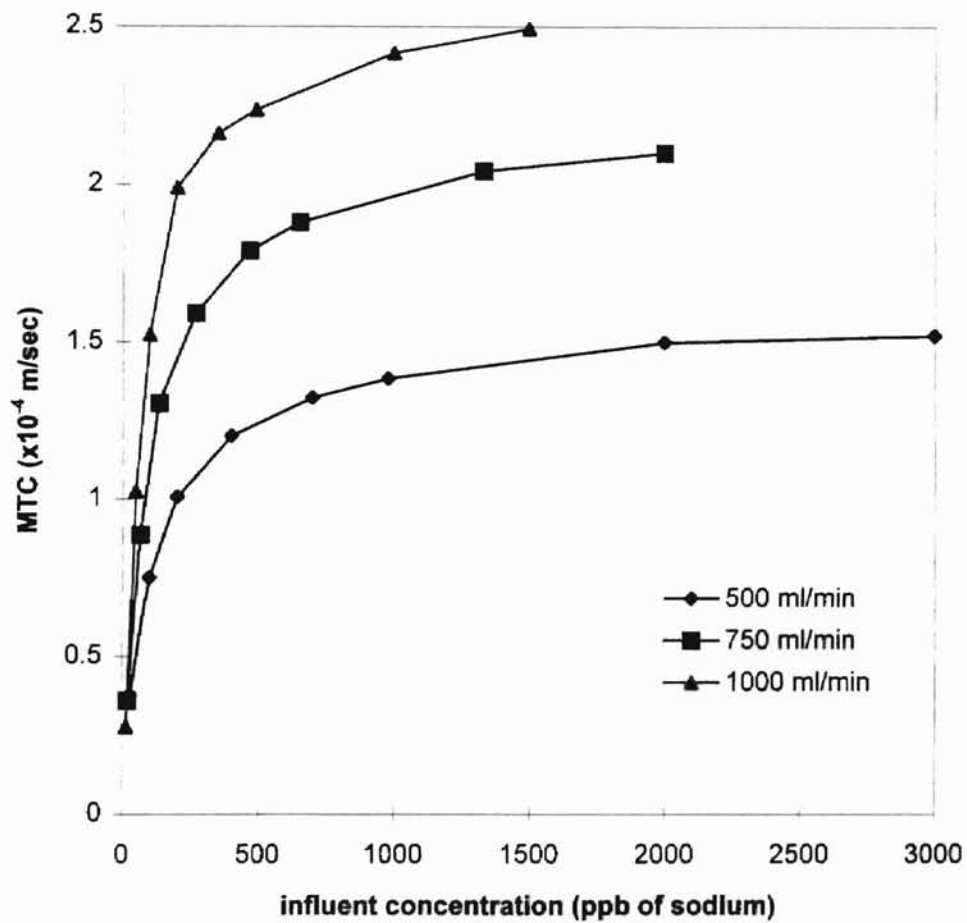


Figure 3. Mass transfer coefficients of sodium for new monosphere resin in a mixed bed at different flow rates

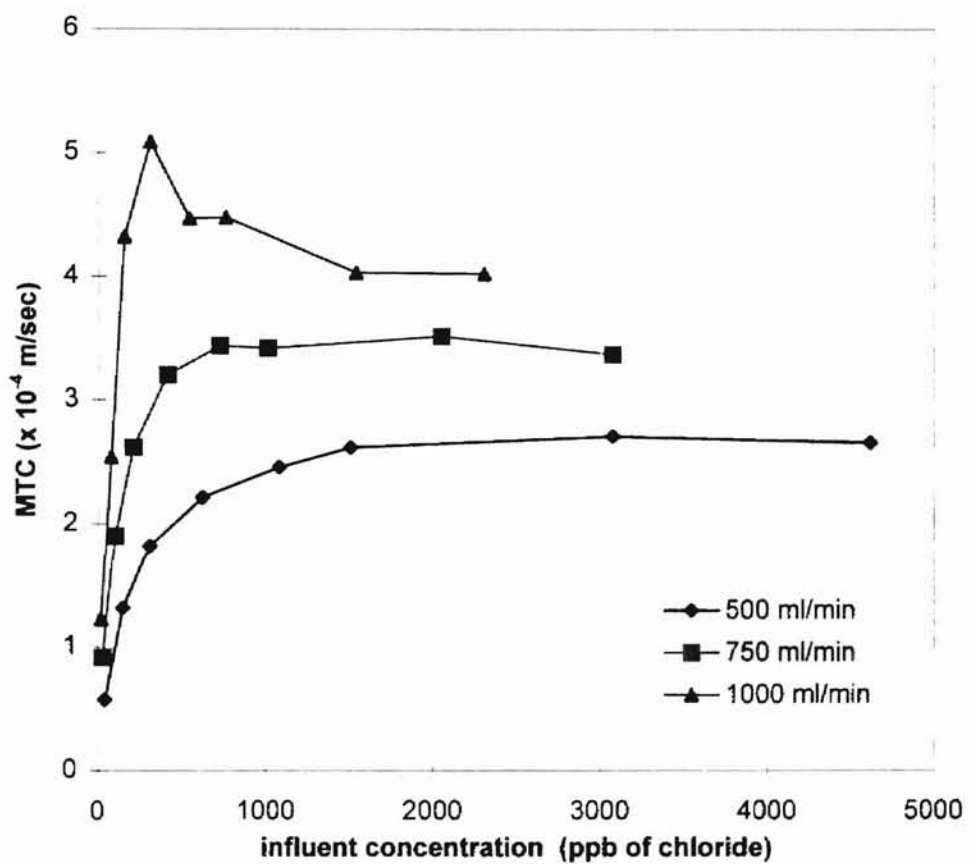
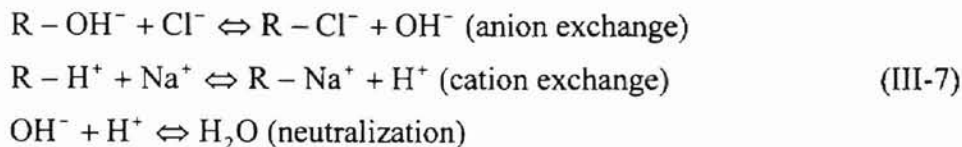


Figure 4. Mass transfer coefficients of chloride for new monosphere resin in a mixed bed at different flow rates

hydrogen and hydroxide ions released by ion exchange resins combine with each other to form water, the flux of other ions through the film is affected. The exchange and neutralization reactions are



Essentially, the hydrogen-hydroxide neutralization reaction works as a sink for removal of these ions in the bulk liquid and maintains the hydrogen and hydroxide concentration gradients around the cationic and anionic beads respectively. This, in turn, affects sodium and chloride diffusion across the respective liquid films because of the electroneutrality constraint.

Figure 5 shows that MTCs of chloride are higher than those of sodium in both mono and mixed beds. This higher MTC is associated with the 2:1 cationic to anionic resin ratio (by volume) which gives an excess cationic exchange capacity. This results in excess hydrogen ions moving the neutralization plane within the film surrounding the anionic resin, thereby increasing the anionic gradient. Also, the chloride-hydroxide resin selectivity is much higher than that for sodium-hydrogen. This results in the film-resin interface equilibrium strongly favoring the anion. The effective driving force for exchange increases by decreasing the film concentration at the resin surface, again increasing the gradient.

Figures 6 through 8 show the MTCs of sodium and chloride for new monosphere resins compared with used resin from the PSO Riverside plant's CP 1 and CP2. The MTCs of sodium and chloride for the used resins are lower than the MTCs of new resins

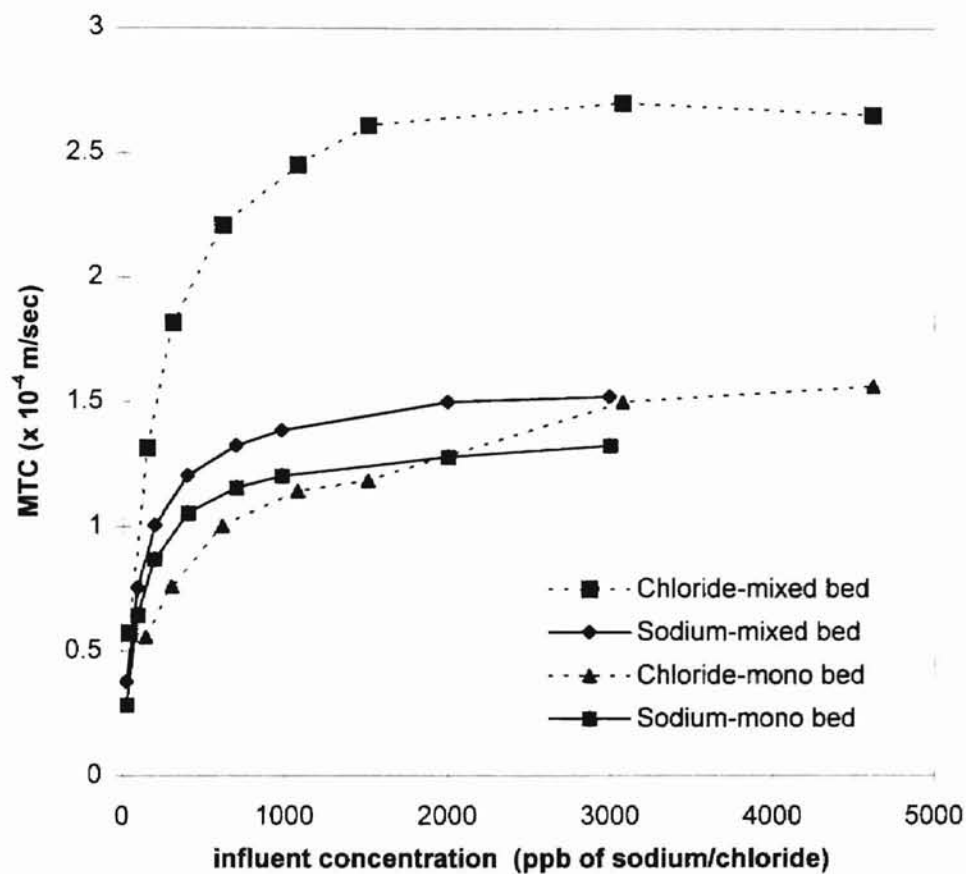


Figure 5. Comparison of mass transfer coefficients of sodium and chloride for new monosphere resin in a mixed bed and in a mono bed at 500 ml/min flow rate

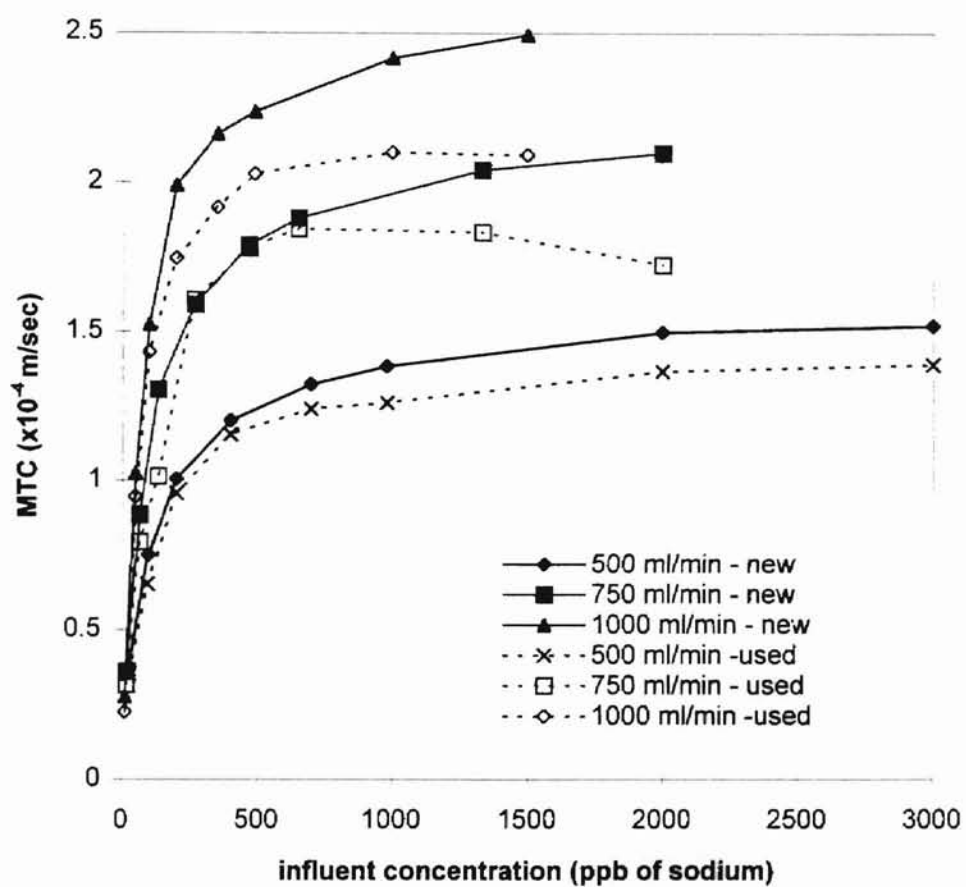


Figure 6. Comparison of mass transfer coefficients of sodium in a mixed bed for new monosphere resin and used resin (RS CP 1) at different flow rates

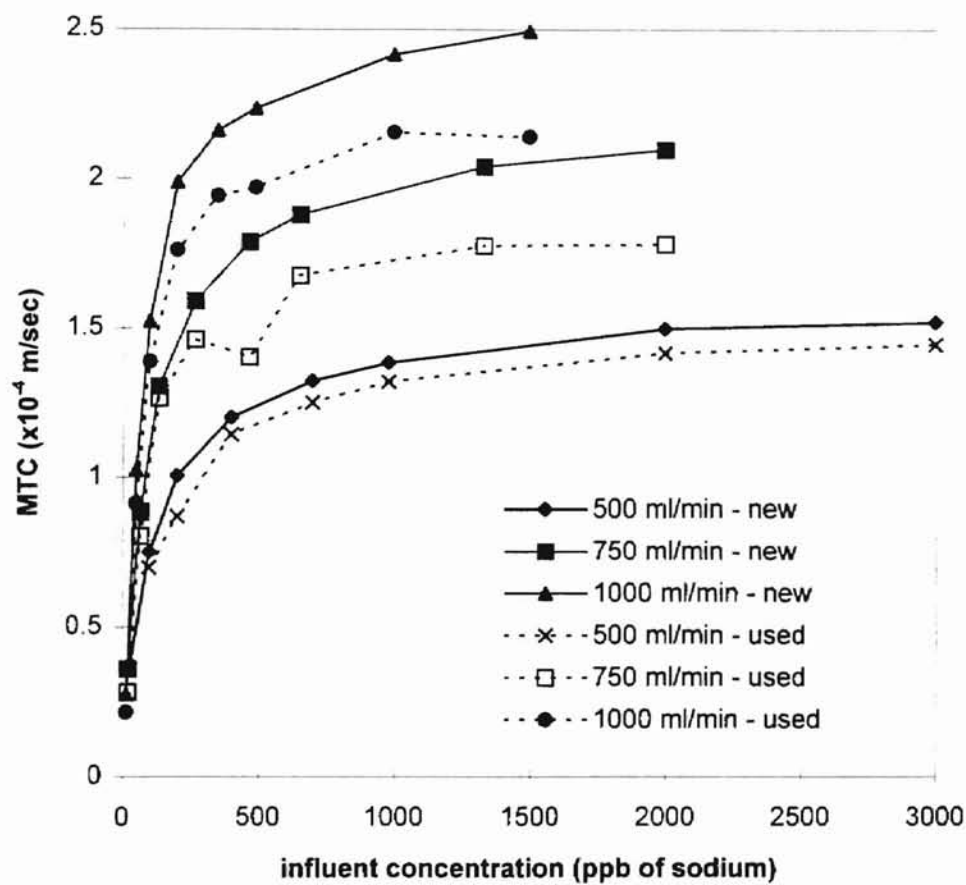


Figure 7. Comparison of mass transfer coefficients of sodium in a mixed bed for new monosphere resin and used resin (RS CP 2) at different flow rates

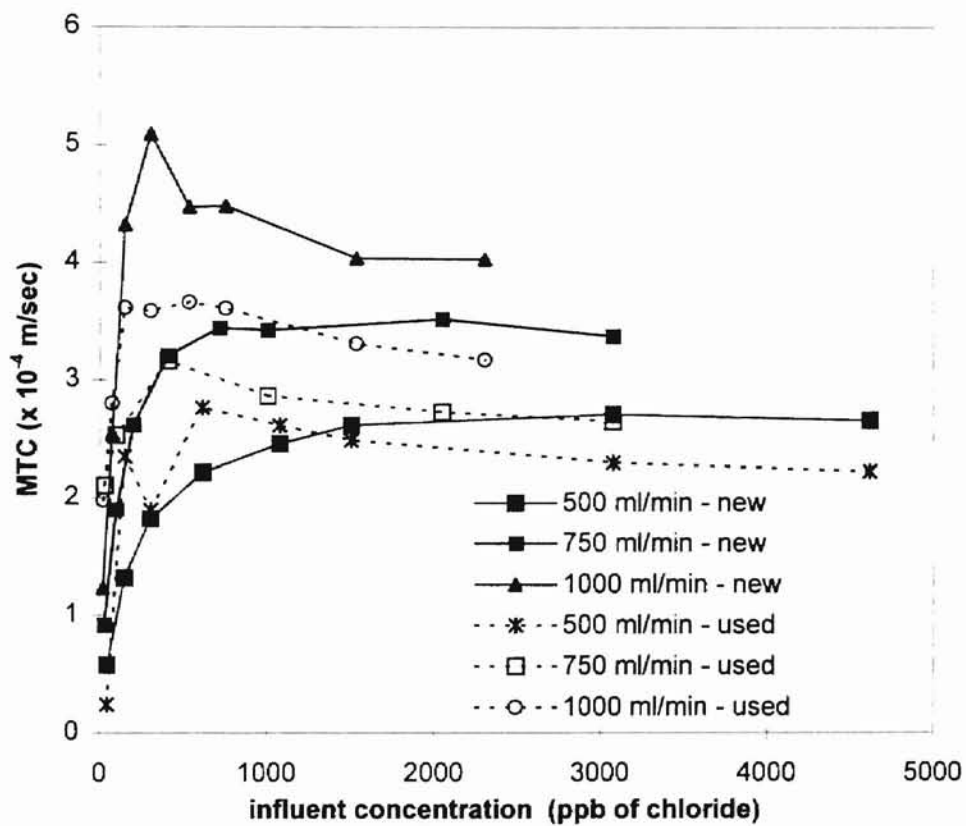


Figure 8. Comparison of mass transfer coefficients of chloride in a mixed bed for new monosphere resin and used resin (RS CP 1) at different flow rates



indicating resin degradation. This is an indication of resin performance in the condensate polishers. The degradation of the used cation resin is only minor when compared with used anion resin degradation. Table IV shows the operating conditions of the plant where the used resins were sampled. This observation of minimal cation resin fouling is typical since cationic resins are inherently stable and resistant to fouling effects. For anionic resins, the MTC decrease of chloride is significant (Figure 8). After only 12 months of use, the MTC decrease is 21 %. The Riverside facility is located downstream of several Tulsa industrial sites and has experienced severe problems associated with turbine blade erosion and corrosion. The excessive anion resin fouling is most likely to have been caused by poor river quality. It is not possible to use this method of kinetic testing of resins to identify reasons for degradation because the overall MTC obtained by this simple experiment is a lumped parameter that includes film, interfacial, and particle effects.

**TABLE IV**

**Operating Conditions of Condensate Polishers at Riverside CPs 1 and 2 and  
Northeast CPs 3 and 4**

Number of Beds per Unit	4
Bed Depth	
Actual, ft (m)	8.24 (2.51)
Resin Packed, ft (m)	4.12 (1.26)
Bed Diameter, ft (m)	6.0 (1.83)
Working Pressure, psig (MPa)	500 (3.45)
Flow Rate per Bed, GPM (m <sup>3</sup> /s)	500 - 1300 (0.032-0.082)
pH of Feed Solution	9.1 - 9.3
Resin	
Cation	Dowex Monosphere™ 650C-H
Anion	Dowex Monosphere™ 550A-OH
Fraction of Cation resin	0.667
Maximum Design Temperature, °F	140
Regeneration Period, days	21

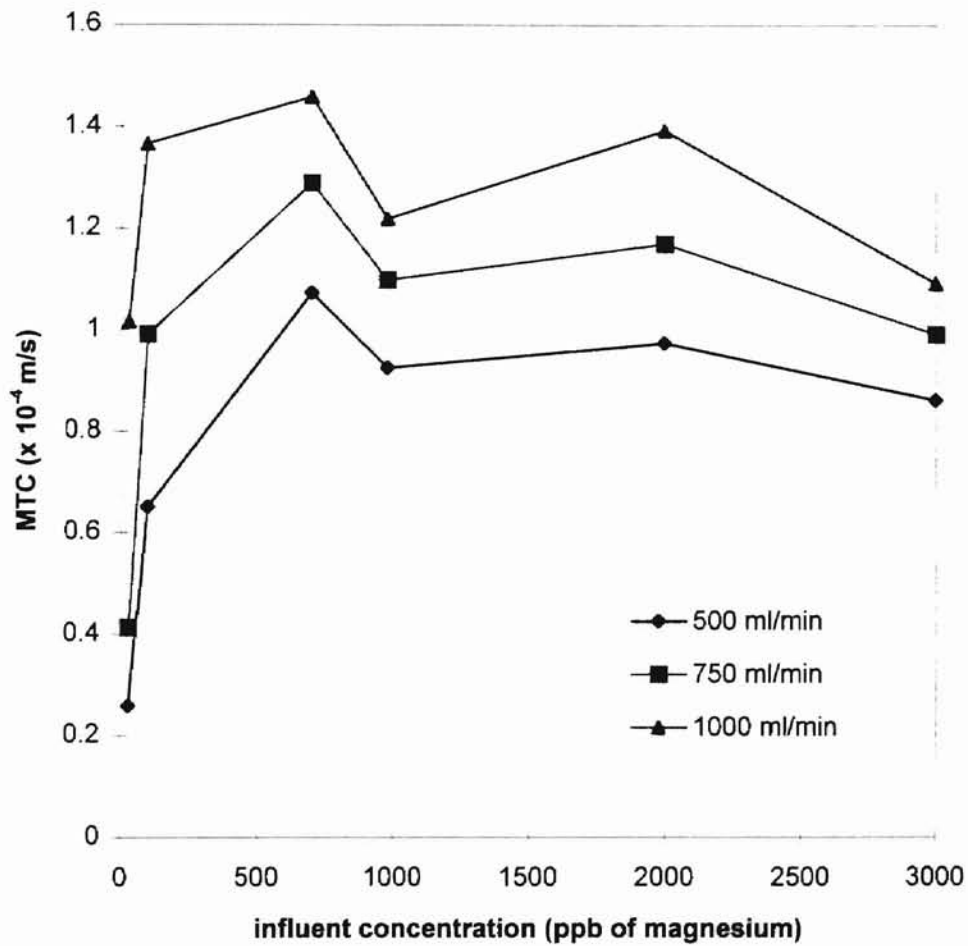


Figure 9. Mass transfer coefficients of magnesium for new monosphere resin in a mono bed at different flow rates

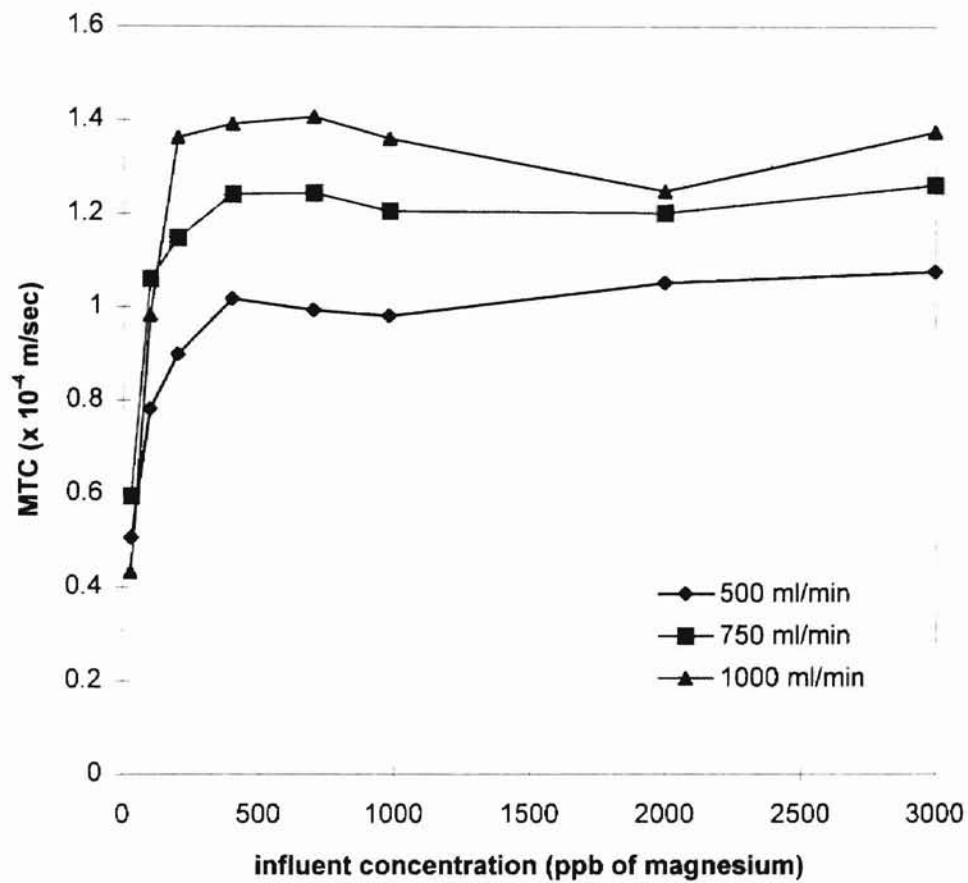


Figure 10. Mass transfer coefficients of magnesium for new monosphere resin in a mixed bed at different flow rates

Figures 9 and 10 show the MTCs of magnesium for new monosphere resin in mono and mixed beds at 500, 750 and 1000 ml/min. The MTCs of magnesium for new resins show the same trends as MTCs of monovalent sodium ions. The kinetics of divalent ion exchange is film diffusion controlled for the case of new resin as proved by the increase in MTC with increasing flow rate. The MTCs in mixed bed are higher than the MTCs in mono bed, confirming the earlier discussion that solution pH affects the value of MTC. The MTCs of magnesium at influent concentrations greater than 200ppb of magnesium and flow rates of 500, 750, and 1000 ml/min are nearly uniform at each flow rate and have average values of  $1.02 \times 10^{-4}$ ,  $1.22 \times 10^{-4}$ , and  $1.35 \times 10^{-4}$  m/s respectively. The MTC of sodium under similar conditions are  $1.38 \times 10^{-4}$ ,  $1.86 \times 10^{-4}$ , and  $2.26 \times 10^{-4}$  m/s respectively. It can be clearly noticed that the MTCs of divalent ions are lower than the MTCs of monovalent ions. This can be explained by the higher diffusion coefficient of sodium as compared to magnesium. In dilute solutions, the ionic diffusion coefficient and equivalent ionic conductance are related through mobility resulting in the Nernst Relation. Nernst's expression for calculating the diffusion coefficient of a single ion is

$$D_i = \left( \frac{RT}{Z_i F^2} \right) \lambda_i \quad (\text{III-8})$$

where  $Z_i$  is the charge on ion and  $\lambda_i$  is the equivalent conductance. Values of equivalent conductance for different ionic species is given in Lange's Handbook of Chemistry (1985). The diffusion coefficients of sodium and magnesium are found to be  $13.34 \times 10^{-6}$  and  $7.064 \times 10^{-6}$   $\text{cm}^2/\text{s}$  respectively that explains the lower MTC of magnesium. Figure 11

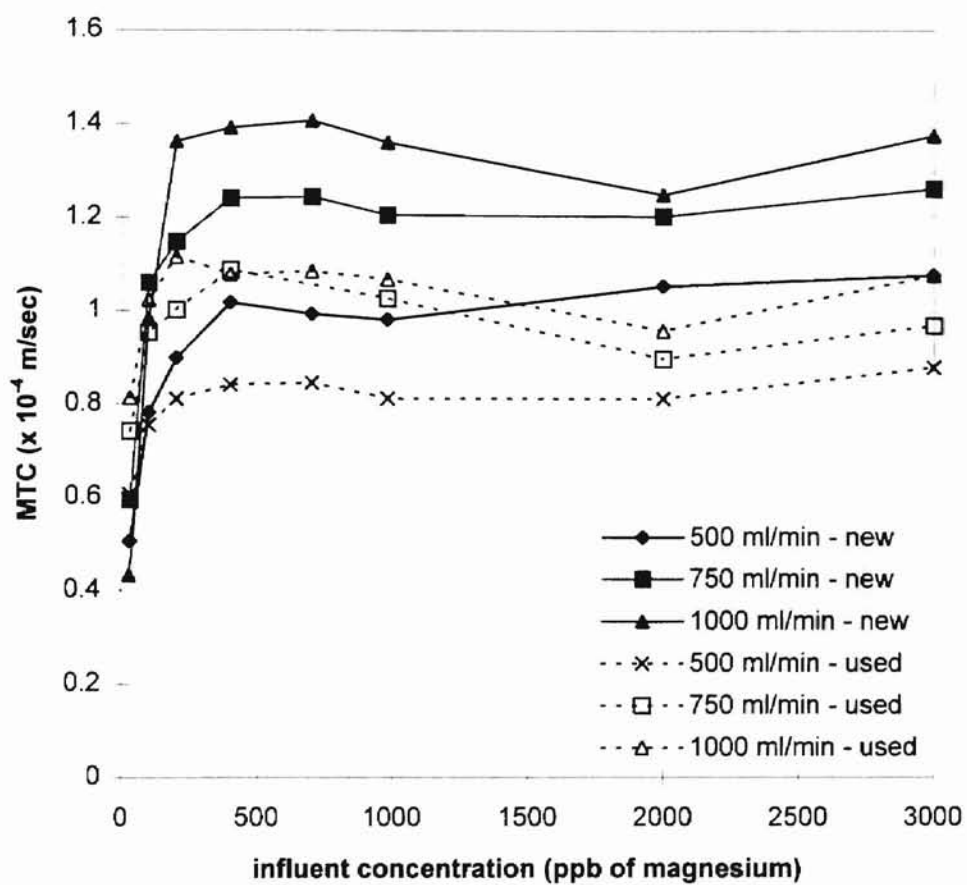


Figure 11. Comparison of mass transfer coefficients of magnesium for new monosphere resin and used resin (RS CP 1) in a mixed bed at different flow rates

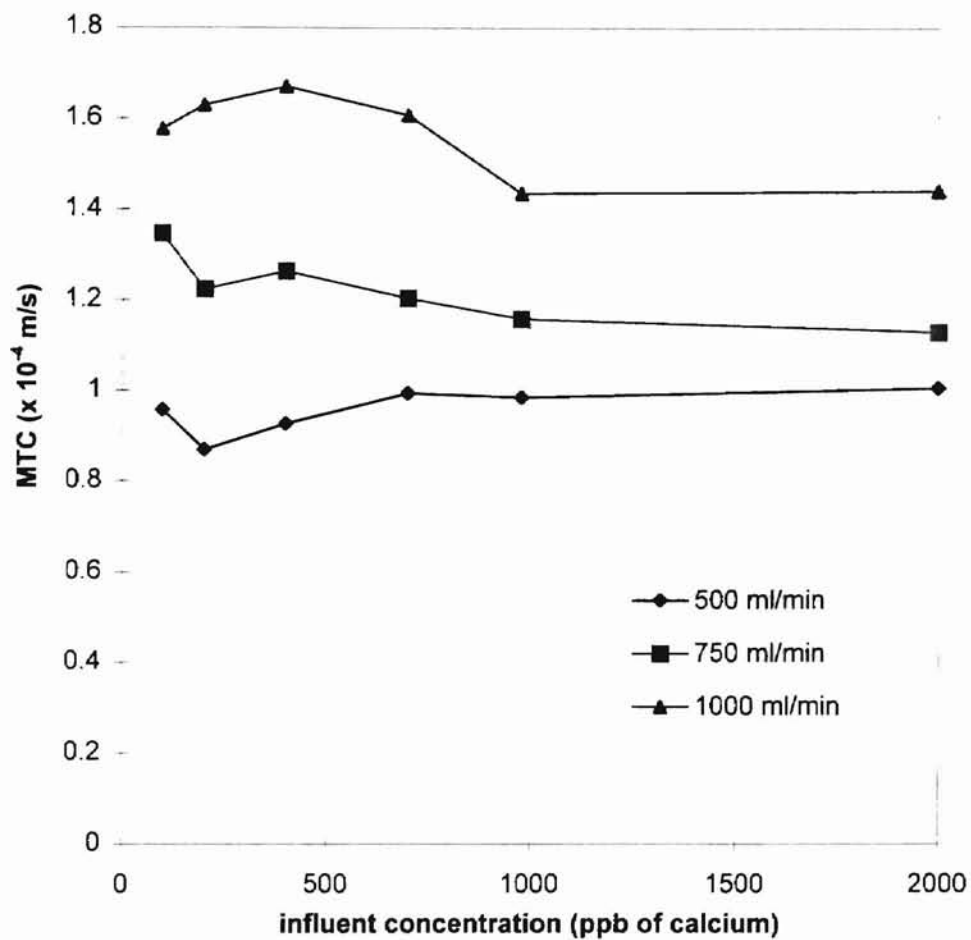


Figure 12. Mass transfer coefficients of calcium for new monosphere resin in a monobed at different flow rates

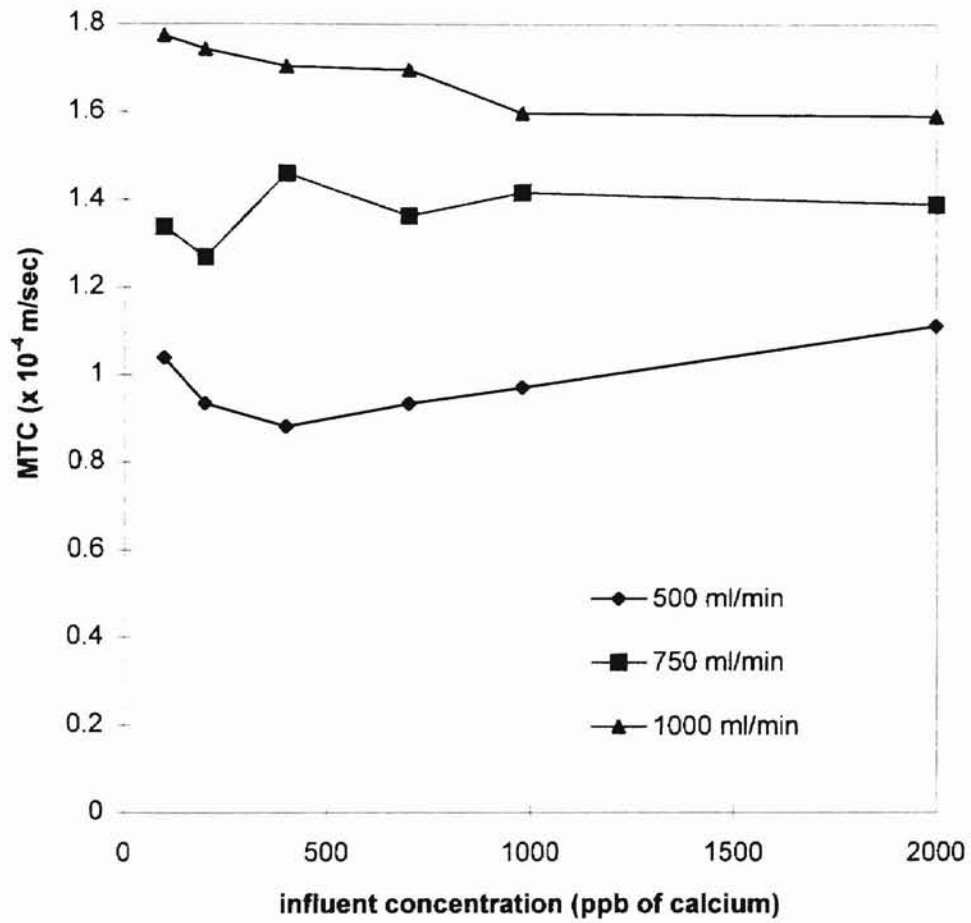


Figure 13. Mass transfer coefficients of calcium for new monosphere resin in a mixed bed at different flow rates

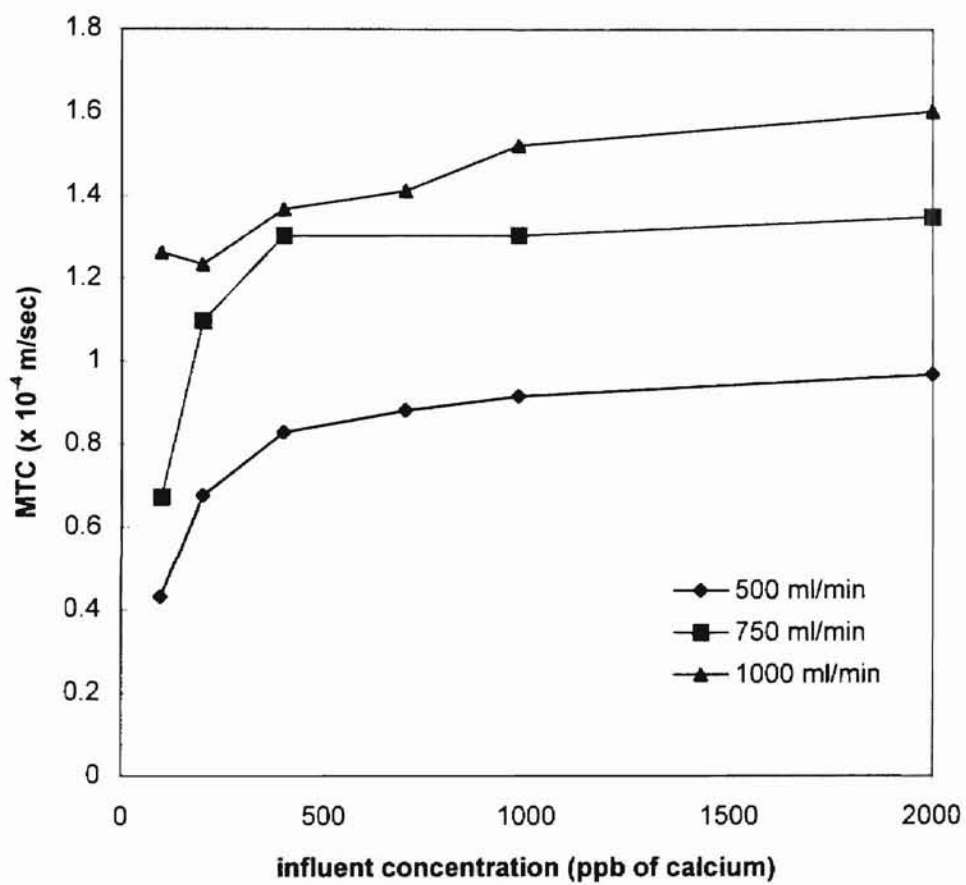


Figure 14. Mass transfer coefficients of calcium for used monosphere resin (RS CP 1) in a mixed bed at different flow rates



shows a comparison of MTC of magnesium for new monosphere resin versus that for used resin from RS CP1. The MTC of magnesium for used resin in a mixed bed is lower than that in a new resin mixed bed indicating the extent of deterioration. Figures 12 through 14 show the MTCs of calcium for new monosphere resin in a monobed, mixed bed, and for used resin in a mixed bed at the Riverside station's condensate polisher 1. The same trends observed in the MTC of magnesium are observed for calcium. The diffusion coefficient of calcium calculated using equation III-8 is  $7.92 \times 10^{-6} \text{ cm}^2/\text{s}$ . Figure 15 is a comparison of MTCs of calcium, magnesium, and sodium at 750 ml/min for new monosphere resin in a mixed bed. One data point on the sodium curve has a lower MTC than the corresponding point on the calcium curve. This is attributed to experimental error. The progressive decrease in MTC values of sodium, calcium, and magnesium indicated in this study is expected because of the differences in their diffusion coefficients.

#### Extraction Of Particle Mass Transfer Properties

The mass transfer coefficient (MTC) evaluated using Equation III-6 is in reality the overall mass transfer coefficient of a single ion. This MTC takes into account film, interfacial, and particle effects. In new ion-exchange resin, the effects of fouling are relatively negligible. The rate controlling mechanism in new resins is predominantly film diffusion control. Interfacial effects can be assumed to be zero for low levels of resin loading observed in kinetic leakage analysis. All resins used in this study were first completely regenerated before being used. Hence, the resin loadings are expected to be

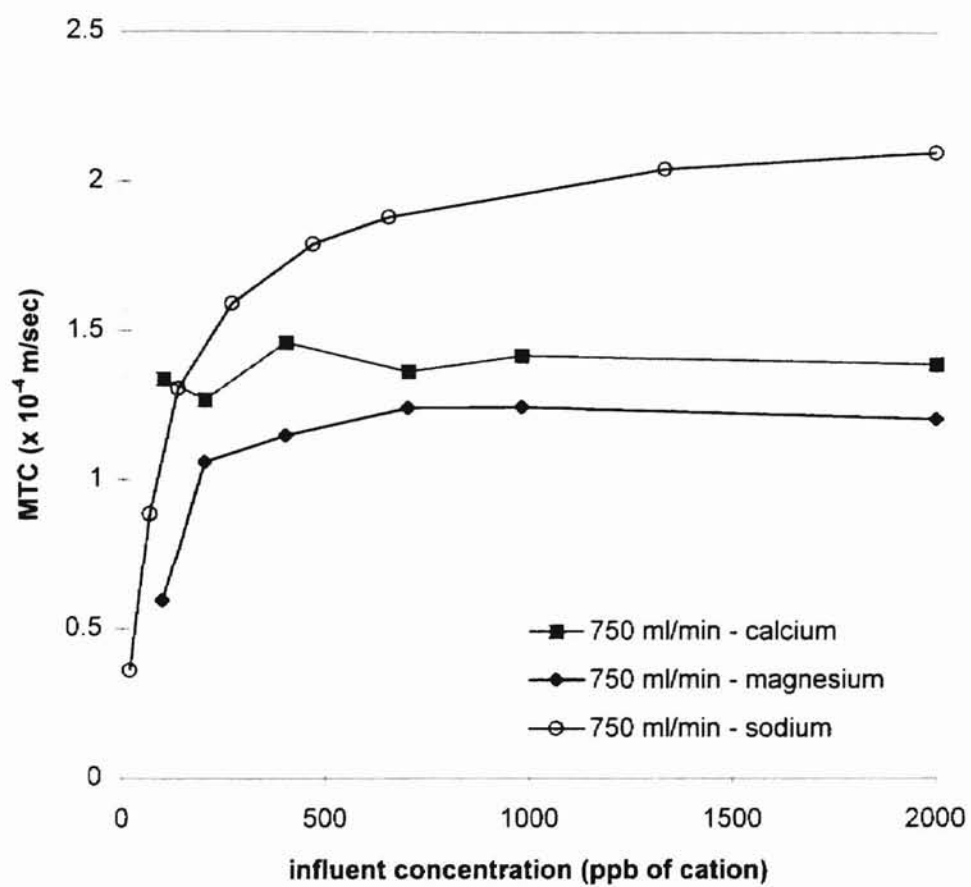


Figure 15. Comparison of mass transfer coefficients of calcium, magnesium, and sodium for new monosphere resin in a mixed bed at 750 ml/min

very low. Lee (1994) calculated the maximum percentage loadings and found them to be 3.4% and 5.8% for sodium and chloride based on total influent ions without ionic leakage at a flow rate of 900 ml/min. Used resin kinetics require both film and particle diffusion mechanisms to describe the exchange process accurately.

Assuming that the solute concentration inside the resin is small compared with that in the bulk solution, the overall exchange rate can be expressed as

$$\frac{\partial q_i}{\partial t} = K_{o,i} a_p C_i \quad (\text{III-9})$$

where  $K_{o,i}$  is the overall mass transfer coefficient. Equation III-9 has the same form as Equation III-3. Hence, Equation III-9 can be rewritten with an overall MTC as

$$\ln \frac{C_i^{\text{eff}}}{C_i^f} = - \left( \frac{K_{o,i} \text{SZAR}}{V} \right) \quad (\text{III-10})$$

The MTC of new resins calculated using the above expression is in reality the film mass transfer coefficient. The overall MTC of used resins is comprised of both, a film mass transfer coefficient and a particle mass transfer coefficient. Evaluation of the particle mass transfer coefficient of anions and cations for different used resins will give a good understanding of the extent of deterioration. Van Deemter et al. (1956) proposed a series resistance model for ion chromatographic columns where the overall mass transfer resistance ( $1/K_o$ ) may be written as the sum of the resistances in the mobile and immobile phase. This series resistance expression is given by

$$\frac{1}{K_o} = \frac{1}{K_f} + \frac{K_{\text{dist}}}{K_p} \quad (\text{III-11})$$

where  $K_{\text{dist}}$  is the distribution factor. The particle MTC,  $K_p$  for used resin may be calculated by rearranging equation III-11 as

$$K_p = \frac{K_{\text{dist}} K_o K_f}{K_f - K_o} \quad (\text{III-12})$$

This particle MTC accounts for resin degradation due to any fouling or deactivation of active sites, but cannot distinguish the mechanisms causing the deterioration of mass transfer kinetics.

Glueckauf and Coates (1947) presented a simple linear driving force model to predict the breakthrough curves of ion chromatographic columns. This model was developed to avoid the complexity of the diffusion solution and used an estimated effective rate constant. A comparison of breakthrough curves calculated from the linear rate model for plug flow and Rosen's solution (Ruthven, 1984) for intraparticle diffusion control shows good agreement with the equivalent rate constant defined as  $15D/R_p^2$ . This was first described by Glueckauf who showed the equivalence between a linear rate model, with  $k=15D/R_p^2$ , and the diffusion model holds for a variety of boundary conditions (Glueckauf, 1955).

Using moments analysis (Ruthven, 1984) for a simple linear rate model with dispersed plug flow and for micropore-macropore diffusion with external film resistance, Ruthven developed the following relationship

$$\frac{1}{K_o K_{\text{dist}}} = \frac{R_p}{3K_f} + \frac{R_p^2}{15\epsilon_p D_p} + \frac{r_c^2}{15K_{\text{dist}} D_c} \quad (\text{III-13})$$

This relationship is an extension of Glueckauf's approximation for systems in which more than one mass transfer resistance is significant. Ignoring the term due to

intraparticle diffusion and combining particle porosity with the measured particle diffusivity, the final form of Equation III-13 is

$$\frac{1}{K_o K_{dist}} = \frac{R_p}{3K_f} + \frac{R_p^2}{15D_p} \quad (\text{III-14})$$

From Equation III-14 the effective particle diffusivity can be estimated. This value of particle diffusivity would account for resin degradation in used resins and can be a valuable tool just like particle mass transfer coefficient to predict the extent of fouling.

### Results And Discussion

In this study, particle mass transfer coefficients and effective particle diffusivities have been obtained for used resin samples from Riverside Station condensate polisher 1, Riverside Station condensate polisher 2, Northeast Station condensate polisher 3, and Northeast Station condensate polisher 4. Since this study did not involve the calculation of overall mass transfer coefficients of sodium and chloride from Riverside Station condensate polisher 2, and Northeast Station condensate polishers 3 and 4, the values of film mass transfer coefficients for new monosphere resin and overall mass transfer coefficients obtained by Lee (1994) in his experimental studies are used here to estimate particle mass transfer properties. Lee's (1994) data has been used because it would be beneficial to observe the effects of particle diffusion control from different plants where operating conditions are different. The problems observed in these plants are different too. Hence, it would be interesting to see if the particle mass transfer properties give insight into the extent of particle diffusion control.

TABLE V

**Average MTCs ( $\times 10^{-4}$  m/s) of New Monosphere Resin (Film MTC), Riverside station CPs 1 And 2, and Northeast Station CPs 3 And 4**

flow rate	MTC of monosphere resin (film)		MTC of used resin Riverside CP1		MTC of used resin Riverside CP2		MTC of used resin Northeast CP3		MTC of used resin Northeast CP4	
	cation	anion	cation	anion	cation	anion	cation	anion	cation	anion
500	1.27	2.03	1.16	1.55	1.23	1.64	1.22	1.96	1.13	2.0
700	1.63	2.53	1.49	1.7	1.47	1.68	1.47	2.25	1.32	2.29
900	1.72	2.65	1.57	1.93	1.58	1.78	1.67	2.47	1.46	2.45

Table V presents the average values of film and overall MTCs for new and used resins respectively from Lee's studies (1994). The arithmetic mean of the MTCs for the influent concentration range greater than 500 ppb for chloride and 324 ppb sodium were used for these estimates. This concentration range was chosen because the MTCs were near uniform. Table VI shows the particle MTCs calculated by equation III-12 with the overall MTCs by equation III-10. For cation resin, particle MTCs are always higher than film MTCs indicating that particle diffusion effects were small relative to film diffusion effects. This observation agrees with Lee's work in which he concluded that fouling effects in cation resin are minimal. The cation resin from Northeast station CP 4 shows slightly lower particle MTCs than the Riverside Station resin indicating the need to consider particle diffusion control in addition to film diffusion control. This is, again, in agreement with Lee's results.

TABLE VI

**Particle Mass Transfer Coefficients Based On Overall Mass Transfer Coefficients  
Estimated By Harries And Ray's Equation (Table V)**

Particle mass transfer coefficient $\times 10^{-4}$ (m/s)								
FR	Riverside No.1		Riverside No.2		NE No.3		NE No.4	
ml/min	cation	anion	cation	anion	cation	anion	cation	anion
500	11.8	0.29	34.5	0.38	27.4	3.6	9.8	9.2
700	15.3	0.23	11.6	0.22	13.2	0.96	6.1	1.1
900	15.9	0.32	17.1	0.24	63.9	2.2	8.5	1.8

NE : Northeast Station

FR : volumetric flow rate

For anion resins from Riverside Station 1 and 2, particle MTCs were lower than film MTCs indicating high resin degradation. Anion resins from NE station CP 3 and 4 have particle MTCs of the same order of magnitude as new anion monosphere resin. This indicates that the rate controlling mechanism in these used anion resins is a function of both film and particle diffusion control. But the particle MTCs of anion resin from NE station is greater than the particle MTCs of anion resin from Riverside station indicating lesser fouling in the Northeast resin. Considering the resin age, the observed influence of particle MTC in both, cation and anion resin from Northeast is minimal. The Northeast Station uses a rural lake as a source of cooling water.

Using Equation III-14, Table VII can be obtained for the data presented in Table V. These data indicate the same trends as those obtained by the other methods. Rixey and King (1989) reported a value of  $D_f$  of  $1 \times 10^{-5}$  cm<sup>2</sup>/s when  $K_f$  is 0.002 cm/s. Hence, a value of  $K_f$  typically an order of magnitude greater than 0.002 cm/s would result in  $D_f$ 's an order of magnitude greater than the reported value too. For a film mass transfer

limited case, effective particle diffusivities are expected to be greater than the film diffusivities.

The values of effective particle diffusivity for cation resin, as shown in Table VII, are of the same order of magnitude as film diffusivity indicating that the cation resin are resistant to fouling effects. The cation resin from Northeast station CP 4 show slightly lower particle diffusivities than the cation resin from other facilities. This is the same observation as done by Lee (1994) and from evaluating particle MTCs. The effective particle diffusivities for all used anion resin samples are an order of magnitude lower than film diffusivity showing significant resin degradation. Thus, for the used anionic resin from both the Riverside and the Northeast facilities particle diffusion does play an important role in the exchange mechanism.

**TABLE VII**

**Effective Particle Diffusivity Based On Linear Driving Force Equation (Film MTCs Based On Harries And Ray's Equation)**

Flow Rate ml/min	Effective Particle Diffusivity, $D_p \times 10^{-4} \text{ cm}^2/\text{s}$							
	Riverside No. 1		Riverside No. 2		NE No. 3		NE No. 4	
	cation	anion	cation	anion	cation	anion	cation	anion
500	3.48	0.0431	4.95	0.0457	4.68	0.0556	3.19	0.0564
700	4.49	0.047	3.92	0.0462	4.19	0.0632	2.68	0.0643
900	4.7	0.0533	4.58	0.049	7.13	0.0701	3.38	0.0692

### Conclusions and Recommendations

1. For new cationic and anionic resins, film diffusion is the predominant rate controlling mechanism.



2. The MTCs of cationic and anionic resin in monobeds are lower than the MTCs in mixed beds which can be attributed to solution pH. The hydrogen and hydroxyl neutralization reaction in a mixed bed serves as a sink for maintaining the hydrogen and hydroxyl concentration gradients around the cation and anion resins respectively. This results in the higher MTCs in mixed beds.
3. The MTCs of cations and anions are apparently dependent on influent concentrations at the low influent concentration range. This dependence could be attributed to the detection limits of the ion chromatographic system. Further analysis on this lower influent concentration range should be done. With greater control on the human errors involved, and by modifying the ion chromatographic equipment to extend the detection limits, the dependence or independence of the MTCs on influent concentration at low influent concentrations can be proved.
4. The increase in MTCs with flow rate would not continue at indefinitely high flow rates due to kinetic slippage at extremely high flow rates. Similarly MTCs may not decrease with flow rate at extremely low flow rates. Work could be done to identify these high and low flow rate regions.
5. The higher MTC of chloride compared to sodium, calcium and magnesium in a mixed bed is due to the higher chloride-hydroxyl selectivity coefficient. The excess cation resin in the mixed bed also serves to enhance the hydroxyl concentration gradient resulting in the higher chloride MTC.
6. The MTCs of used resins are lower than the MTCs of new resins indicating the extent of deterioration in used resin kinetics.

7. Use of the series resistance model along with the linear driving force modification indicate the effect of particle diffusion control. It should be understood that this method of quantifying the deterioration results in a specific mass transfer property. Now, other methods of mass transfer property evaluations can be developed to compare the results obtained using this single parameter experiment.
8. The MTCs of divalent ions, magnesium and calcium are found to be lesser than the MTCs of sodium which is explained by their respective ionic diffusion coefficients.
9. The fouling effects appear to be worse in anion exchange resins agreeing with contemporary understanding of kinetics.
10. Another avenue for further work could be in the analysis of the impurity concentrations at different heights in the mixed bed resin column. The actual profile of impurity concentrations at different slices of the mixed bed could be studied to give a better understanding of kinetics while modeling breakthrough curves of mixed-bed ion-exchange columns.

## CHAPTER IV

### SPECTROSCOPIC ANALYSIS OF USED RESINS

#### Introduction

The Raman effect is a light scattering effect most easily seen as the change in frequency for a small percentage of the intensity in a monochromatic beam as the result of interacting with some material. This change in frequency is the result of coupling between the incident radiation and vibrational energy levels of molecules. Raman scattering is observed as the appearance of a signal at a frequency where this signal did not exist previously or as an increase in an existing signal (Grasselli and Bulkin, 1991). The spectroscopic region of the observed Raman effect depends on the energy of the incident radiation and on the molecular energy levels that are involved in shifting this radiation.

Even without microscopes, Raman spectra can be obtained on very small samples. Single crystals comparable in size to those used for x-ray diffraction, single grains of powder, individual filaments from synthetic or natural polymers, and liquid sample volumes as small as 1 nl can all be readily examined usually without additional sample preparation (Grasselli and Bulkin, 1991). Applications of Raman spectroscopy have been

restricted by one major point - fluorescence. As a phenomenon, fluorescence is approximately  $10^6$  -  $10^8$  times stronger than Raman scattering. Often, when one tries to excite a Raman spectrum, fluorescence is the only phenomenon observed (Grasselli and Bulkin, 1991). Trace impurities, coatings on polymers, additives, etc. may fluoresce so strongly that it is impossible to observe the Raman spectrum of a major component. The use of UV or near infrared excitation has proved to be effective in reducing this problem. It has also been shown that the fluorescent background produced by some samples will decay gradually with time if they are left in the laser beam. Therefore, good practice is to wait sometime before recording the spectrum of a strongly fluorescent material as the background may reduce considerably (Loader, 1970).

A major problem in ion exchange processes is deterioration of the cationic and anionic exchange resins. This deterioration is detected as chloride or sulfate leakage in the case of anion resins and as sodium or ammonium leakage in the case of cation resins. Harries (1991) has tried to establish causes of cation exchange resin fouling using X-ray photoelectron spectroscopy on the surface of the cation resin. He suspected residual oligomers from anion exchange resin to be responsible for fouling the surface and expected these oligomers to be associated with nitrogen - containing active exchange groups. If the oligomers are sufficiently large, some of these exchange groups would not be associated with a cation exchange site on the cation resin surface. Hence, during regeneration of the cation resin with hydrogen chloride, these groups would be converted to the chloride form. The results of his analysis for nitrogen and chlorine were not satisfactory. Chlorine was not found on both, new and used resins. Nitrogen was detected on the surfaces of used resins but was present as N-O grouping instead of the

expected N-C grouping if it were present as an anion exchange group. Noh (1992) analyzed new and used resins using Raman Laser Spectroscopy and reported no significant differences in the constituents of new and used resins.

### Theory

Raman spectroscopy is a powerful tool for the study of inorganic species. The vibrational spectrum provides frequencies, intensities and other band properties that allow identification of species present and even their concentrations to a limited extent. Hence, analysis of resin surfaces using Raman spectroscopy could reveal the presence of any foulants that are responsible for poor resin kinetics.

Spontaneous Raman scattering (Loader, 1970) is generally measured by collecting scattered radiation contained within a solid collection angle that depends on the collection geometry and optics at each frequency of interest,  $\nu$ , and plotting the intensity of the radiation,  $I(\nu)$ , versus  $\nu$ . The measured Raman intensity,  $I(\nu)$  is given by

$$I(\nu) = C (\nu_0 - \nu_i)^4 \nu_i^{-1} B^{-1} S_i \quad (\text{IV-1})$$

where  $C$  is a constant that depends on the instrument response, slitwidth, collection angle, and attenuation due to absorptivity of the sample;  $\nu_0$  is the absolute frequency (in wavenumber units) of the laser excitation line;  $\nu_i$  is the frequency difference of the scattered radiation (i.e. the Raman shift);  $B$  is a temperature factor given by

$$B = 1 - \exp(-h \nu_i c / kT) \quad (\text{IV-2})$$

when the Boltzmann distribution is applied; and  $S_i$  is the intrinsic molar scattering coefficient at frequency  $\nu_i$ . Most of the published spectra of species in solution are presented in this  $I(\nu)$  versus  $\nu$  format.

The objectives of this study are to identify the presence of silica, nitrogen, sodium, chloride and sulfate on the surface of new and used cation and anion exchange resins. Silica is a foulant that could form a physical layer on the surface of the resin, inhibiting penetration of counter ions into the resin. Nitrogen containing active exchange groups on cation exchange resin are suspected to associate with residual oligomers from anion resin, causing kinetic deterioration in cation resin. Anion exchange groups on cation resin and cation exchange groups on anion resin cause sodium, chloride and sulfate to be present as foulants on the surface when cation resin is regenerated with hydrochloric acid or hydrosulfuric acid and when anion resin is regenerated with sodium hydroxide. For purposes of this study, a Laser Raman Spectroscopic apparatus was used. This apparatus is available at the Physics Department of Oklahoma State University. The Professor-in-charge of the Raman Spectroscopic apparatus is Dr. Wicksted and the student who carried out this experiment is Karen Suhm.

### Results And Discussion

The results of the Raman spectroscopic analysis on new and used anion and cation exchange resins are seen in figures 16 to 19. Figure 16 is the result of the surface scan on a new anion monosphere resin bead. The bead was scanned in the frequency range of

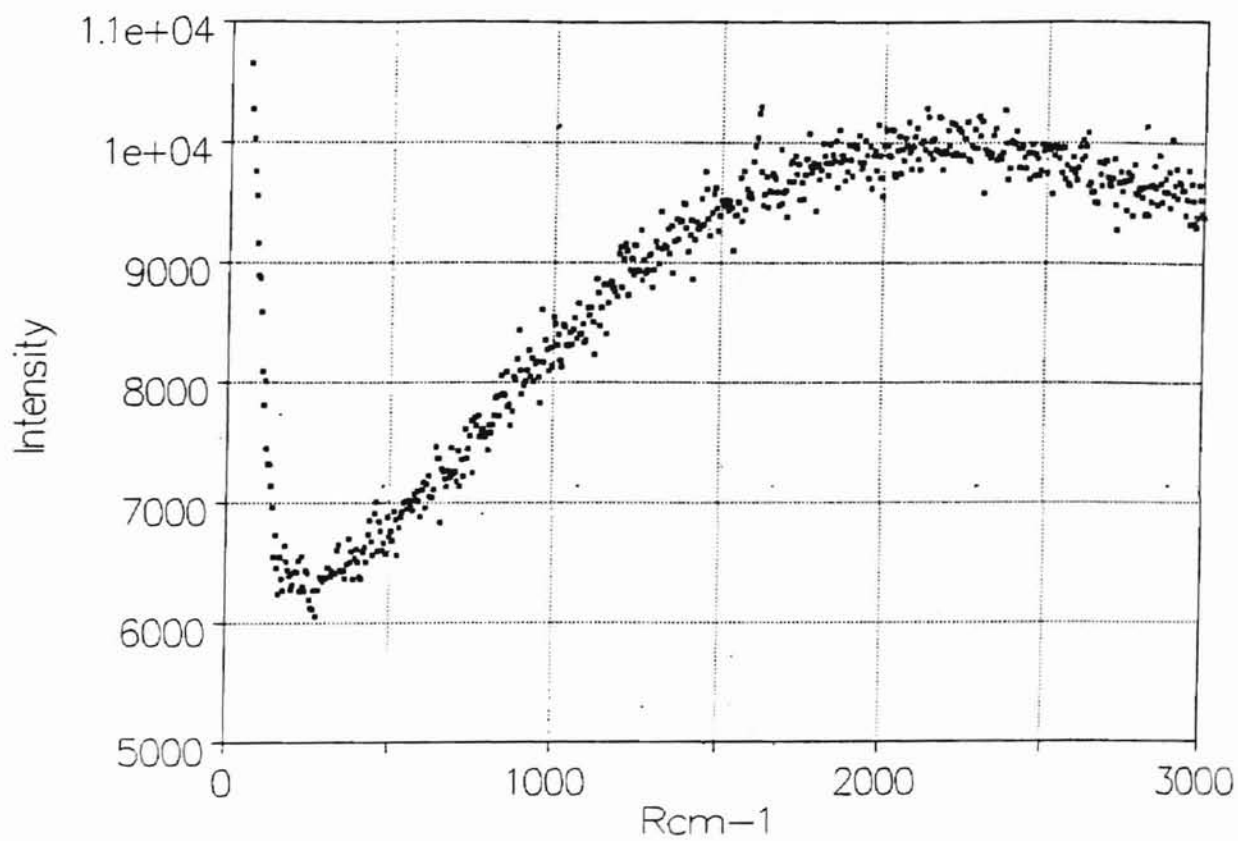


Figure 16. Raman Spectroscopic Analysis of new anion monosphere resin bead (Surface scan at 400 mW intensity laser beam)

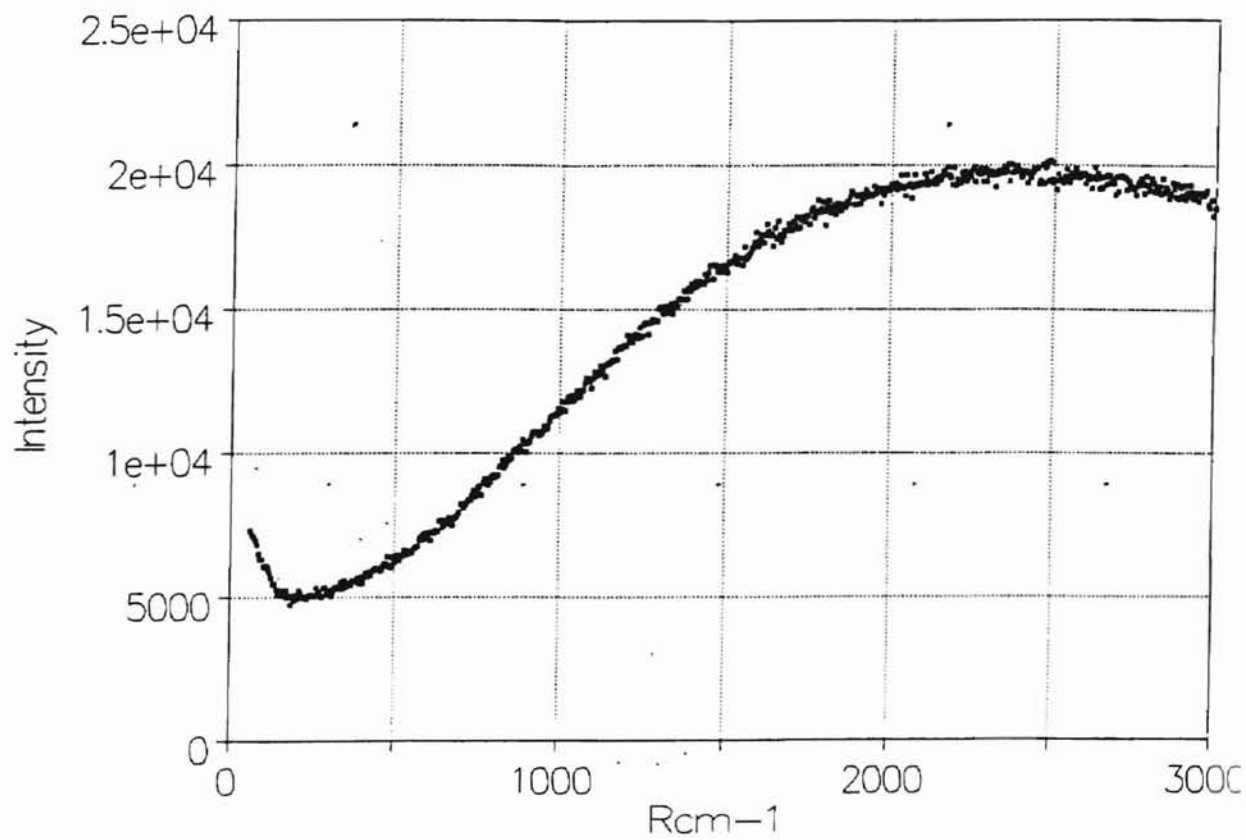


Figure 17. Raman Spectroscopic Analysis of used anion resin from Riverside Station CP2

(Surface scan at 400 mW intensity laser beam)



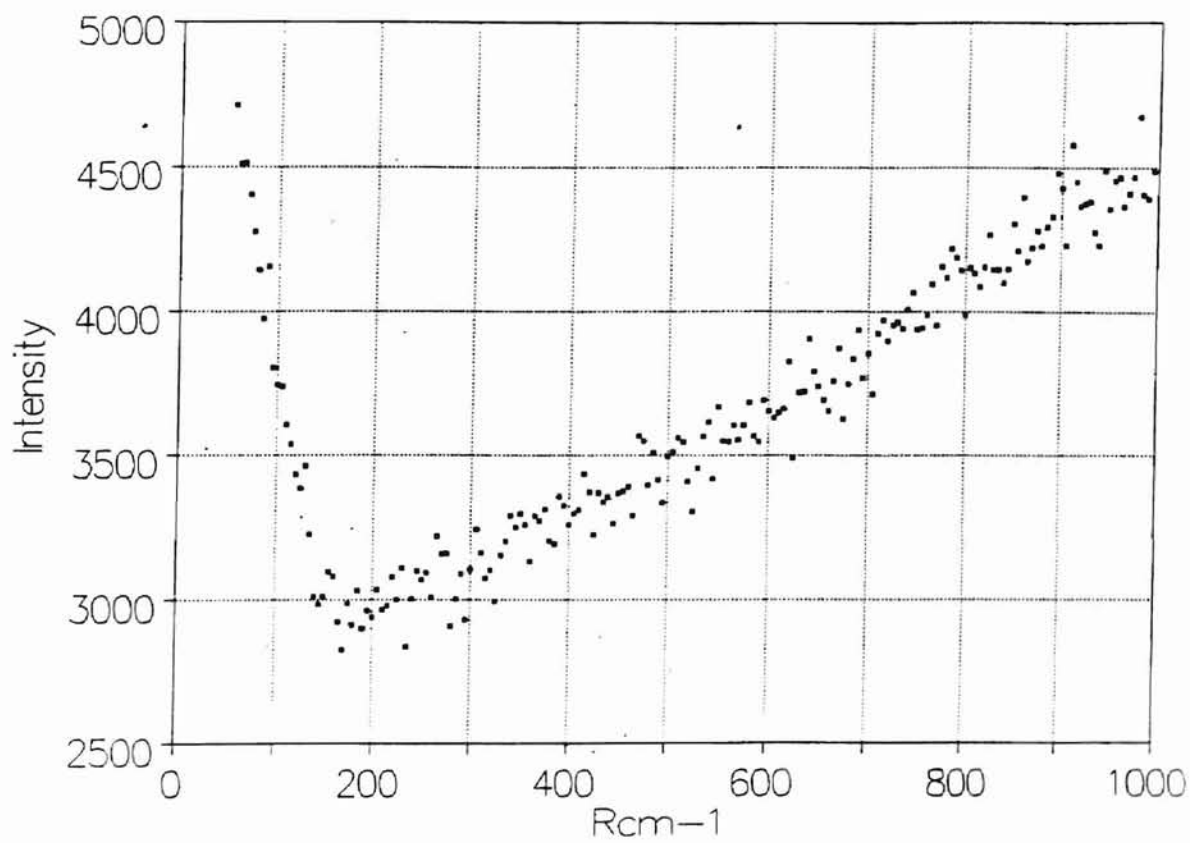


Figure 18. Raman spectroscopic analysis of a second bead of new anion monosphere resin (Surface scan at 200 mW intensity)

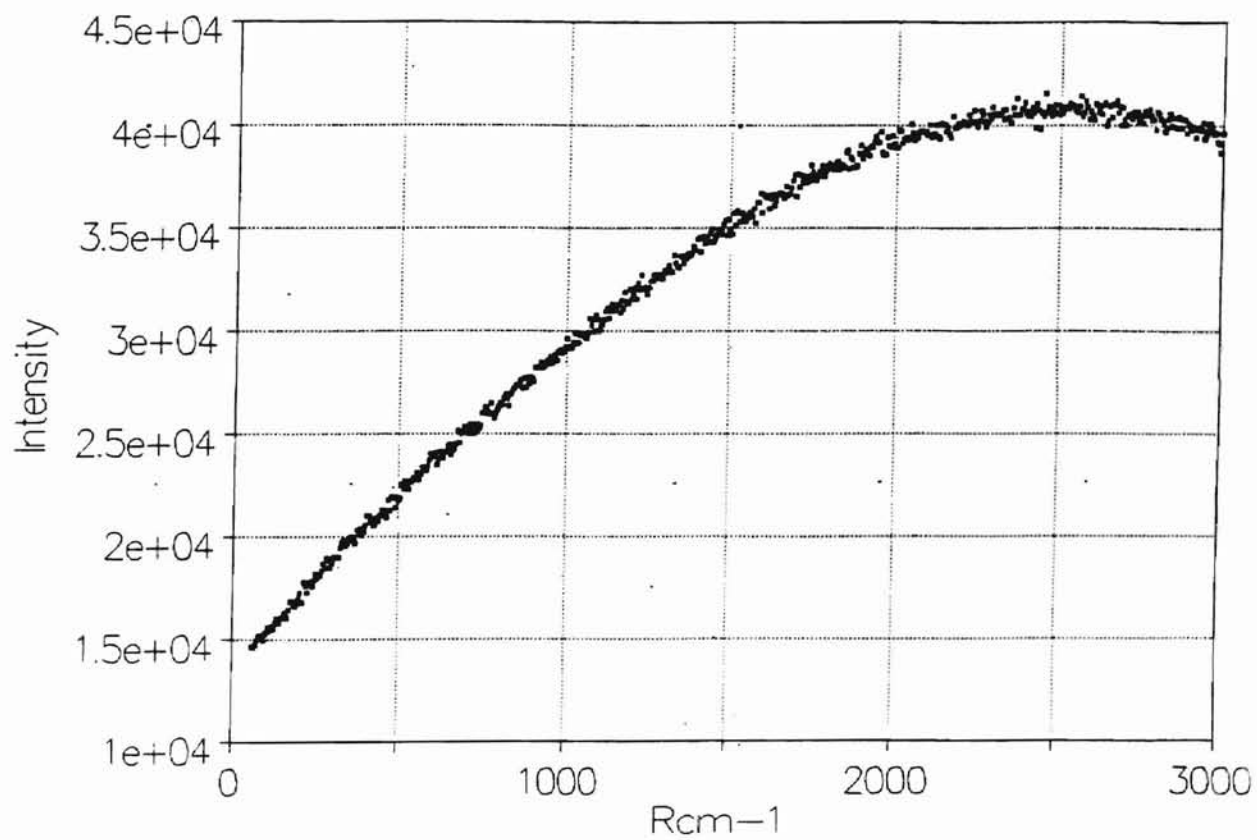


Figure 19. Raman spectroscopic analysis of used anion monosphere resin from Northeast station CP2 (Surface scan at 400 mW intensity)

0-3000  $\text{cm}^{-1}$ . The scan did not reveal any peaks. There was a decrease in the intensity of scattering until around 250  $\text{cm}^{-1}$  after which a fluorescent peak is observed in the remaining frequency range. This peak inhibited the observation of any expected foulants in this sample. The surface scan on used anion monosphere resin from Riverside Station CP 2 (Figure 17) again resulted in a fluorescent peak that drowned out the observation of any other peaks. The same observation was made in scans on a different new monosphere resin (Figure 18) and on used anion resin from NE Station CP 2 (Figure 19). It was noticed in all figures that intensity of scattering was greater in the used resin samples than in the new samples. Attempts were made to study used cation resins, but thermal degradation of the sample prevented any useful observations to be made. Thermal degradation of cation exchange resin was observed even when the intensity of radiation of the laser beam was lowered progressively from 500 mW to 100 mW.

Anion exchange resin withstood thermal degradation better than the cation exchange resin. Fluorescence occurs because the resin absorbs light very strongly and then starts emitting this absorbed light which is observed as the high intensity curve that drastically reduces the sensitivity of the Raman system. To circumvent this problem, the samples were irradiated with the laser beam for fifteen minutes expecting the fluorescent impurity to be 'photobleached'. This is one of the most successful approaches to overcoming fluorescence, but does not help when the sample itself is fluorescent. In our study, the irradiation did not help in improving the observations. From the results obtained, it was also observed that the intensity of scattering in the used resins was higher at all frequencies observed than the new resin samples. This is expected because of the higher trace impurities present in the used resins.

## Conclusions and Recommendations

1. The presence of background fluorescence in all the resin samples inhibited the observation of any trace impurities.
2. Since the peak of the fluorescence usually occurs in the visible region, UV Resonance Raman Techniques and techniques using red or near - IR lasers often can be used to avoid fluorescent interference (Wicksted, 1995). The Raman spectroscopic system available to us for the study did not have this capability and hence, further work could not be done. Further work in identifying the foulants on used resins can be done using spectroscopic methods in the near IR or UV regions. Mass spectrophotometry is another possible method for identifying the foulants present in used resins.
3. The thermal degradation of cation exchange resin under the intense focused laser beam prevented the study of these resins. The standard approach to this problem has been to spin the sample rapidly, allowing the thermal energy to dissipate for any given part of the sample between exposures (Eng et al., 1985). In severe cases, dilution with a thermal conductive matrix can help (Nimmo et al., 1985). It may be difficult to analyze used cation resins using spectroscopic methods because of the heat degradation of the cation resin at the temperatures involved. Mass spectrophotometry may be an ideal technique to overcome this problem.

## BIBLIOGRAPHY

- Anderson, R. E., Bauman, W. C., and Harrington, D. F., Sulphate-Bisulphate equilibrium on anion exchange resins, Ind. Eng. Chem., **1955**, 47, 1620-1623.
- Bates, J. C., and Johnson, T. D., The Development of a Computer Model, AMM LEAK, for Sodium Leakage from  $\text{NH}_4^+/\text{OH}^-$  form mixed beds, Ion Exchange Technology, Editors Naden, D., and Streat, M., Ellis Horwood Limited, **1984**.
- Bolden, W. B., White, T., and Groves, F. R. Jr., Continuous Fixed Bed Ligand Exchange: The Shrinking-Core Model, AIChE J., **1989**, 35(5), 849-852.
- Boyd, G. E., Schubert, J., and Adamson, A. W., The Exchange Adsorption of Ions from Aqueous Solutions by Organic Zeolites. I. Ion-Exchange Equilibria, J. Am. Chem. Soc., **1947**, 69, 2818-2829.
- Boyd, G.E., Adamson, A. W., and Myers, L. W., The Exchange Adsorption of Ions from Aqueous Solutions by Organic Zeolites. II. Kinetics, J. Am. Chem. Soc., **1947**, 69, 2836-2859.
- Carberry, J. J., A Boundary-Layer Model of Fluid-Particle Mass Transfer in Fixed Beds, AIChE J., **1960**, 6(3), 460-463.
- Emmett, J. R., Condensate Polishing: Ammonia Cycle Operation, Effl. and Water Treat. J., **1983**, 23, 507-510.
- Emmett, J. R., and Hebbs, A., Factors Affecting the Performance of Condensate Polishing Plant, "44th Annual Meeting", International Water Conference, Pittsburgh, PA, **1983**.
- Eng J., Czenuszewicz, R., Spiro, T., "Name of Article", J. Raman Spectroscopy, 16(6), 432, **1985**.
- Foutch, G. L. and Chowdiah, V., Resin Degradation Effects in Mixed-Bed Ion Exchange, Ultrapure Water, **1992**, 9(2), 29-32.
- Frisch, N. W. and Kunin, R., Kinetics of Mixed-Bed Deionization: I, AIChE J., **1960**, 6(4), 640-647.

OKT. AHOMA STATE UNIVERSITY

- Glueckauf, E., and Coates, J. I., Theory of Chromatography. IV. The Influence of Incomplete Equilibrium on the Front Boundary of Chromatograms and on the Effectiveness of Separation, J. Chem. Soc., **1947**, 1315.
- Glueckauf, E., Formulae for Diffusion into Spheres and their Application to Chromatography, Trans. Faraday Soc., **1955**, 15, 1540-1551.
- Gopala Rao, M. and Gupta, A. K., Ion Exchange Processes Accompanied by Ionic Reactions, Chem. Engr. J., **1982**, 24, 181-190.
- Goto, S., Goto, M., and Teshimo, H., Simplified evaluations of mass transfer resistances from batch-wise adsorption and Ion-exchange data. 1. Linear Isotherms", Ind. Eng. Chem. Fund., **1981**, 20(4), 368-371.
- Goto, S., Goto, M., and Teshimo, H., Simplified evaluations of mass transfer resistances from batch-wise adsorption and Ion-exchange data. 2. Nonlinear Isotherms, Ind. Eng. Chem. Fund., **1981**, 20(4), 371-375.
- Grasselli, J. G., and Bulkin, B., Analytical Raman Spectroscopy, John Wiley and Sons, Inc., New York, **1991**.
- Gregor, H.P., General Thermodynamic Theory of Ion Exchange Processes, J. Am. Chem. Soc., **1948**, 70, 1293.
- Gregor, H. P., Gibbs-Donnan Equilibria in Ion Exchange Resin Systems, J. Am. Chem. Soc., **1951**, 73(1), 642-650.
- Griffin, J. W., Causes of Ion Exchange Resin Fouling, Ind. Water Treat., **1991**, 23(6), 30-33.
- Harries, R. R. and Ray, N. J., Acid Sulfate Leakage from Mixed Beds, Effl. and Water Treat. J., **1978**, 18, 487-495.
- Harries, R. R. and Ray, N. J., Anion Exchange in High Flow Rate Mixed Beds, Effl. and Water Treat. J., **1984**, 24(4), 131-139.
- Harries, R. R., Water Purification by Ion Exchange Mixed Bed, Ph.D. Dissertation, Loughborough University of Technology, **1986**.
- Harries, R. R., Ion Exchange Kinetics in Condensate Purification, Chem. and Ind., **1987**, 4, 104-109.
- Harries, R. R., Ion Exchange Kinetics in Ultra Pure Water Systems, J. of Chem. Tech. and Biotech., **1991**, 51, 437-447.

- Haub, C. E. and Foutch, G. L., Mixed-Bed Ion Exchange at Concentrations Approaching the Dissociation of Water. 1. Model Development, Ind. and Engr. Chem. Fund., **1986a**, 25(3), 373-380.
- Haub, C. E. and Foutch, G. L., Mixed-Bed Ion Exchange at Concentrations Approaching the Dissociation of Water. 2. Column Model Application, Ind. and Engr. Chem. Fund., **1986b**, 25(3), 381-385.
- Hills, J. H., An Investigation of the Linear Driving Force Approximation to Diffusion in Spherical Particles, Chem. Engr. Sci., **1986**, 41(11), 2779-2785.
- Huang, T.C. and Li, K.Y., Ion-Exchange Kinetics for calcium radiotracer in a batch system, Ind. Eng. Chem. Fund., **1973**, 12(1), 50-55.
- Kataoka, T. and Yoshida, H., Mass Transfer in Laminar Region Liquid and Packing Material Surface in the Packed Bed, J. Chem. Engr. Jpn., **1972**, 5(2), 132-136.
- Kataoka, T. and Yoshida, H., Breakthrough Curve in Equal Valence Ion Exchange: Liquid Phase Diffusion Control, J. Chem. Engr. Jpn., **1976**, 9(5), 383-387.
- Katchalsky, A., and Lifson, S., The Electrostatic Free Energy of Polyelectrolyte Solutions. I. Randomly Kinked Macromolecules, J. Poly. Sci., **1953**, 11(5), 409-423.
- Kielland, J. J., Thermodynamics of Base-Exchange Equilibria of some Different Kinds of Clays, J. Soc. Chem. Ind., **1935**, 54, 232-234.
- Kressman, T. R. E., and Kitchener, J. A., Cation Exchange with a Synthetic Phenolsulphonate Resin. Part I. Equilibria with Univalent Cations, J. Chem. Soc., **1949**, 1190-1208.
- Lange, N. A., Lange's Handbook of Chemistry, Editor J. A. Dean, McGraw-Hill, New York, **1985**.
- Lee, G. C., The Ionic Mass Transfer Coefficients of cation and anion exchange resins at various flow rates and influent concentrations in single and mixed beds, Ph.D. Dissertation, Oklahoma State University, Stillwater, OK, **1994**.
- Loader, J., Basic Laser Raman Spectroscopy, Hyden & Sons Ltd., **1970**.
- McNulty, J. T., Anion Exchange Resin Kinetics in Mixed Bed Condensate Polishing, Ion Exchange Technology, editors Naden, D., and Streat, M., Ellis Horwood Limited, **1984**.

ART AHUMA SIAIB UHIT 2222

- McNulty, J. T., Eumann, M., Bevan, C. A., and Tan, V. C. T., Anion Exchange Resin Kinetic Testing an Indispensable Diagnostic Tool for Condensate Polisher Troubleshooting, "47th Annual Meeting International Water Conference", Pittsburgh, Pennsylvania, 1986.
- Nimmo, J., Bouill, A., McConnell, A., and Smith, W., J. Raman Spectroscopy, 16(4), 245, 1985.
- Noh, B. I., Effect of Step Changes in Feed Concentration and Incomplete Mixing of Anion and Cation Resins on the Performance of Mixed-Bed Ion Exchange, Ph.D. Dissertation, Oklahoma State University, Stillwater, Oklahoma, 1992.
- Pan, S. H. and David, M. M., Design Effect of Liquid Phase Ionic Migration on a Moving Packed-Bed Ion Exchange Process, AIChE Sym. Ser., 1978, 74(179), 74-82.
- Periyasamy, M. and Ford, W. T., Rates of Exchange of Solvent in and out of Crosslinked Polystyrene Beads, React. Polym. 1985, 3, 351-355.
- Petruzzelli, D., Liberti, L., Boghetich, G., Helfferich, F.G., and Passino, R., Ion exchange kinetics on anion resins. Concentration profiles and Transient Phenomena in the solid phase, React. Poly., 1988, 7, 151-157.
- Pickup, S., Blum, F. D. and Ford, W. T., Self-Diffusion Coefficients of Boc-Amino Acid Anhydrides Under Conditions of Solid Phase Peptide Synthesis, J. Polym. Sci., 1990, 28, 931-934.
- Rahman, K. and Streat, M., Mass Transfer in Liquid Fluidized Beds of Ion Exchange Particles, Chem. Engr. Sci., 1981, 36(2), 293-300.
- Rice, S. A., and Nagasawa, M., Polyelectrolyte solutions, Academic Press Inc., New York, 1961.
- Rixey, W. G. and King, C. J., Fixed-Bed Multisolute Adsorption Characteristics of Nonwet Adsorbents, AIChE J., 1989, 35(1), 69-74.
- Robinson, R. A. and Stokes, R. H., Electrolyte Solutions, Butterworths Scientific Publications, London, 1968.
- Rowe, P. N., Particle-To-Liquid Mass Transfer in Fluidized Beds, Chem. Engr. Sci., 1975, 30(1), 7-9.
- Ruthven, D. M., Principles of Adsorption and Adsorption Processes, John Wiley and Sons, 1984.

OKT AHUMA DIALE UIN 12345



- Spalding D. B., The Prediction of Mass Transfer Rates when equilibrium does not prevail at the phase interface, Int. J. Heat Mass Trans., **1961**, 2, 283-313.
- Tittle, K., Mixed-Bed Performance in a Condensate Polishing Plant, Proceed. of the Am. Power Conf., **1981**, 43, 1126-1130.
- Turse, R., and Rieman III, W., Kinetics of Ion Exchange in a Chelating Resin, J. Phys. Chem., **1961**, 65(2), 1821-1824.
- Van Deemter, J. J., Zuiderweg, F. J. And Klinberg, A., Longitudinal diffusion and resistance to mass transfer as causes of nonideality in chromatography, Chem. Eng. Sci., **1956**, 5, 271-289.
- Wicksted, J. P., Personal Communication, School of Physics, Oklahoma State University, **1995**.
- Yoon, T. K., The Effect of The Cation to Anion Resin Ratio on Mixed-Bed Ion Exchange Performance at Ultra-Low Concentrations, Ph.D. Dissertation, Oklahoma State University, Stillwater, Oklahoma, **1990**.

APPENDIXES

ART. HUMANA DIALE. URS. 1000

## APPENDIX A

### EXPERIMENTAL SYSTEM

The experimental system was originally set up by King (1991). The system was designed to reduce pressure drop at high flow rates and to reduce contaminants from materials of construction. The Tygon tubing with an inside diameter of  $\frac{1}{4}$  inch used earlier (Yoon, 1990; King, 1991; Noh, 1992) was replaced by polyethylene pipe (Lee, 1994). The reason for doing this was that the Tygon tubing was not appropriate for high flow rate experiments, and produced leakage problems around line connectors and high back pressure to a feed pump (Lee, 1994). The pipe used in this system has a larger diameter, so the effects of the pressure drop are reduced.

The deionized water, stored in a carboy, can be contaminated by foulants in the carboy itself and by air. Pure water to make feed solutions of a particular ionic concentration was supplied directly into the system on-line through a big mixed bed. The water used by this mixed bed, previously, was deionized using a deionizing cartridge. Due to space constraints, this system was modified and a second column for makeup water was constructed and placed next to the mixed bed. Hence, distilled water was first passed through this mixed bed column to deionize it further. This deionized water was

AKI AHUMASIAIE UMI

then used in the experimental setup where it was passed through another mixed bed column after which it was mixed with an impurity of a particular concentration.

The main system used in this study is composed of an experimental column, resistivity meters, feeding and dosing pumps, and an ion chromatographic system to measure effluent concentrations from the test column. Figure 20 shows the flow diagram of the main system. Thus, distilled water is first passed through a mixed bed column to deionize it. This once-deionized water is then circulated continuously as in Figure 20 without dosing concentrated solution until the resistivity (RS1 in Figure 20) of the water became 17.8 M $\Omega$ -cm. Theoretically, resistivity of deionized water is 18.3 M $\Omega$ -cm. The observed resistivity in RS2 was 18.3 M $\Omega$ -cm after deionization through the circulation routine in Figure 20. Therefore, the lower resistivity in RS1 was assumed to occur due to air bubbles or eddies inside the Pyrex resistivity sensor holder. To ensure absence of ions in the water, the water from the circulation routine was analyzed by ion chromatography before every experiment. There were no ions (no peaks) detected in that water.

The ion chromatographic system was controlled by a personal computer connected with an interface using Dionex software already installed. The ion chromatographic system and the analysis of effluent samples are described in Appendix C.

### Test Column

The test column used in this study was made by the Materials Laboratory at Oklahoma State University. The column was built of Pyrex glass. Pyrex was used as the material of construction because it is transparent and, hence, the flow distribution and the resin bed condition inside the column could be checked. The resin supporter was a sponge. The size of the column was one inch inside diameter  $\times$  18 inch length  $\times$  0.13 inch wall thickness (2.54 cm  $\times$  46 cm  $\times$  0.32 cm). The inlet and outlet diameter of the test column was 0.5 inch.

Before the experimental run was started, deionized water was filled to at least 20 cm above the top level of resin in the test column. This was to ensure uniform distribution of feed solution through the resin bed and to prevent floating of resins in the top portion of the column. Floating separates the mixed resins which is not desirable. Any air bubbles trapped inside the resin bed was removed by tapping the outside column wall.

### Ion Exchange Resin

The resins used in this study were the Dowex resins, Monosphere 650C-H for cation resin, and Monosphere 550A-OH for anion resin. Both resins are made by copolymerization of polystyrene and divinylbenzene. The new resins were provided by the Dow Chemical Company, and the used resins were sampled from two different condensate polishers of Public Service of Oklahoma's plant at Riverside, Tulsa. Table II

shows the plant location, installation, and sampling dates of the used resins. Table III shows the physical properties of the resin.

Before the new and used resins were used, the resins were regenerated using concentrated regenerants. The regeneration step was needed to ensure the  $H^+$  form on cation resins and the  $OH^-$  form on anion resins. The regeneration process is described in detail in Appendix B.

### Accessories

The auxiliary equipment for this experimental study included resistivity meters, pumps, carboys and a personal computer. The ion chromatographic system is explained in detail in Appendix C. Table VIII lists the accessories along with their specifications. The syringe pump, which was used as a dosing pump, made it possible to feed the solution of very low influent concentration. The calibration curves were prepared for the concentration range 33-120 ppb for chloride, 75-600 ppb for sulfate, and 20-198 ppb for sodium, magnesium and calcium. These very low concentration solutions for the calibration were obtained using the syringe pump. The calibration curves for all ions analyzed are described in Appendix C. The pipe and fittings were bought from Orion Corporation, and were made of contaminant resistant polyethylene. The inside diameter was 0.5 inch. The specifications of the auxiliary mixed bed purification column was 3 in. inside diameter  $\times$  48 in. height and 41 in. bed depth. The size of the column in the main experimental system was 3 in. inside diameter  $\times$  42.5 in. height and 29.5 in. bed depth. Monosphere resins were used in both columns.

TABLE VIII

## List Of Equipment

Equipment	Unit	Capacity	Manufacturer
resistivity and temperature probe (RS 1)	1		Signet Sci.
resistivity and temperature probe (RS 2)	1		Thornton Associates, Inc.
resistivity monitor	2		Signet Sci. (RS1) Thornton Associates, Inc. (RS2)
carboy	2	50 liter	
	2	30 liter	Nalge Comp.
sampling bottle	50	110 ml	
piston pump	1	60 liter/hr	Madden Corp.
syringe pump (SAGA Model 341B)	1	min. 0.00011 $\mu$ l/hr max. 20 ml/hr	Orion Research Inc.
syringe		plastipak 10 ml	Becton-Dickinson Corp.

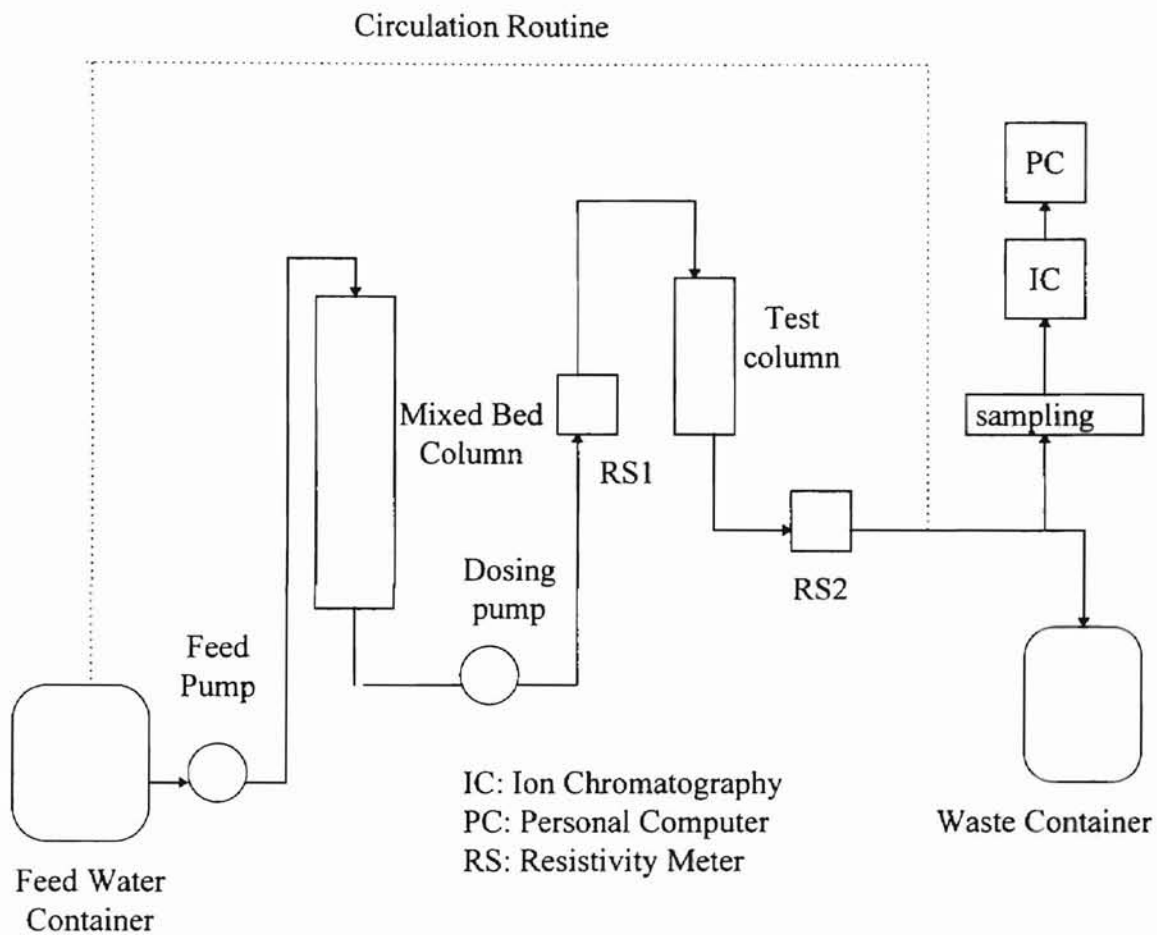


Figure 20: Flow Diagram of Experimental System



## APPENDIX B

### EXPERIMENTAL PROCEDURE

Several operations were performed before the main experiment was carried out - the preparation of deionized water, the preparation of feed solution, the separation of mixed resins and the regeneration of resins. This chapter describes the resin separation, the regeneration process and the experimental procedure of the main experiments. This overall procedure is similar to that used by Harries (1986). Harries' experimental procedure is widely used in industry to carry out kinetic testing of resins

#### Separation of Mixed bed

Used resins samples from PSO were obtained as mixed resin. Therefore, the resins had to be separated prior to regeneration. Separation was done by feeding deionized water upward through a column of the used resin. First, the appropriate amount of mixed resins was loaded into a column of 1.9 inches inside diameter  $\times$  15.7 inches height. Deionized water was fed at the rate of about 150 ml/min to backwash the resins. During this backwash, the anion and cation resin get separated due to the lower density of anion resin. Using a siphon, the anion resin located in the upper portion of the

column is separated. The interfacial region between the anion and the cation resin is discarded to prevent any cross contamination during regeneration. The collected resin is then stored in plastic bottles prior to regeneration.

### Regeneration Procedure

All new and used resins were regenerated to ensure identical treatment, and to eliminate rinse residues that can be present in new resins. All new anion resins were received in hydroxide form, and all new cation resins in hydrogen form. 1N HCl was used as the regenerant for cation resin and 1N NaOH was used for anion resin. The regenerant is dosed through the column at a specific flow rate. After regeneration, the resin is backwashed with deionized water until outlet conductivity from top of the column was lesser than  $5 \mu\text{Scm}^{-1}$ . The resins, whether new or used, were all regenerated in an identical manner. The following is the step-by-step regeneration procedure for cation and anion resins.

#### Cation resin

Step 1: 300 ml cation resin was loaded into the column.

Step 2: The resins were backwashed with deionized water through the column at the rate of 150 ml/min for 5 minutes.

Step 3: 750 ml of 1 M HCl solution was fed into the top of the column at the rate of

85 ml/min. The amount of solution can be varied depending on the amount of loaded resin in the reactor. The regenerant solution is needed in the ratio of 4 liter resin to 10 liter of 1 M HCl solution

Step 4: Deionized water was continuously fed into the bottom of the column at 150 ml/min flow rate until the conductivity of effluent from the column is lesser than  $5 \mu\text{S}\cdot\text{cm}^{-1}$ .

Step 5: The regenerated resins were stored in special contaminant resistant polyethylene bottle with deionized water for future use. The resins were used within one month to avoid contamination.

#### Anion resin

Step 1: 300 ml anion resin was loaded into the column.

Step 2: The resins were backwashed with deionized water through the column at the rate of 150 ml/min for 5 minutes.

Step 3: 0.33 liter of 1 mole of NaOH solution was fed into the top of the column at 85 ml/min flow rate. The amount of regenerant solution was calculated by Harries' procedure. Harries used 1 liter of 1 M NaOH solution per liter resin.

Step 4: Deionized water was continuously fed into the bottom of the column at 150 ml/min flow rate until the conductivity of effluent from the column is lesser than  $5 \mu\text{S}\cdot\text{cm}^{-1}$ .

Step 5: The regenerated resins were stored in special contaminant resistant polyethylene bottle with deionized water for future use. The resins were used within one month to avoid contamination.

## Experimental Procedure

The feed concentrations in this study were very low (Table I), and it is difficult to accurately prepare a solution under 1 ppm concentration. In addition, minimizing water contamination was essential for accurate experimentation. These problems were solved by using a syringe pump and the on-line purification as explained in Appendix A. Before starting an experimental run, a test bed and concentrated feed solution were prepared. Special attention was given to the preparation of the mixed bed, because the densities of cation and anion resins were different, and it is not easy to mix both resins well. The following algorithm describes the experimental procedure in detail.

- Step 1: About 50 liters of deionized water was prepared by passing distilled water through a mixed-bed ion exchange purification column, as in Figure 20.
- Step 2: The deionized water made in Step 1 was continuously circulated until the resistivity in RS1 approached  $18.3 \text{ M}\Omega\text{-cm}$ . The second deionization was also achieved by a mixed bed purification column. During circulation, the test column was removed to prepare the mixed bed. To make sure of water resistivity, the secondary deionized water was injected into the ion chromatography.
- Step 3: During the preparation of make-up water, a mixed bed and a concentrated feed solution were prepared. Resin is mixed generally by inert gas passing upward through a test column. However, the mixed bed in this study was prepared using a measuring spoon in a 100 ml beaker because the amount of resin was small. The volumes of cation and anion resin needed in a mixed bed were 40

and 20 ml, respectively. The resin volume was measured using a 50 ml capacity measuring cylinder, removing the resins from a reservoir by siphon, and pouring into the beaker. Deionized water coexisting with the resins in the beaker was removed by syringe. This was necessary because the resins immersed in water could not be mixed appropriately due to density differences. The resins in the beaker were mixed slowly with a measuring spoon. The degree of mixing could be checked by color, because both resins have different colors. The mixed or single resins were transferred into the test column without extra water, using a measuring spoon. To pack the mixed resin uniformly and tightly in the test bed, deionized water was filled at least 20 cm past the resins and the column was tapped several times until the loaded resins were steady. This procedure was needed to prevent channeling and remove air bubble between resins. The concentrated feed solution was prepared to match eight influent concentrations at each flow rate using the syringe pump.

Step 4: The single or mixed bed prepared in Step 3 was connected in the proper location in Figure 20 during temporary stop of the feed pump.

Step 5: Without dosing the concentrated solution, the test bed was rinsed again by deionized water prepared in Step 2 at the operating flow rates until resistivity in RS2 became 18.3 M $\Omega$ -cm.

Step 6: The flow rate was measured with a 1 liter measuring cylinder between every sampling to make sure that it was steady.

Step 7: The dosing pump was turned on at a certain flow level which corresponds

to the lowest influent concentration.

Step 8: When the resistivity in RS2 was constant, effluent was sampled in a polyethylene bottle . During this operation, the resistivity of water was checked in RS1 continuously to ensure uniform influent concentration. The time needed to get uniform effluent resistivity was measured by a stop watch. At the most, it took 4 minutes to reach uniform resistivity. This was repeated until the samples for seven different influent concentrations were collected.

Step 9: The flow rate from the pump was changed to a higher level and the procedure followed in step 8 was carried out at the new flow rate. Before carrying out the experiment at the new flow rate, the system was shut down and the resin in the test bed was changed to new resin. Step 1 through 8 were then repeated at each different flow rate.

Step 10: The collected samples were analyzed within two days using ion chromatography.

## APPENDIX C

### ION CHROMATOGRAPHIC APPARATUS

The effluent samples from the experimental column were analyzed by a Dionex Series 4500i Ion Chromatographic system (IC). This chapter describes the IC, the preparation of chemicals needed in IC, the operating procedure and the calibration curves for cation and anion concentrations.

#### Components of Ion Chromatography

The Dionex Series 4500i Ion Chromatographic system is designed for dual-system operation to measure cation and anion concentrations simultaneously. The IC consists of an injection pump, a gradient Pump, a conductivity detector, an advanced high-pressure chromatography module, an advanced computer interface and an eluant degas module for cation and anion separately. The gradient pump is used to load eluant solution into a column. It is designed to load up to four different eluant solutions accurately, and to mix them at a programmed flow rate using a microprocessor-based

eluant delivery system. The Conductivity detector can automatically offset background conductivity up to  $1600 \mu\text{Scm}^{-1}$  and is designed to compensate for conductivity variation due to temperature. The advanced high-pressure chromatography module consists of a column and a micromembrane suppresser. The injection pump is used to inject the sample into IC.

The IC is controlled and operated by the Dionex software, AutoIon 450 Data System (AI-450 version 3.2) installed on a 486 computer, through the Advanced Computer Interface. The IC was operated by schedule and method files which were already programmed in the software. The method file controls all systems of the IC for a given operation comprising of a number of runs. The schedule file defines the sequence of method files to be used in one complete operation, and the data files save the results of each run in the operation. The software automatically collects all data and calculates peak areas. The detection level of this IC was 0.2 ppb of sodium and 0.3 ppb of chloride.

#### Preparation of Eluant and Regenerant

The eluant in an IC is used as the carrier of ions through the column. A mixture of 1.8 mM sodium carbonate and 1.7 mM sodium bicarbonate was used as anion eluant, and the mixture of 27 mM hydrochloric acid and 2.25 mM DL-2,3-diaminopropionic acid monohydrochloride as cation eluant for detection of monovalent ions. For divalent cations, a stronger cation eluant consisting of 27 mM hydrochloric acid and 6 mM DL-2,3-diaminopropionic acid monohydrochloride was used. The flow rates of anion and cation eluants were 2.0 and 1.0 ml/min, respectively. Four plastic bottles of 1.5 liter



capacity, two bottles for each ion, were used to store cation and anion eluant solution. The concentrated anion eluant was made by dissolving 9.54 g sodium carbonate and 7.14 g sodium bicarbonate in a 500 ml volumetric flask and making up to 500 ml with deionized water. The anion eluant was prepared by diluting 10 ml of the concentrated eluant to 1 liter with deionized water. The cation eluant for monovalent ions was prepared by diluting a mixture of 25 ml of DAP stock solution and 25 ml of 1 M HCl to 1 liter with deionized water. The DAP stock solution was made by dissolving 0.141 g DAP in 100 ml deionized water. The cation and anion eluants were stored in two bottles with the same concentration eluant, respectively, and fifty percent eluant of needed volume from one bottle was mixed with 50 % eluant from the other bottle through inert solenoid valves. The percentages can be altered depending on eluant concentrations in each bottle. The outlets from the valves were combined in the manifold and fed to the gradient pump through the gradient mixer.

Regenerant is used to regenerate an IC column. 0.05 M sulfuric acid solution was used as anion regenerant and 70 mM tetrabutylammonium hydroxide as cation regenerant. The flow rates were 2.5 and 5.0 ml/min for anion and cation column regeneration respectively. The anion regenerant was prepared by diluting 100 ml of 0.5 N  $\text{H}_2\text{SO}_4$  to 1 liter with deionized water. 0.5 N  $\text{H}_2\text{SO}_4$  was made by diluting 7 ml of 36 N  $\text{H}_2\text{SO}_4$  to 500 ml with deionized water. The cation regenerant was made by diluting 100 ml of TBAOH to 2 liter with deionized water. Two 4 liter plastic bottles were used as reservoirs of cation and anion regenerant. The used cation regenerant was collected, treated by an Auto Regeneration System purchased from Dionex and reused because the price of TBAOH was expensive. The Auto Regeneration System consists of a electric

metering pump of 6 GPD maximum outlet (from PULSAtron), an Auto Regeneration Cation Cartridge and two plastic bottles which are reservoirs for used and treated regenerant. The treated regenerant was poured into the reservoir of cation regenerant. Table xx shows the specifications of chemicals used for regenerant and eluant.

Nitrogen and helium were used to degas eluant bottles and pressurize the eluant and regenerant reservoirs. The degassing procedure was necessary to prevent air bubbles from loading into the Gradient Pump and valves. If bubbles were loaded into the Gradient Module, the Gradient Pump can not work or be operated at optimum condition. This phenomenon happened sometimes, even though the Degas Module was used. This was due to prolonged shut down periods, and the air bubbles had to be removed by a technique obtained from the Dionex operating manual.

**TABLE IX**

**Characteristic Of Chemicals For Regenerant And Eluant**

name	assay	service	manufacturer
DAP*	99 %	cation eluant	Fluka Chemie
hydrochloric acid	36.5 - 38 %	cation eluant	Fisher Sci.
sodium bicarbonate	99 %	anion eluant	Fisher Sci.
sodium carbonate	99 %	anion eluant	Fisher Sci.
sulfuric acid	95 - 98 %	anion regenerant	Fisher Sci.
TBAOH*	55% aqueous solution	cation regenerant	Southwestern Analytical Chemicals Inc.

\* DAP : DL-2,3-Diaminopropionic Acid Monohydrochloride

TBAOH : Tetrabutylammonium Hydroxide

## Operating Procedure of IC

The procedures of start up, software operation and shut down was carried out using the following step-by-step description:

Step 1: Screw tightly the caps of eluant and regenerant bottles to prevent gas leakage.

Step 2: Turn on the valves of helium and nitrogen gas cylinder.

Step 3: Turn on the system switch of eluant degas module.

Step 4: After 5 minutes, the two mode switches for cation and anion eluants in the are changed from sparge to pressure position. At this time, the reservoirs can be checked for gas leakage using a soap solution. If gas leakage is detected, step 5 is carried out, else step 6 is followed.

Step 5: The gas cylinder valves are turned off and the actual points of gas leakage from six reservoirs of eluants and regenerants are found and corrected. Normally, gas leaks occur because of improper closing of reservoir lids, and because of wear and tear of tubes carrying gas to the eluant and regenerant reservoirs. The gas cylinder valves are then turned on again.

Step 6: The pressures for the eluant and regenerant bottles are checked in the pressure gauges. The pressure for eluant and regenerant bottles is fixed to be between 5 and 10 psi.

Step 7: The computer is turned on. It is connected with the Advanced Computer Interface (ACI) and has the installed AI-450 software.

Step 8: Select "run" icon after having verified appropriateness of method and schedule files.

Step 9: At this point, the main switch of ACI may have to be turned off and on immediately. This is necessary to electrically connect the ACI and AI-450 software.

Step 10: Load schedule files for both cation and anion analyses if the dual operating system is needed.

Step 11: All valves on the IC are set to remote operation. The operating pressure of the gradient pump is normally about 550 psi for the anion port and about 1100 psi for cation port. The minimum and maximum pump pressures are 100 psi, and 1500 psi respectively, for both cation and anion detection systems. Thus if pump pressure is below minimum or over maximum pressure, the gradient pump module stops its operation and IC does not work. This phenomenon happens sometimes because of the penetration of air bubbles into the gradient pump module. On such occasions, the IC operating manual is referred to and the problem is identified and corrected.

Step 12: The IC is operated on a few blank runs to elute any peaks from the last run in any previous operation. Once the conductivities in both the anion and cation conductivity detectors have stabilized, the present run can be started.

Step 13: In order to wash out ionic contaminants that can exist in the gradient pump, mixer and lines of IC, the pure deionized water was injected 2 or 3 times. The base line of conductivity in real-time analysis through a computer monitor

showed some fluctuation for the first injection. However it became steady for next injections. The injection is carried out by clicking on "run" in menu.

Step 14: All prepared samples are analyzed. The resulting graphs of conductivity Vs time for cation and anion are saved in data files which are assigned in schedule files. The data files are used to calculate peak areas and then, the concentrations of selected ions based on peak areas and concentrations of standards for those ions. The peak areas and concentrations are calculated immediately after each run is over and can be viewed based on data files in the "Optimize" menu of the AI-450 software. The calibration curves can be viewed in the "CalPlot" menu of the software.

Step 15: Deionized water is injected 2 or 3 times to clean out all parts of IC used after analyzing all samples.

Step 16: After finishing step 14, IC is stopped by pushing "abort" button on ACI or in a menu of AI-450.

Step 17: The mode switches for cation and anion eluants in the eluant degas module are changed from pressure to sparge position.

Step 18: The system switch in the eluant degas module is turned off.

Step 19: The two gas cylinders are turned off.

Step 20: The caps of eluant and regenerant bottles are opened and then closed tightly. This is for releasing the pressure applied and preventing the penetration of contaminants in air during shut-down period.

Step 21: The main switch in ACI is turned off and on immediately.

Step 22: The AI-450 software is closed.

### Calibration Curves

The ion chromatographic system was calibrated with 6 different standards every time after startup. The AI-450 software used for analysis of samples has a Calplot program that provides the calibration curves for each Method program. The calibration curves are plotted for Instrument response (peak area) versus amount (standard concentration). In addition to the actual calibration curve, the component name, the calibration fit type, and the mathematical equation used to calculate the concentration and response are provided by the software. The calibration curve and the additional information are used primarily to verify the linearity of the method over the concentration range for which the method was developed. Linear type fits were obtained for four to six standard concentrations in the 20-198 ppb concentration range for cations and the 35-600 ppb concentration range for anions. This concentration range was chosen after observing the effluent concentrations for the entire range of influent concentrations. The effluent concentrations were typically in the range of the standard concentrations chosen. The correlation coefficient,  $r^2$  provides a measure of the method's linearity. The calibration curves for sodium, magnesium, calcium, chloride and sulfate are shown in figures 21 to 25. The correlation coefficients for sodium, magnesium, calcium, chloride and sulfate were 0.998, 0.997, 0.953, 0.992 and 0.993 respectively, indicating good linearity.

To minimize errors in preparing the very low concentration solutions, the syringe pump was used to dose high concentrations of the salt solutions in deionized water

flowing at the rate of 500 ml/min. The standard solutions were newly prepared whenever the IC was started up. This was necessary because the system conditions of the IC could change each time the IC was started. The changes in system conditions could result in error in determining unknown concentrations if new calibration curves were not obtained each time after start up.

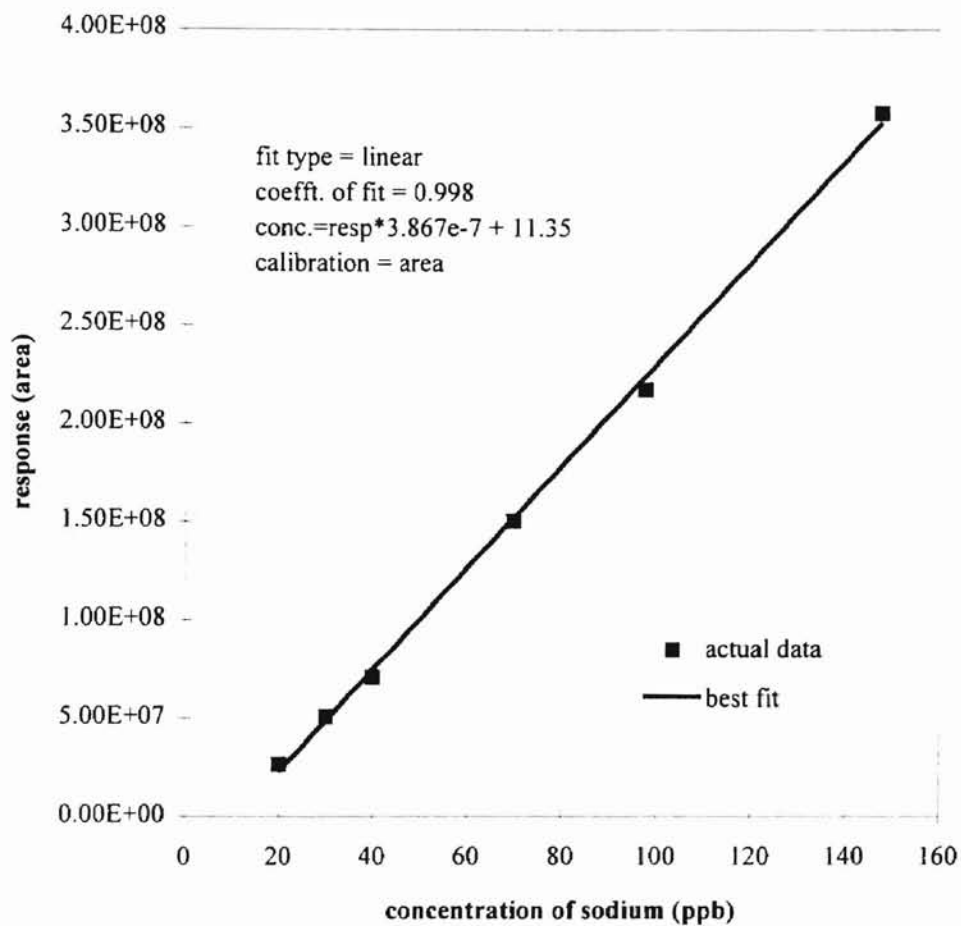


Figure 21. Calibration Curve For Sodium As Obtained From Dionex Software



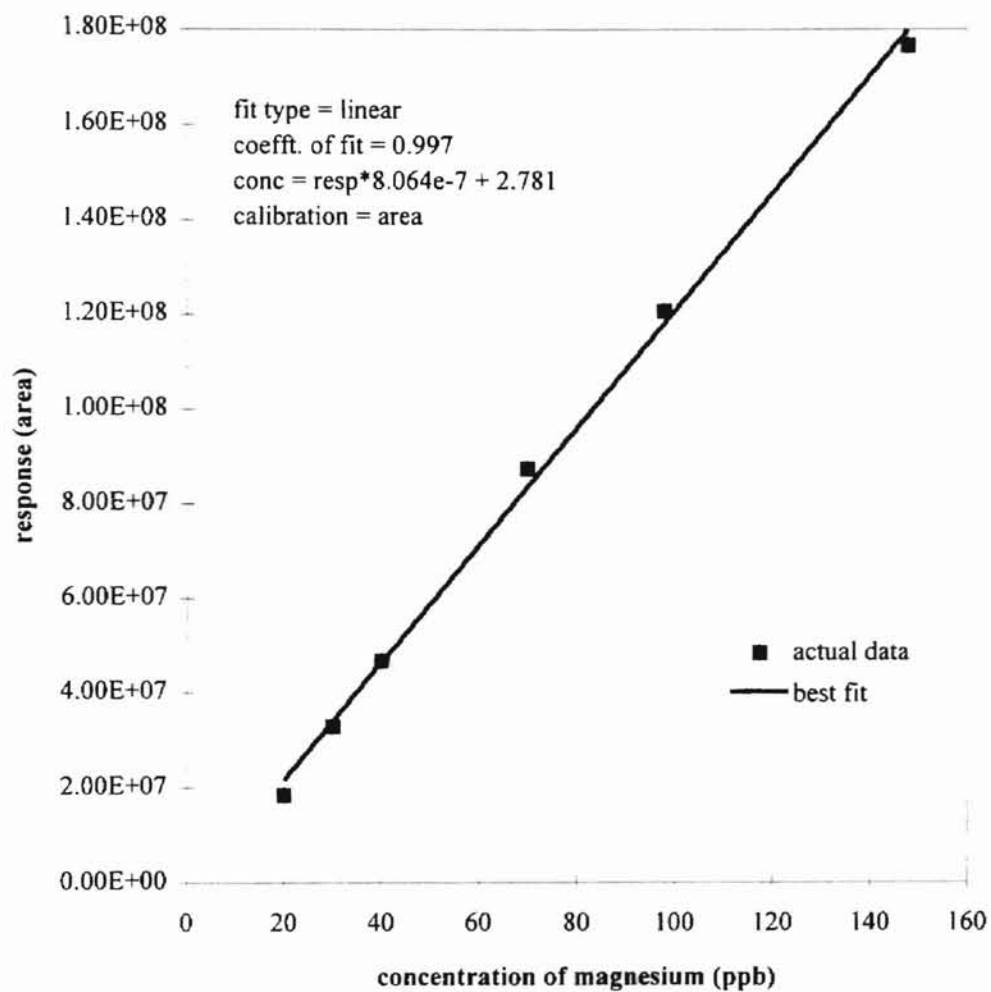


Figure 22. Calibration Curve For Magnesium As Obtained From Dionex Software

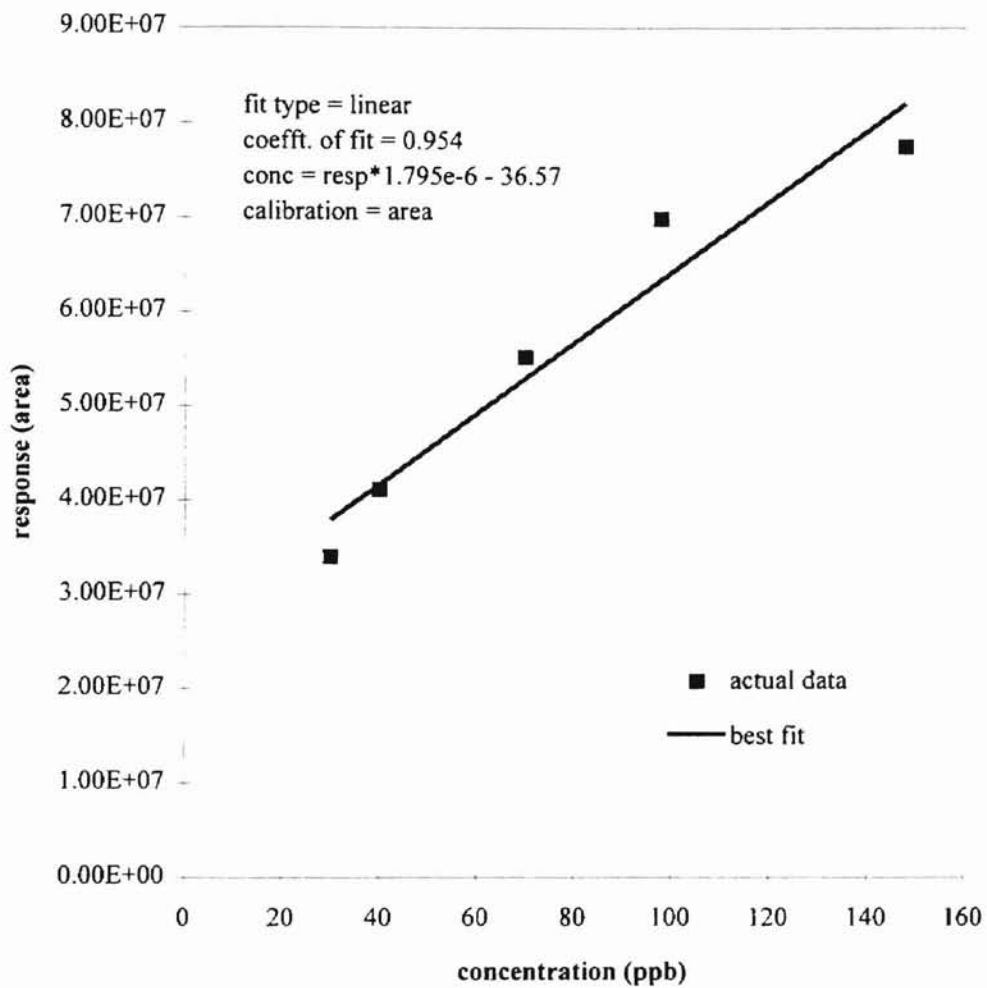


Figure 23. Calibration Curve For Calcium As Obtained From Dionex Software

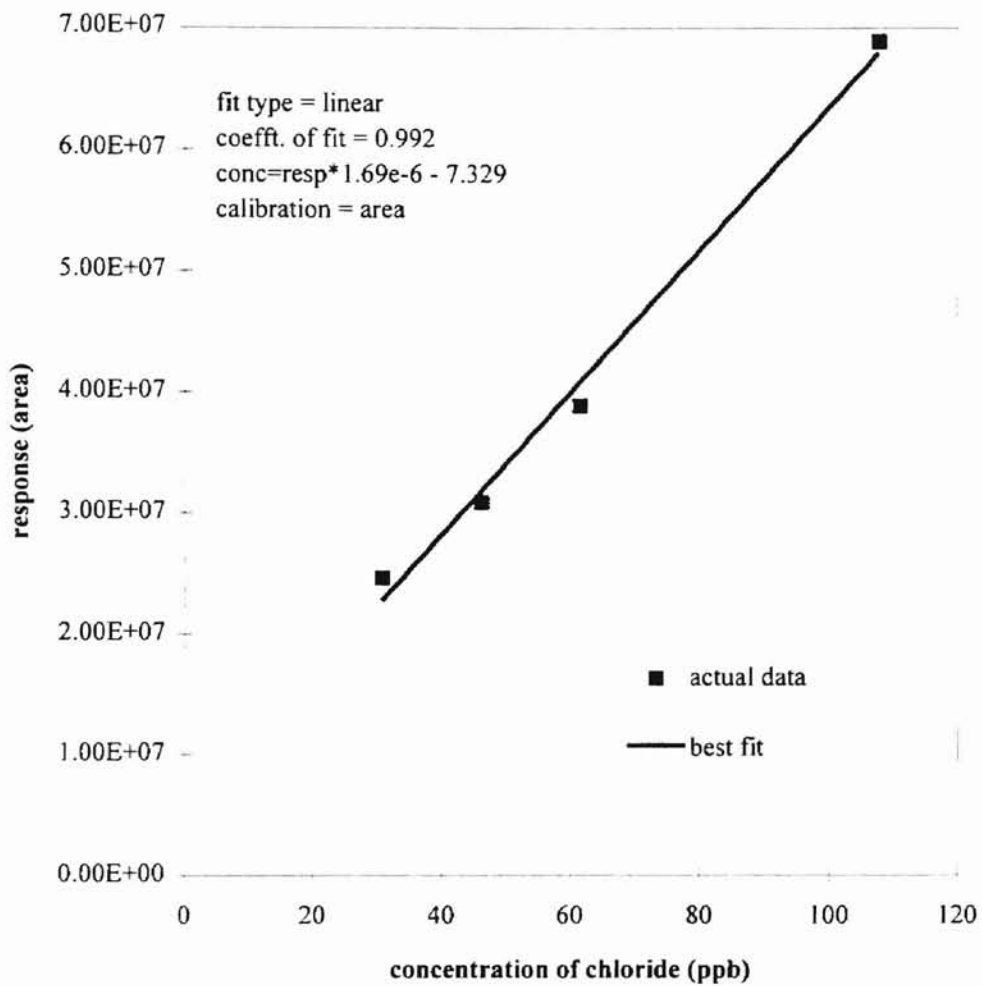


Figure 24. Calibration Curve For Chloride As Obtained From Dionex Software

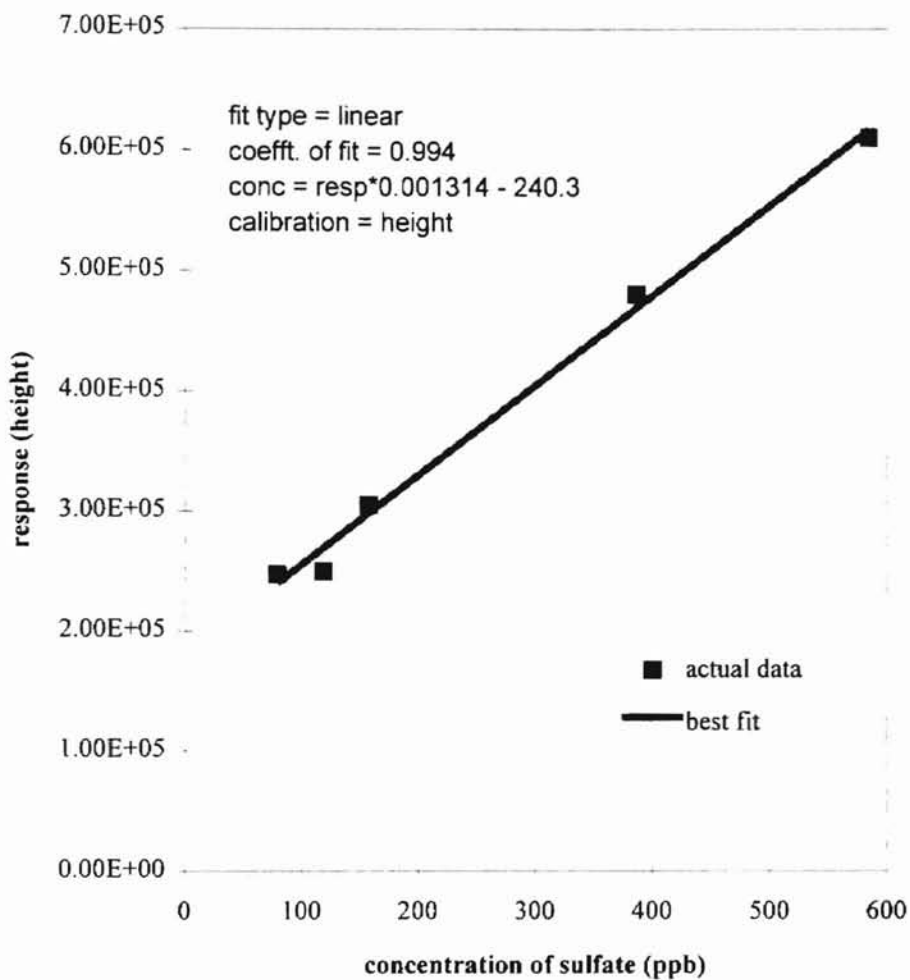


Figure 25. Calibration Curve For Sulfate As Obtained From Dionex Software

## APPENDIX D

### ERROR ANALYSIS

An error is the difference between a measured value and the true exact value, and it follows statistical laws. The absolute error of any measurement is the difference between the measured value and the true value. This does not indicate the accuracy of the measurement. The relative error of a measurement is the absolute error divided by the measured value. The number of significant figures in a measurement is determined by the gradation of the scale. The magnitude of the smallest gradation on the readout scale is its discrimination. The absolute error of any measurement ( $E_a$ ) is given by the relation  $E_a = X_t - X_m$  where  $X_t$  is the true value and  $X_m$  is the measured value. The relative error is given by  $E_r = \frac{E_a}{X_m}$ . It is customary to group errors into inherent, mathematical, instrumental, human, and natural errors. The errors in this study are mainly personal or human errors (in the measurement of bed height, volume of resin, and volumetric flow rate of water through bed, and in the weighing of salts and preparation of salt solutions), and experimental errors (weighing of salts, measurement of effluent concentrations, inaccuracies of flow rate of water, and dosing rate of salt).

The errors from human measurement, instrumental limitations and reproducibility of data are discussed in this section. The salts sodium chloride, magnesium sulfate, and calcium chloride dihydrate were weighed with an electronic digital balance from Mettler (model AE 100). Concentrated salt solutions (1000-2000 ppm) were prepared as dosing solutions. The amount of salt needed to prepare these solutions was always between 10 and 4 grams. The error in weighing these salts using the digital reading on the scale as specified by the manufacturer was  $\pm 0.0002$  g. The maximum relative error was therefore between 0.002 % and 0.005%.

The measurement of wet resin volume was carried out with a 50 ml measuring cylinder to measure resin in volumes of 40 ml and 20 ml. The error was estimated to be one half scale of the lowest gradation which was  $\pm 0.5$  ml. Therefore, the maximum relative error was 1.25% and 2.5% respectively.

The measurement of bed depth was conducted after the procedure of removing air bubbles and making the resin bed as compact as possible. The error was estimated to be  $\pm 0.125$  inches or 0.3175 cm. The bed depth was always lesser than 11.6 cm. The corresponding relative error was 2.7%.

The instrumental error from the feeding pump was estimated by the repeated measurements of effluents of test column with a 500 ml measuring cylinder and stopwatch during the experimental run. The errors were  $\pm 25$  ml/min at 1000 ml/min,  $\pm 15$  ml/min at 750 ml/min, and  $\pm 10$  ml/min at 500 ml/min. The relative errors amounted to 2.5%, 2%, and 2% respectively.

The error from the syringe pump (Sage Model 341 B) was specified by the manufacturer (Orion Corporation) to be  $\pm 10\%$  (based on B-D plastipak syringes). Other accessories such as pH meters, and resistivity meters were not analyzed for error because their readings were used only as guidelines rather than as actual implemented values in the mass transfer equation.

The void fractions in the resin bed for both cation and anion monosphere resin was specified by the manufacturer to be between 0.335 and 0.350. The bed porosity affects specific surface area in the mass transfer equation. The relative error in specific surface area due to boundary values of the bed porosity for monosphere resins (both, cation and anion) was  $\pm 1.4\%$ .

All the errors discussed above propagate to affect the mass transfer equation. Water flow rate and bed depth are linearly related to MTC, and are constant for one experimental run (for eight different influent concentrations at one flow rate). Hence, the effects of uncertainty of flow rate and bed depth are the same as the relative errors of the variables and are constant for each experimental run. The uncertainty in specific surface area of resin is also linearly related to MTC and is the same as the relative errors in surface area for the entire experiment.

The effect of uncertainty of the dosing pump on the MTC is different for each influent concentration. The error in MTC is related to the natural logarithm of each influent concentration. If all variables except the influent concentration ( $C_i^f$ ) are kept constant, then the relative error in mass transfer coefficient is bounded by

$$\% \text{age error} = \text{between } \frac{\ln 1.1}{\ln C_i^{\text{eff}} - \ln C_i^f} \times 100 \text{ and } \frac{\ln 0.9}{\ln C_i^{\text{eff}} - \ln C_i^f} \times 100 \quad (\text{D-1})$$

These sources of uncertainties are combined to give maximum and minimum mass transfer coefficients for each influent concentration at every flow rate. The values of mass transfer coefficients are bounded by the following limiting expressions

$$K_{\max} = - \left( \frac{V_{\max}}{S_{\min} Z_{\min} AR_i} \right) \ln \frac{C_i^{\text{eff}}}{(C_i^f)_{\max}} \quad (\text{D-2})$$

$$K_{\min} = - \left( \frac{V_{\min}}{S_{\max} Z_{\max} AR_i} \right) \ln \frac{C_i^{\text{eff}}}{(C_i^f)_{\min}} \quad (\text{D-3})$$

Equations D1 and eq D2 can be used to obtain the upper and lower bounds on values of mass transfer coefficients after combining the uncertainties of each variable. The maximum and minimum relative errors were between 13.87% and -14.42%, but most relative errors were between  $\pm 9\%$  and  $\pm 12\%$ . The bounds on mass transfer coefficients are listed in Table XII (Appendix E).

### Reproducibility of Runs

The MTC of sodium was evaluated at 750 ml/min in a mixed bed. The experiment was repeated to estimate reproducibility. The average difference in MTC at 750 ml/min was 3.73%. The highest difference occurred at an influent concentration of 65 ppb sodium and was 10.9%. For most other influent concentrations, difference in MTC was less than 1.6%.



### Analytical Error of effluent samples

Instrumental error is a source for error in experiments. This error was estimated by repeating the measurements of the same sample with the IC. The peak area was obtained and the difference in peak area was used as the criterion of analytical error. The maximum absolute deviation was measured to be 2.172 %.

## APPENDIX E

### EXPERIMENTAL DATA

The following tables present calculated mass transfer coefficients (mtc) and effluent concentrations for various ions as estimated by Harries and Ray's equation, and the bounds on mtc using uncertainties in the various variables.

TABLE X

Mass Transfer Coefficient Data Of Monosphere Resin Estimated By  
Harries And Ray's Equation

<b>MTC of Sodium at 500 ml/min</b>				
New resin mono bed			New resin mixed bed	
Ci (feed)	Ci (eff)	mtc (x 10 <sup>-4</sup> m/s)	Ci (eff)	mtc (x 10 <sup>-4</sup> m/s)
30	12.77	0.28	9.97	0.38
98	14.13	0.64	10.81	0.75
200	14.67	0.87	10.48	1.01
400	16.84	1.05	11.79	1.20
700	21.67	1.15	14.42	1.32
980	26.42	1.20	16.89	1.38
2000	42.80	1.28	24.67	1.50
3000	56.02	1.28	34.67	1.50

---

**MTC of Sodium at 500 ml/min**


---

Used resin RS CP1    Used resin RS CP2

Ci (feed)	Ci (eff)	mtc (x 10 <sup>-4</sup> m/s)	Ci (eff)	mtc (x 10 <sup>-4</sup> m/s)
30	10.73	0.35		
98	14.45	0.65	12.60	0.70
200	12.06	0.96	15.49	0.87
400	13.51	1.15	13.96	1.14
700	18.39	1.24	17.85	1.25
980	24.19	1.26	20.39	1.32
2000	36.33	1.37	31.32	1.42
3000	50.75	1.39	43.19	1.45

---

**MTC of sodium at 750 ml/min**


---

New resin mono bed    New resin mixed bed

Ci (feed)	Ci (eff)	mtc (x 10 <sup>-4</sup> m/s)	Ci (eff)	mtc (x 10 <sup>-4</sup> m/s)
20	12.28	0.24	9.89	0.36
65.3	14.31	0.76	11.56	0.88
133.3	13.36	1.15	10.39	1.30
266.7	16.59	1.38	11.88	1.59
466.7	21.11	1.54	14.10	1.79
653.3	25.74	1.61	16.52	1.88
1333.33	42.85	1.71	24.57	2.04
2000	59.69	1.75	32.97	2.10

---

**MTC of sodium at 750 ml/min**


---

Used resin RS CP1    Used resin RS CP2

Ci (feed)	Ci (eff)	mtc (x 10 <sup>-4</sup> m/s)	Ci (eff)	mtc (x 10 <sup>-4</sup> m/s)
20	10.79	0.32	11.53	0.28
65.3	13.78	0.80	13.52	0.81
133.3	18.37	1.01	11.22	1.27
266.7	11.53	1.61	15.29	1.46
466.7	14.33	1.78	29.98	1.40
653.3	17.70	1.84	24.60	1.68
1333.33	36.98	1.83	41.27	1.78
2000	68.56	1.72	61.30	1.78

---

**MTC of sodium at 1000 ml/min**


---

New resin mono bed			New resin mixed bed		
Ci (feed)	Ci (eff)	mtc (x $10^{-4}$ m/s)	Ci (eff)	mtc (x $10^{-4}$ m/s)	
15	12.37	0.13	10.00	0.28	
49	13.74	0.84	10.90	1.02	
100	13.13	1.35	10.70	1.52	
200	15.39	1.70	10.80	1.99	
350	20.68	1.88	14.67	2.16	
490	25.35	1.97	18.43	2.24	
1000	46.80	2.03	28.88	2.42	
1500	62.57	2.11	38.68	2.49	

---

**MTC of sodium at 1000 ml/min**


---

Used resin RS CP1			Used resin RS CP2		
Ci (feed)	Ci (eff)	mtc (x $10^{-4}$ m/s)	Ci (eff)	mtc (x $10^{-4}$ m/s)	
15	10.80	0.22	10.95	0.21	
49	12.24	0.95	12.83	0.91	
100	12.26	1.43	13.06	1.39	
200	15.44	1.75	15.11	1.76	
350	21.09	1.91	20.21	1.94	
490	25.03	2.03	27.21	1.97	
1000	45.93	2.10	42.36	2.15	
1500	69.77	2.09	64.94	2.14	

---

**MTC of Cl at 500 ml/min**


---

New resin mono bed			New resin mixed bed			Used resin RS CP2	
Ci (feed)	Ci (eff)	mtc (x $10^{-4}$ m/s)	Ci (eff)	mtc (x $10^{-4}$ m/s)	Ci (eff)	mtc (x $10^{-4}$ m/s)	
46.2			18.32	0.57	31.54	0.24	
150.92	23.94	0.56	18.09	1.31	3.42	2.34	
308	24.93	0.76	16.36	1.82	14.48	1.89	
616	22.15	1.00	17.31	2.21	7.14	2.76	
1078	24.52	1.14	20.50	2.45	15.92	2.61	
1509.2	29.94	1.18	22.16	2.61	27.33	2.48	
3080	21.37	1.50	39.16	2.70	76.02	2.29	
4620	25.92	1.56	63.67	2.65	127.79	2.22	

---

**MTC of Cl at 750 ml/min**


---

Ci (feed)	New resin mono bed			New resin mixed bed			Used resin RS CP2		
	Ci (eff)	mtc	(x 10 <sup>-4</sup> m/s)	Ci (eff)	mtc	(x 10 <sup>-4</sup> m/s)	Ci (eff)	mtc	(x 10 <sup>-4</sup> m/s)
30.8	22.33		0.15	11.50		0.91	3.20		2.10
100.5	24.05		0.65	13.03		1.90	6.61		2.53
205.2	20.05		1.05	12.29		2.61			
410.7	41.85		1.03	13.05		3.20	13.68		3.16
718.7	43.29		1.27	17.69		3.44			
1006.1	39.66		1.46	25.27		3.42	46.21		2.86
2053.3	35.67		1.83	46.57		3.51	109.43		2.72
3080	47.07		1.89	81.76		3.37	178.73		2.64

---

**MTC of Cl at 1000 ml/min**


---

Ci (feed)	New resin mono bed			New resin mixed bed			Used resin RS CP2		
	Ci (eff)	mtc	(x 10 <sup>-4</sup> m/s)	Ci (eff)	mtc	(x 10 <sup>-4</sup> m/s)	Ci (eff)	mtc	(x 10 <sup>-4</sup> m/s)
23.1				8.58		1.23	4.68		1.98
75.5	29.55		0.57	9.72		2.54	7.89		2.80
154	59.87		0.57	4.69		4.32	8.34		3.61
308	59.06		1.00	5.04		5.09	17.06		3.58
539	33.67		1.67	14.59		4.47	28.07		3.66
754.6	17.60		2.27	20.27		4.48	41.04		3.60
1540	38.55		2.22	59.22		4.03	106.77		3.30
2310	72.87		2.08	89.50		4.02	179.21		3.16

---

**MTC of Mg at 500 ml/min**


---

Ci (feed)	New resin mono bed			New resin mixed bed			Used resin RS CP1		
	Ci (eff)	mtc	(x 10 <sup>-4</sup> m/s)	Ci (eff)	mtc	(x 10 <sup>-4</sup> m/s)	Ci (eff)	mtc	(x 10 <sup>-4</sup> m/s)
30	13.80		0.26	6.81		0.51	5.08		0.61
98	13.85		0.65	9.92		0.78	10.72		0.75
200				14.35		0.90	18.55		0.81
400				20.21		1.02	33.94		0.84
700	27.70		1.07	37.96		0.99	58.67		0.84
980	60.51		0.92	55.13		0.98	90.72		0.81
2000	106.72		0.97	91.23		1.05	185.35		0.81
3000	224.29		0.86	127.66		1.08	227.88		0.88

---

**MTC of Mg at 750 ml/min**


---

New resin mono bed			New resin mixed bed			Used resin RS CPI		
Ci (feed)	Ci (eff)	mtc (x $10^{-4}$ m/s)	Ci (eff)	mtc (x $10^{-4}$ m/s)	Ci (eff)	mtc (x $10^{-4}$ m/s)	Ci (eff)	mtc (x $10^{-4}$ m/s)
30	12.28	0.24	9.38	0.59	7.04	0.74		
98	14.31	0.76	12.34	1.06	15.20	0.95		
200			21.18	1.15	28.22	1.00		
400			35.25	1.24	47.70	1.09		
700	52.62	1.29	61.37	1.24		0.00		
980	108.05	1.10	92.70	1.20	131.71	1.03		
2000	191.45	1.17	190.59	1.20	346.93	0.90		
3000	410.34	0.99	254.25	1.26	451.60	0.97		

---

**MTC of Mg at 1000 ml/min**


---

New resin mono bed			New resin mixed bed			Used resin RS CPI		
Ci (feed)	Ci (eff)	mtc (x $10^{-4}$ m/s)	Ci (eff)	mtc (x $10^{-4}$ m/s)	Ci (eff)	mtc (x $10^{-4}$ m/s)	Ci (eff)	mtc (x $10^{-4}$ m/s)
30	6.50	1.02	15.91	0.43	9.11	0.81		
98	12.53	1.37	23.18	0.98	21.86	1.02		
200			27.09	1.36	38.97	1.11		
400			78.58	1.39	82.19	1.08		
700	77.91	1.46	88.82	1.41	142.59	1.08		
980	156.39	1.22	133.17	1.36	204.77	1.07		
2000	245.95	1.39	320.22	1.25	491.76	0.96		
3000	579.66	1.09	398.95	1.37	618.66	1.08		

---

**MTC of SO<sub>4</sub> at 500, 750, 1000 ml/min flowrates**


---

 New resin mixed bed
 

---

Ci(feed)	Ci(eff)	mtc (x 10 <sup>-4</sup> m/s) (500 ml/min)	Ci(eff)	mtc (x 10 <sup>-4</sup> m/s) (750 ml/min)	Ci(eff)	mtc (x 10 <sup>-4</sup> m/s) (1000 ml/min)
119	47.53	0.51	56.24	0.63	56.82	0.83
387			221.04	0.47	176.71	0.88
790					182.22	1.64
1581	186.53	1.51	228.27	1.63	194.35	2.35
2767	248.66	1.54	240.28	2.05	283.38	2.55
3873	266.41	1.90	323.18	2.09	346.25	2.71
7904	360.61	1.96	760.51	1.97	774.87	2.60
11857			847.37	2.22	861.34	2.94

---

**MTC of Ca at 500 ml/min**


---

New resin mono bed			New resin mixed bed			Used resin RS CP1		
Ci (feed)	Ci (eff)	mtc (x 10 <sup>-4</sup> m/s)	Ci (eff)	mtc (x 10 <sup>-4</sup> m/s)	Ci (eff)	mtc (x 10 <sup>-4</sup> m/s)		
98	5.49	0.96	4.65	1.04	27.60	0.43		
200	14.61	0.87	12.91	0.93	27.60	0.67		
400	24.56	0.93	30.15	0.88	35.19	0.83		
700	35.14	0.99	45.21	0.93	52.75	0.88		
980	50.56	0.98	56.74	0.97	66.76	0.92		
2000	96.72	1.01	76.50	1.11	116.57	0.97		

---

**MTC of Ca at 750 ml/min**


---

New resin mono bed			New resin mixed bed			Used resin RS CP1		
Ci (feed)	Ci (eff)	mtc (x 10 <sup>-4</sup> m/s)	Ci (eff)	mtc (x 10 <sup>-4</sup> m/s)	Ci (eff)	mtc (x 10 <sup>-4</sup> m/s)		
98	6.57	1.35	7.15	1.34	26.35	0.67		
200	17.15	1.22	16.71	1.27	23.36	1.10		
400	31.63	1.26	22.97	1.46	31.23	1.30		
700	62.48	1.20	48.58	1.36				
980	95.91	1.16	61.29	1.42	76.42	1.30		
2000	206.83	1.13	131.99	1.39	142.66	1.35		

---

**MTC of Ca at 1000 ml/min**


---

New resin mono bed			New resin mixed bed			Used resin RS CP1		
Ci (feed)	Ci (eff)	mtc (x 10 <sup>-4</sup> m/s)	Ci (eff)	mtc (x 10 <sup>-4</sup> m/s)	Ci (eff)	mtc (x 10 <sup>-4</sup> m/s)	Ci (eff)	mtc (x 10 <sup>-4</sup> m/s)
98	9.12	1.58	7.26	1.77	15.36	1.26		
200	17.19	1.63	15.51	1.74	32.70	1.23		
400	32.37	1.67	32.85	1.70	53.75	1.37		
700	62.24	1.61	58.17	1.69	88.14	1.41		
980	112.94	1.43	94.02	1.60	105.12	1.52		
2000	228.62	1.44	193.82	1.59	190.32	1.60		



TABLE XI

Maximum And Minimum Relative Errors Of Mass Transfer Coefficients  
Due To Experimental Uncertainties

MTC of Sodium at 500 ml/min						
New resin mono bed						
MTC (*10 <sup>-4</sup> m/s)					Relative Error (%age)	
Ci (feed)	Ci (eff)	K	Kmax	Kmin	max	min
30	12.77	0.28	0.34	0.23	18.28	-19.30
98	14.13	0.64	0.72	0.56	11.64	-12.96
200	14.67	0.87	0.96	0.77	10.29	-11.67
400	16.84	1.05	1.15	0.94	9.61	-11.01
700	21.67	1.15	1.26	1.03	9.32	-10.74
980	26.42	1.20	1.31	1.07	9.21	-10.64
2000	42.80	1.28	1.39	1.14	9.04	-10.48
3000	56.02	1.28	1.44	1.18	12.82	-7.21
New resin mixed bed						
MTC (*10 <sup>-4</sup> m/s)					Relative Error (%age)	
Ci (feed)	Ci (eff)	K	Kmax	Kmin	max	min
30	9.97	0.38	0.43	0.32	14.12	-15.81
98	10.81	0.75	0.82	0.67	9.57	-11.35
200	10.48	1.01	1.09	0.90	8.43	-10.23
400	11.79	1.20	1.30	1.08	7.87	-9.69
700	14.42	1.32	1.42	1.20	7.61	-9.43
980	16.89	1.38	1.49	1.25	7.50	-9.32
2000	24.67	1.50	1.61	1.36	7.31	-9.14
3000	34.67	1.50	1.63	1.38	8.87	-7.75

## Used resin RS CP1

Ci (feed)	Ci (eff)	MTC (*10 <sup>-4</sup> m/s)			Relative Error (%age)	
		K	Kmax	Kmin	max	min
30	10.73	0.35	0.40	0.29	14.77	-16.44
98	14.45	0.65	0.72	0.57	10.26	-12.03
200	12.06	0.96	1.04	0.86	8.60	-10.40
400	13.51	1.15	1.25	1.04	7.99	-9.80
700	18.39	1.24	1.34	1.12	7.78	-9.60
980	24.19	1.26	1.36	1.14	7.74	-9.56
2000	36.33	1.37	1.47	1.24	7.53	-9.35
3000	50.75	1.39	1.49	1.26	7.49	-9.31

## Used resin RS CP2

Ci (feed)	Ci (eff)	MTC (*10 <sup>-4</sup> m/s)			Relative Error (%age)	
		K	Kmax	Kmin	max	min
98	12.60	0.70	0.77	0.62	9.91	-11.69
200	15.49	0.87	0.95	0.78	8.95	-10.74
400	13.96	1.14	1.24	1.03	8.02	-9.83
700	17.85	1.25	1.35	1.13	7.76	-9.58
980	20.39	1.32	1.42	1.20	7.62	-9.44
2000	31.32	1.42	1.52	1.29	7.44	-9.27
3000	43.19	1.45	1.55	1.31	7.39	-9.22

**MTC of sodium at 750 ml/min**New resin mono  
bed

Ci (feed)	Ci (eff)	MTC (*10 <sup>-4</sup> m/s)			Relative Error (%age)	
		K	Kmax	Kmin	max	min
20	12.28	0.24	0.31	0.18	27.18	-27.82
65.3	14.31	0.76	0.86	0.65	13.09	-14.34
133.3	13.36	1.15	1.27	1.01	10.82	-12.17
266.7	16.59	1.38	1.52	1.23	10.06	-11.44
466.7	21.11	1.54	1.69	1.37	9.68	-11.09
653.3	25.74	1.61	1.76	1.43	9.54	-10.95
1333.33	42.85	1.71	1.87	1.53	9.36	-10.77
2000	59.69	1.75	1.91	1.56	9.29	-10.71

New resin mixed  
bed

		MTC (*10 <sup>-4</sup> m/s)			Relative Error (%age)	
Ci (feed)	Ci (eff)	K	Kmax	Kmin	max	min
20	9.89	0.36	0.43	0.28	19.25	-20.84
65.3	11.56	0.88	0.98	0.77	10.81	-12.57
133.3	10.39	1.30	1.42	1.16	8.96	-10.75
266.7	11.88	1.59	1.72	1.43	8.25	-10.06
466.7	14.10	1.79	1.93	1.62	7.89	-9.71
653.3	16.52	1.88	2.03	1.70	7.75	-9.57
1333.33	24.57	2.04	2.20	1.85	7.54	-9.36
2000	32.97	2.10	2.26	1.90	7.47	-9.29

Used resin RS CP1

		MTC (*10 <sup>-4</sup> m/s)			Relative Error (%age)	
Ci (feed)	Ci (eff)	K	Kmax	Kmin	max	min
20	10.79	0.32	0.38	0.24	21.25	-22.80
65.3	13.78	0.80	0.89	0.69	11.47	-13.21
133.3	18.37	1.01	1.12	0.89	10.08	-11.85
266.7	11.53	1.61	1.74	1.44	8.22	-10.03
466.7	14.33	1.78	1.92	1.61	7.91	-9.72
653.3	17.70	1.84	1.99	1.67	7.81	-9.62
1333.33	36.98	1.83	1.98	1.66	7.82	-9.64
2000	68.56	1.72	1.86	1.56	8.00	-9.81

Used resin RS CP2

		MTC (*10 <sup>-4</sup> m/s)			Relative Error (%age)	
Ci (feed)	Ci (eff)	K	Kmax	Kmin	max	min
20	11.53	0.28	0.35	0.21	23.21	-24.72
65.3	13.52	0.81	0.90	0.70	11.39	-13.13
133.3	11.22	1.27	1.38	1.13	9.08	-10.87
266.7	15.29	1.46	1.59	1.31	8.53	-10.34
466.7	29.98	1.40	1.52	1.26	8.68	-10.48
653.3	24.60	1.68	1.81	1.51	8.08	-9.90
1333.33	41.27	1.78	1.92	1.60	7.91	-9.73
2000	61.30	1.78	1.92	1.61	7.90	-9.72

---

**MTC of sodium at 1000 ml/min**


---

 New resin mono  
bed
 

---

		MTC (*10 <sup>-4</sup> m/s)			Relative Error (%age)	
Ci (feed)	Ci (eff)	K	Kmax	Kmin	max	min
15	12.37	0.13	0.20	0.05	59.75	-58.43
100	13.13	1.35	1.51	1.17	11.95	-13.17
200	15.39	1.70	1.89	1.50	10.90	-12.18
350	20.68	1.88	2.08	1.66	10.53	-11.83
490	25.35	1.97	2.17	1.74	10.37	-11.68
1000	46.80	2.03	2.24	1.80	10.26	-11.57
1500	62.57	2.11	2.32	1.87	10.14	-11.46

 New resin mixed  
bed
 

---

		MTC (*10 <sup>-4</sup> m/s)			Relative Error (%age)	
Ci (feed)	Ci (eff)	K	Kmax	Kmin	max	min
15	10.00	0.28	0.36	0.19	30.38	-31.47
49	10.90	1.02	1.15	0.88	12.24	-13.87
100	10.70	1.52	1.68	1.34	10.05	-11.75
200	10.80	1.99	2.17	1.78	8.99	-10.72
350	14.67	2.16	2.35	1.94	8.72	-10.46
490	18.43	2.24	2.43	2.00	8.61	-10.36
1000	28.88	2.42	2.62	2.17	8.38	-10.13
1500	38.68	2.49	2.70	2.24	8.30	-10.05

 Used resin RS CPI
 

---

		MTC (*10 <sup>-4</sup> m/s)			Relative Error (%age)	
Ci (feed)	Ci (eff)	K	Kmax	Kmin	max	min
15	10.80	0.22	0.31	0.14	36.15	-37.07
49	12.24	0.95	1.07	0.81	12.80	-14.42
100	12.26	1.43	1.58	1.26	10.34	-12.03
200	15.44	1.75	1.91	1.55	9.47	-11.19
350	21.09	1.91	2.09	1.71	9.13	-10.85
490	25.03	2.03	2.21	1.81	8.93	-10.66
1000	45.93	2.10	2.28	1.88	8.81	-10.55
1500	69.77	2.09	2.28	1.87	8.83	-10.56

Used resin RS CP2

Ci (feed)	Ci (eff)	MTC (*10 <sup>-4</sup> m/s)			Relative Error (%age)	
		K	Kmax	Kmin	max	min
15	10.95	0.21	0.30	0.13	37.50	-38.38
49	12.83	0.91	1.03	0.78	13.06	-14.66
100	13.06	1.39	1.53	1.22	10.49	-12.17
200	15.11	1.76	1.93	1.56	9.44	-11.16
350	20.21	1.94	2.12	1.73	9.07	-10.80
490	27.21	1.97	2.15	1.76	9.03	-10.76
1000	42.36	2.15	2.34	1.93	8.73	-10.47
1500	64.94	2.14	2.33	1.92	8.75	-10.49

MTC of Cl at 500 ml/min

New resin mono  
bed

Ci (feed)	Ci (eff)	MTC (*10 <sup>-4</sup> m/s)			Relative Error (%age)	
		K	Kmax	Kmin	max	min
150.92	23.94	0.56	0.62	0.48	11.91	-13.22
308	24.93	0.76	0.84	0.67	10.44	-11.81
616	22.15	1.00	1.10	0.89	9.46	-10.87
1078	24.52	1.14	1.24	1.02	9.09	-10.52
1509.2	29.94	1.18	1.29	1.06	8.99	-10.43
3080	21.37	1.50	1.62	1.35	8.45	-9.90
4620	25.92	1.56	1.69	1.41	8.36	-9.82

New resin mixed  
bed

Ci (feed)	Ci (eff)	MTC (*10 <sup>-4</sup> m/s)			Relative Error (%age)	
		K	Kmax	Kmin	max	min
46.2	18.32	0.57	0.66	0.47	16.01	-17.40
150.92	18.09	1.31	1.44	1.16	9.90	-11.41
308	16.36	1.82	1.97	1.63	8.59	-10.13
616	17.31	2.21	2.39	2.00	7.98	-9.53
1078	20.50	2.45	2.64	2.22	7.70	-9.26
1509.2	22.16	2.61	2.81	2.37	7.55	-9.11
3080	39.16	2.70	2.90	2.46	7.47	-9.03
4620	63.67	2.65	2.85	2.41	7.51	-9.07

## Used resin RS CP2

		MTC (*10 <sup>-4</sup> m/s)			Relative Error (%age)	
Ci (feed)	Ci (eff)	K	Kmax	Kmin	max	min
46.2	31.54	0.24	0.31	0.16	31.44	-32.52
150.92	3.42	2.34	2.53	2.12	7.82	-9.37
308	14.48	1.89	2.05	1.70	8.45	-9.99
616	7.14	2.76	2.96	2.51	7.42	-8.98
1078	15.92	2.61	2.81	2.37	7.55	-9.11
1509.2	27.33	2.48	2.67	2.25	7.67	-9.23
3080	76.02	2.29	2.47	2.07	7.88	-9.43
4620	127.79	2.22	2.40	2.01	7.97	-9.52

## MTC of Cl at 750 ml/min

New resin mono  
bed

		MTC (*10 <sup>-4</sup> m/s)			Relative Error (%age)	
Ci (feed)	Ci (eff)	K	Kmax	Kmin	max	min
30.8	22.33	0.15	0.20	0.09	37.95	-38.11
100.562	24.05	0.65	0.73	0.55	13.49	-14.73
205.282	20.05	1.05	1.16	0.92	10.77	-12.12
410.718	41.85	1.03	1.14	0.91	10.85	-12.20
718.718	43.29	1.27	1.40	1.13	10.02	-11.40
1006.082	39.66	1.46	1.60	1.30	9.54	-10.95
2053.328	35.67	1.83	2.00	1.64	8.91	-10.35
3080	47.07	1.89	2.06	1.70	8.83	-10.27

New resin mixed  
bed

		MTC (*10 <sup>-4</sup> m/s)			Relative Error (%age)	
Ci (feed)	Ci (eff)	K	Kmax	Kmin	max	min
30.8	11.50	0.91	1.05	0.76	15.35	-16.75
100.562	13.03	1.90	2.09	1.68	10.08	-11.59
205.282	12.29	2.61	2.84	2.35	8.73	-10.27
410.718	13.05	3.20	3.46	2.89	8.08	-9.63
718.718	17.69	3.44	3.71	3.11	7.88	-9.43
1006.082	25.27	3.42	3.69	3.10	7.89	-9.45
2053.328	46.57	3.51	3.79	3.18	7.82	-9.37
3080	81.76	3.37	3.64	3.05	7.94	-9.49

Used resin RS CP2

		MTC (*10 <sup>-4</sup> m/s)			Relative Error (%age)	
Ci (feed)	Ci (eff)	K	Kmax	Kmin	max	min
30.8	3.20	2.10	2.30	1.87	9.60	-11.12
100.562	6.61	2.53	2.75	2.26	8.86	-10.39
410.718	13.68	3.16	3.41	2.85	8.12	-9.67
1006.082	46.21	2.86	3.10	2.57	8.43	-9.97
2053.328	109.43	2.72	2.96	2.45	8.59	-10.13
3080	178.73	2.64	2.87	2.37	8.69	-10.23

**MTC of CI at 1000 ml/min**New resin mono  
bed

		MTC (*10 <sup>-4</sup> m/s)			Relative Error (%age)	
Ci (feed)	Ci (eff)	K	Kmax	Kmin	max	min
75.46	29.55	0.57	0.67	0.46	17.80	-18.71
154	59.87	0.60	0.67	0.46	11.75	-22.76
308	59.06	1.00	1.13	0.85	13.10	-14.27
539	33.67	1.67	1.85	1.47	10.60	-11.90
754.6	17.60	2.27	2.48	2.02	9.64	-10.99
1540	38.55	2.22	2.44	1.98	9.69	-11.04
2310	72.87	2.08	2.29	1.85	9.88	-11.21

New resin mixed  
bed

		MTC (*10 <sup>-4</sup> m/s)			Relative Error (%age)	
Ci (feed)	Ci (eff)	K	Kmax	Kmin	max	min
23.1	8.58	1.23	1.42	1.02	15.86	-17.12
75.46	9.72	2.54	2.81	2.23	10.60	-12.02
154	4.69	4.32	4.69	3.89	8.57	-10.05
308	5.04	5.09	5.50	4.60	8.14	-9.63
539	14.59	4.47	4.85	4.02	8.48	-9.96
754.6	20.27	4.48	4.86	4.03	8.47	-9.96
1540	59.22	4.03	4.39	3.62	8.78	-10.25
2310	89.50	4.02	4.38	3.61	8.79	-10.26

Used resin RS CP2

		MTC (*10 <sup>-4</sup> m/s)			Relative Error (%age)	
Ci (feed)	Ci (eff)	K	Kmax	Kmin	max	min
23.1	4.68	1.98	2.21	1.71	12.00	-13.38
75.46	7.89	2.80	3.08	2.47	10.15	-11.58
154	8.34	3.61	3.94	3.23	9.14	-10.61
308	17.06	3.58	3.91	3.20	9.17	-10.63
539	28.07	3.66	3.99	3.27	9.10	-10.56
754.6	41.04	3.60	3.93	3.22	9.15	-10.61
1540	106.77	3.30	3.62	2.94	9.46	-10.92
2310	179.21	3.16	3.47	2.81	9.63	-11.08

MTC of Mg at 500 ml/min

New resin mono  
bed

		MTC (*10 <sup>-4</sup> m/s)			Relative Error (%age)	
Ci (feed)	Ci (eff)	K	Kmax	Kmin	max	min
30	13.80	0.26	0.31	0.21	19.47	-20.44
98	13.85	0.65	0.72	0.57	11.59	-12.91
700	27.70	1.07	1.17	0.95	9.55	-10.96
980	60.51	0.92	1.02	0.82	10.05	-11.44
2000	106.72	0.97	1.07	0.86	9.87	-11.26
3000	224.29	0.86	0.95	0.76	10.32	-11.69

New resin mixed  
bed

		MTC (*10 <sup>-4</sup> m/s)			Relative Error (%age)	
Ci (feed)	Ci (eff)	K	Kmax	Kmin	max	min
30	6.81	0.51	0.57	0.44	11.83	-13.48
98	9.92	0.78	0.85	0.69	9.45	-11.15
200	14.35	0.90	0.98	0.80	8.88	-10.59
400	20.21	1.02	1.10	0.91	8.43	-10.15
700	37.96	0.99	1.08	0.89	8.52	-10.23
980	55.13	0.98	1.06	0.88	8.56	-10.27
2000	91.23	1.05	1.14	0.95	8.32	-10.04
3000	127.66	1.08	1.16	0.97	8.25	-9.97



## Used resin RS CPI

Ci (feed)	Ci (eff)	K	MTC (*10 <sup>-4</sup> m/s)		Relative Error (%age)	
			Kmax	Kmin	max	min
30	5.08	0.61	0.67	0.53	10.72	-12.39
98	10.72	0.75	0.83	0.67	9.61	-11.30
200	18.55	0.81	0.89	0.72	9.29	-10.99
400	33.94	0.84	0.92	0.75	9.14	-10.84
700	58.67	0.84	0.92	0.75	9.12	-10.82
980	90.72	0.81	0.89	0.72	9.29	-10.99
2000	185.35	0.81	0.89	0.72	9.29	-10.99
3000	227.88	0.88	0.96	0.78	8.96	-10.67

## MTC of Mg at 750 ml/min

New resin mono  
bed

Ci (feed)	Ci (eff)	K	MTC (*10 <sup>-4</sup> m/s)		Relative Error (%age)	
			Kmax	Kmin	max	min
30	12.28	0.42	0.52	0.36	24.80	-13.95
98	14.31	0.96	1.07	0.83	11.48	-13.15
700	52.62	1.29	1.42	1.14	10.33	-11.70
980	108.05	1.10	1.22	0.96	11.01	-12.35
2000	191.45	1.17	1.29	1.03	10.73	-12.09
3000	410.34	0.99	1.10	0.86	11.50	-12.83

New resin mixed  
bed

Ci (feed)	Ci (eff)	K	MTC (*10 <sup>-4</sup> m/s)		Relative Error (%age)	
			Kmax	Kmin	max	min
30	9.38	0.59	0.68	0.50	13.70	-15.31
98	12.34	1.06	1.16	0.94	9.91	-11.60
200	21.18	1.15	1.26	1.02	9.54	-11.23
400	35.25	1.24	1.36	1.11	9.20	-10.90
700	61.37	1.24	1.36	1.11	9.19	-10.90
980	92.70	1.20	1.32	1.07	9.33	-11.02
2000	190.59	1.20	1.31	1.07	9.34	-11.04
3000	254.25	1.26	1.38	1.12	9.14	-10.84

## Used resin RS CP1

Ci (feed)	Cj (eff)	K	MTC (*10 <sup>-4</sup> m/s)		Relative Error (%age)	
			Kmax	Kmin	max	min
30	7.04	0.74	0.83	0.64	11.98	-13.63
98	15.20	0.95	1.05	0.84	10.45	-12.13
200	28.22	1.00	1.10	0.88	10.19	-11.88
400	47.70	1.09	1.19	0.96	9.79	-11.48
980	131.71	1.03	1.13	0.90	10.07	-11.75
2000	346.93	0.90	0.99	0.78	10.80	-12.47
3000	451.60	0.97	1.07	0.85	10.37	-12.05

## MTC of Mg at 1000 ml/min

New resin mono  
bed

Ci (feed)	Ci (eff)	K	MTC (*10 <sup>-4</sup> m/s)		Relative Error (%age)	
			Kmax	Kmin	max	min
30	6.50	1.02	1.15	0.87	13.59	-14.73
98	12.53	1.37	1.53	1.19	11.88	-13.11
700	77.91	1.46	1.63	1.27	11.57	-12.82
980	156.39	1.22	1.37	1.05	12.48	-13.68
2000	245.95	1.39	1.56	1.21	11.79	-13.03
3000	579.66	1.09	1.24	0.94	13.13	-14.29

New resin mixed  
bed

Ci (feed)	Ci (eff)	K	MTC (*10 <sup>-4</sup> m/s)		Relative Error (%age)	
			Kmax	Kmin	max	min
30	15.91	0.43	0.53	0.33	21.46	-22.73
98	23.18	0.98	1.11	0.84	12.57	-14.11
200	27.09	1.36	1.51	1.20	10.63	-12.22
700	88.82	1.41	1.55	1.24	10.47	-12.07
980	133.17	1.36	1.50	1.19	10.64	-12.23
2000	320.22	1.25	1.39	1.09	11.09	-12.67
3000	398.95	1.37	1.52	1.21	10.58	-12.18

## Used resin RS CP1

		MTC (*10 <sup>-4</sup> m/s)			Relative Error (%age)	
Ci (feed)	Ci (eff)	K	Kmax	Kmin	max	min
30	9.11	0.81	0.93	0.69	14.04	-15.53
98	21.86	1.02	1.15	0.88	12.30	-13.85
200	38.97	1.11	1.25	0.97	11.75	-13.31
400	82.19	1.08	1.21	0.93	11.95	-13.51
700	142.59	1.08	1.21	0.94	11.92	-13.47
980	204.77	1.07	1.19	0.92	12.02	-13.57
2000	491.76	0.96	1.08	0.82	12.77	-14.30
3000	618.66	1.08	1.20	0.93	11.97	-13.52

## MTC of Ca at 500 ml/min

New resin mono  
bed

		MTC (*10 <sup>-4</sup> m/s)			Relative Error (%age)	
Ci (feed)	Ci (eff)	K	Kmax	Kmin	max	min
98	5.49	0.96	1.05	0.85	9.93	-11.32
200	14.61	0.87	0.96	0.77	10.28	-11.66
400	24.56	0.93	1.02	0.82	10.04	-11.43
700	35.14	0.99	1.09	0.88	9.80	-11.19
980	50.56	0.98	1.08	0.87	9.83	-11.22
2000	96.72	1.01	1.10	0.89	9.75	-11.15

New resin mixed  
bed

		MTC (*10 <sup>-4</sup> m/s)			Relative Error (%age)	
Ci (feed)	Ci (eff)	K	Kmax	Kmin	max	min
98	4.65	1.04	1.13	0.93	8.37	-10.08
200	12.91	0.93	1.01	0.84	8.73	-10.44
400	30.15	0.88	0.96	0.79	8.95	-10.66
700	45.21	0.93	1.01	0.84	8.73	-10.45
980	56.74	0.97	1.05	0.87	8.59	-10.31
2000	76.50	1.11	1.20	1.00	8.15	-9.87

Used resin RS CP1

		MTC (*10 <sup>-4</sup> m/s)			Relative Error (%age)	
Ci (feed)	Ci (eff)	K	Kmax	Kmin	max	min
98	27.60	0.43	0.49	0.37	12.98	-14.61
200	27.60	0.67	0.74	0.59	10.14	-11.82
400	35.19	0.83	0.90	0.74	9.20	-10.90
700	52.75	0.88	0.96	0.79	8.95	-10.66
980	66.76	0.92	1.00	0.82	8.81	-10.52
2000	116.57	0.97	1.05	0.87	8.60	-10.32

MTC of Ca at 750 ml/min

New resin mono  
bed

		MTC (*10 <sup>-4</sup> m/s)			Relative Error (%age)	
Ci (feed)	Ci (eff)	K	Kmax	Kmin	max	min
98	6.57	1.35	1.48	1.19	10.16	-11.54
200	17.15	1.22	1.35	1.08	10.54	-11.90
400	31.63	1.26	1.40	1.12	10.40	-11.78
700	62.48	1.20	1.33	1.06	10.60	-11.97
980	95.91	1.16	1.28	1.02	10.77	-12.13
2000	206.83	1.13	1.25	0.99	10.88	-12.23

New resin mixed  
bed

		MTC (*10 <sup>-4</sup> m/s)			Relative Error (%age)	
Ci (feed)	Ci (eff)	K	Kmax	Kmin	max	min
98	7.15	1.34	1.46	1.20	8.90	-10.61
200	16.71	1.27	1.38	1.13	9.11	-10.82
400	22.97	1.46	1.59	1.31	8.58	-10.30
700	48.58	1.36	1.48	1.22	8.83	-10.54
980	61.29	1.42	1.54	1.27	8.69	-10.40
2000	131.99	1.39	1.51	1.24	8.76	-10.47

Used resin RS CP1

		MTC (*10 <sup>-4</sup> m/s)			Relative Error (%age)	
Ci (feed)	Ci (eff)	K	Kmax	Kmin	max	min
98	26.35	0.67	0.76	0.57	12.70	-14.33
200	23.36	1.10	1.20	0.97	9.74	-11.43
400	31.23	1.30	1.42	1.16	9.01	-10.71
980	76.42	1.30	1.42	1.16	9.00	-10.71
2000	142.66	1.35	1.47	1.21	8.87	-10.58

MTC of Ca at 1000 ml/min

New resin mono  
bed

		MTC (*10 <sup>-4</sup> m/s)			Relative Error (%age)	
Ci (feed)	Ci (eff)	K	Kmax	Kmin	max	min
98	9.12	1.58	1.75	1.38	11.22	-12.49
200	17.19	1.63	1.81	1.43	11.08	-12.35
400	32.37	1.67	1.85	1.46	10.98	-12.26
700	62.24	1.61	1.79	1.41	11.14	-12.41
980	112.94	1.43	1.60	1.25	11.64	-12.89
2000	228.62	1.44	1.61	1.25	11.63	-12.87

New resin mixed  
bed

		MTC (*10 <sup>-4</sup> m/s)			Relative Error (%age)	
Ci (feed)	Ci (eff)	K	Kmax	Kmin	max	min
98	7.26	1.77	1.94	1.58	9.46	-11.09
200	15.51	1.74	1.91	1.55	9.53	-11.16
400	32.85	1.70	1.87	1.51	9.62	-11.25
700	58.17	1.69	1.86	1.50	9.64	-11.26
980	94.02	1.60	1.75	1.41	9.89	-11.50
2000	193.82	1.59	1.75	1.41	9.91	-11.52

Used resin RS CP1

		MTC (*10 <sup>-4</sup> m/s)			Relative Error (%age)	
Ci (feed)	Ci (eff)	K	Kmax	Kmin	max	min
98	15.36	1.26	1.40	1.10	11.03	-12.61
200	32.70	1.23	1.37	1.08	11.15	-12.73
400	53.75	1.37	1.51	1.20	10.61	-12.20
700	88.14	1.41	1.56	1.24	10.45	-12.05
980	105.12	1.52	1.67	1.34	10.10	-11.71
2000	190.32	1.60	1.76	1.42	9.87	-11.49

VITA

Alagappan Arunachalam

Candidate for the Degree of

Master of Science

Thesis: EXPERIMENTAL RESIN TESTING: MASS TRANSFER CHARACTERISTICS AND SPECTROSCOPIC ANALYSIS OF NEW AND USED RESINS

Major Field: Chemical Engineering

Biographical:

Personal Data: Born in Madras, Tamil Nadu, India, on May 11, 1973, the son of Alagappa Arunachalam and Nachamai Arunachalam.

Education: Graduated from Don Bosco Matriculation Higher Secondary School, Madras, India, in May 1990; received Bachelor of Engineering degree in Chemical Engineering from Birla Institute of Technology and Science, Pilani, India, in June 1994. Completed the requirements for the Master of Science degree with a major in Chemical Engineering at Oklahoma State University in July 1996.

Experience: Summer internship at Madras Rubber Factory Limited, Madras, India, 1992; summer internship at TamilNadu Petroproducts Limited, Madras, India, in 1993; six month internship at Karnataka State Council for Science and Technology, Bangalore, India, 1994; employed as a Teaching Assistant by the School of Chemical Engineering, Oklahoma State University, Stillwater, Oklahoma, August, 1994 to December, 1994; employed as a Graduate Research Assistant by the School of Chemical Engineering, Oklahoma State University, Stillwater, Oklahoma, January, 1995 to present.

Professional Memberships: American Institute of Chemical Engineers, Phi Lambda Upsilon.